

Using NMR to study Macromolecular Interactions

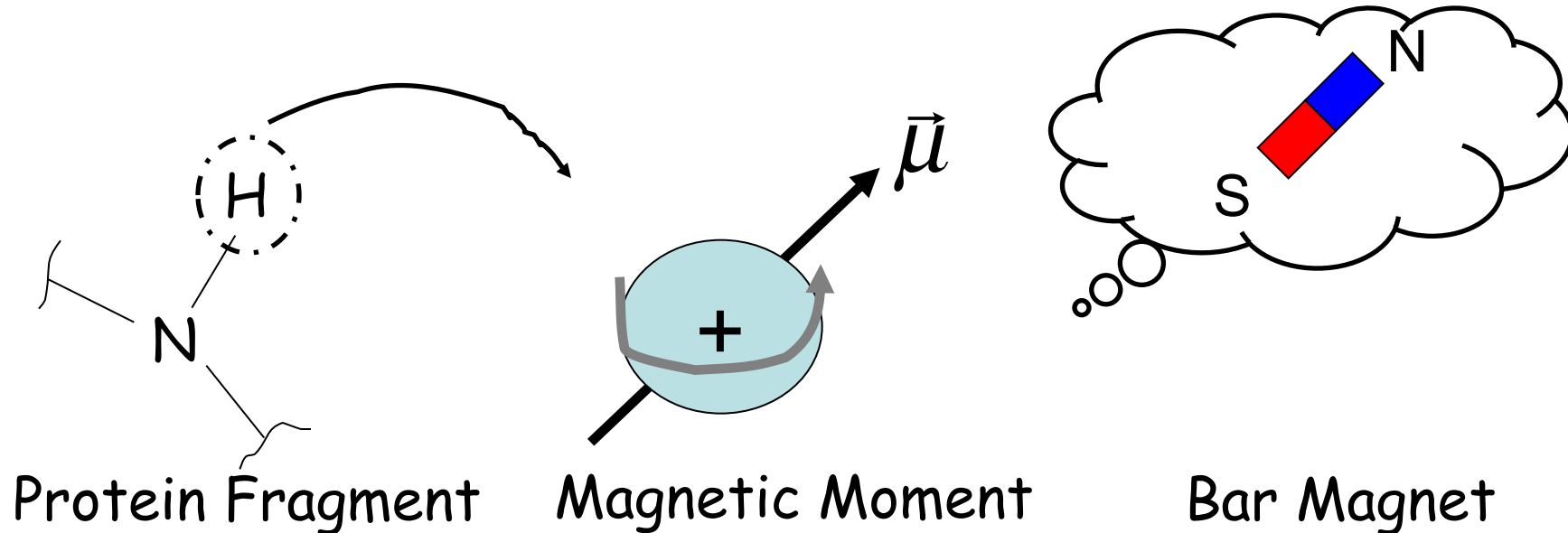
John Gross, BP204A
UCSF

presented by Stephen Floor

Outline

- Multidimensional NMR
- Macromolecular Interactions
- Dynamics
- Dealing with large complexes
- Structure Determination

Review: Nuclear Spins are Microscopic Bar Magnets



Magnetic moment $\vec{\mu} = \gamma \vec{S}$ Angular Momentum

The proportionality constant γ : strength of bar magnet

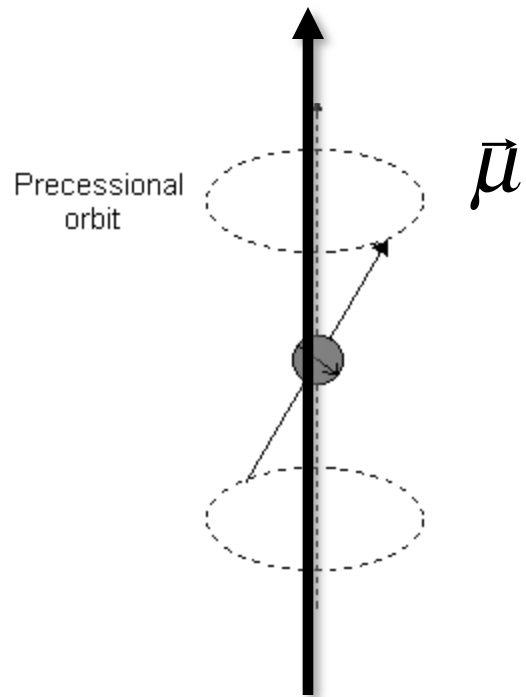
Equation of Motion

$$\frac{d\vec{\mu}}{dt} = \gamma \vec{B} \times \vec{\mu}$$

Based on magnetic torque:

$$\frac{d\vec{L}}{dt} = \vec{B} \times \vec{L}$$

Spin Precession



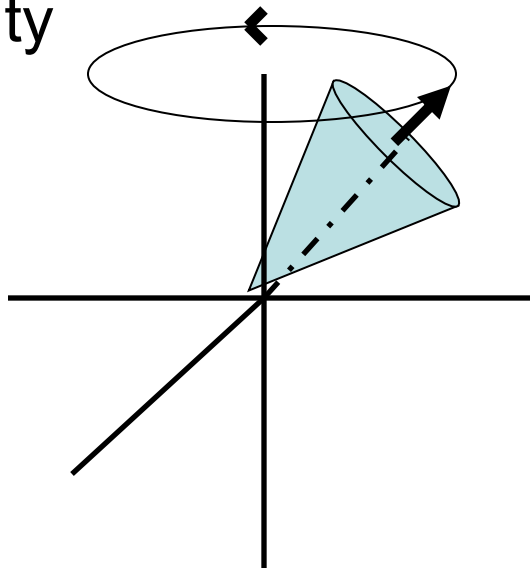
Magnetic Field, B_0

Precession frequency: $\gamma B_0 = \omega_0$

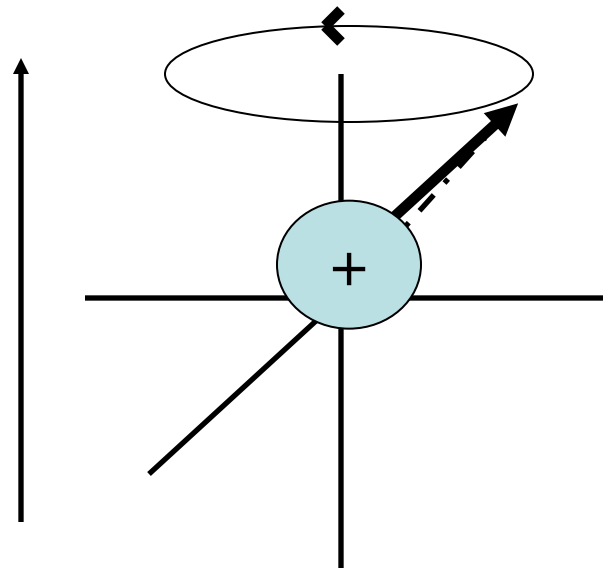
Driving Forces for Precession

Precessional Orbits

Gravity



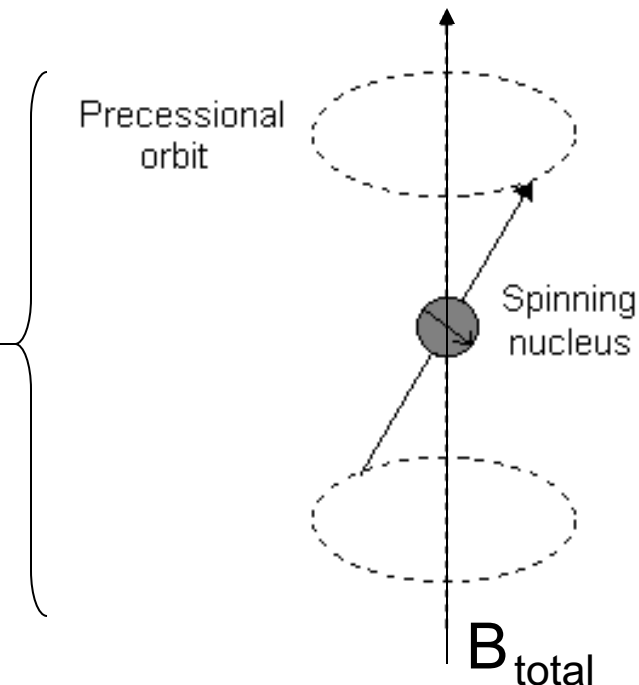
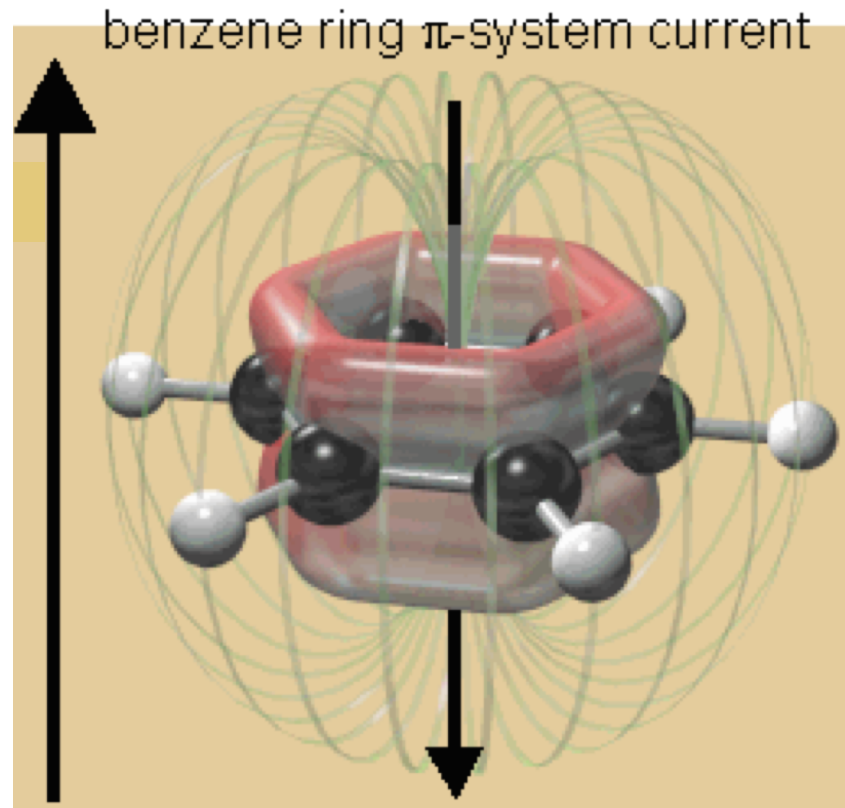
Spinning Top



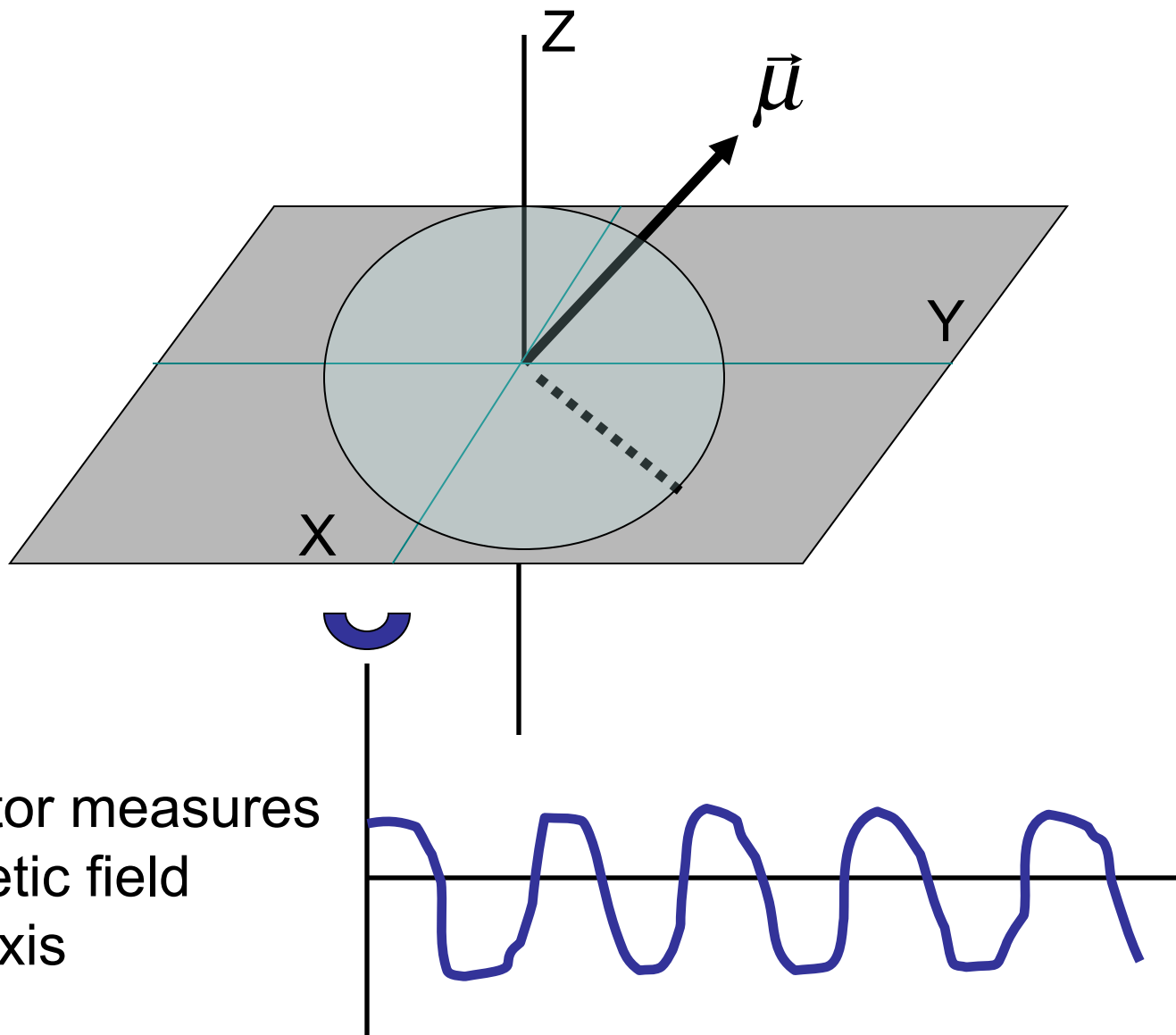
Applied magnetic field, B_0

Spinning Nucleus

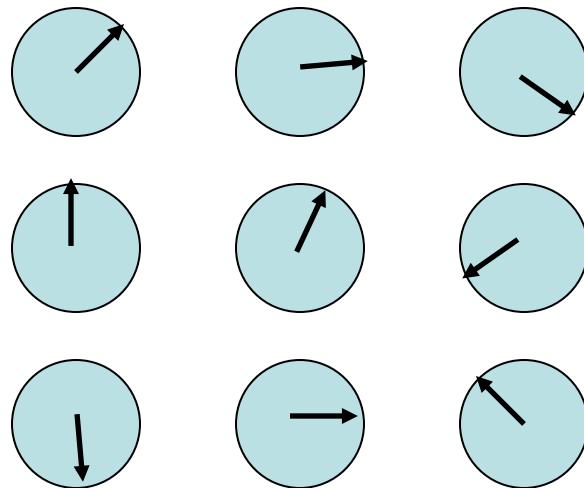
Nuclear Spins Report Local Environment


$$B_{\text{applied}} + B_{\text{local}} = B_{\text{total}} \text{ determines precession}$$

Detection of Spin Precession



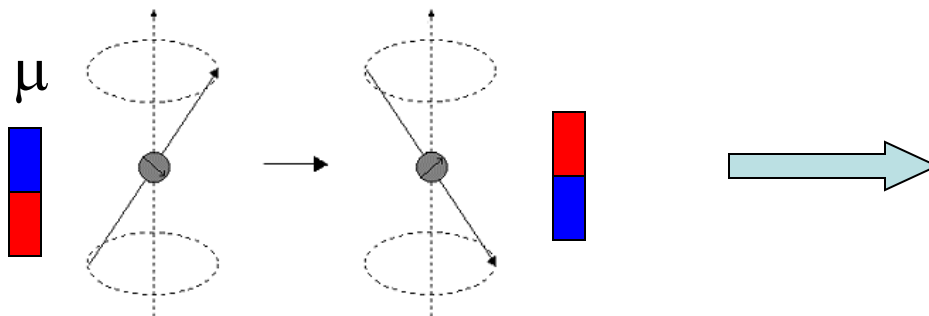
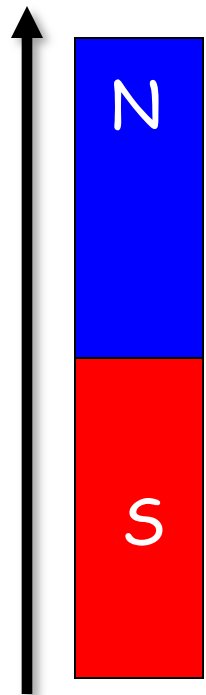
Net Magnetization



$$\left. \begin{aligned} M_x &= \sum_j \mu_x^j = 0 \\ M_y &= \sum_j \mu_y^j = 0 \end{aligned} \right\} \text{No Transverse Magnetization at equilibrium}$$

Magnetic Energy

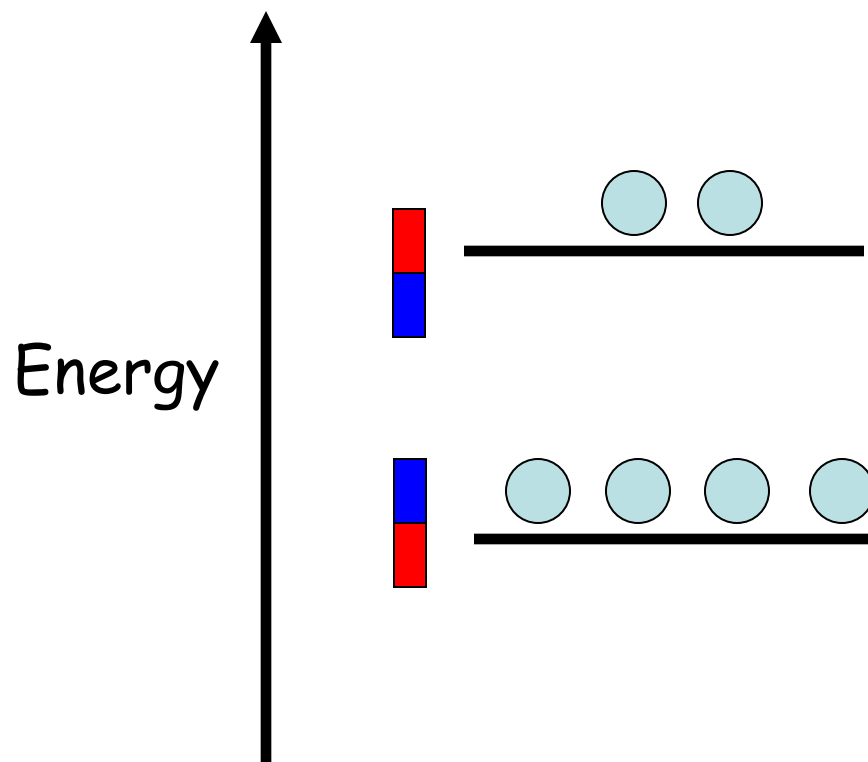
$$E = -\vec{\mu} \bullet \vec{B}$$



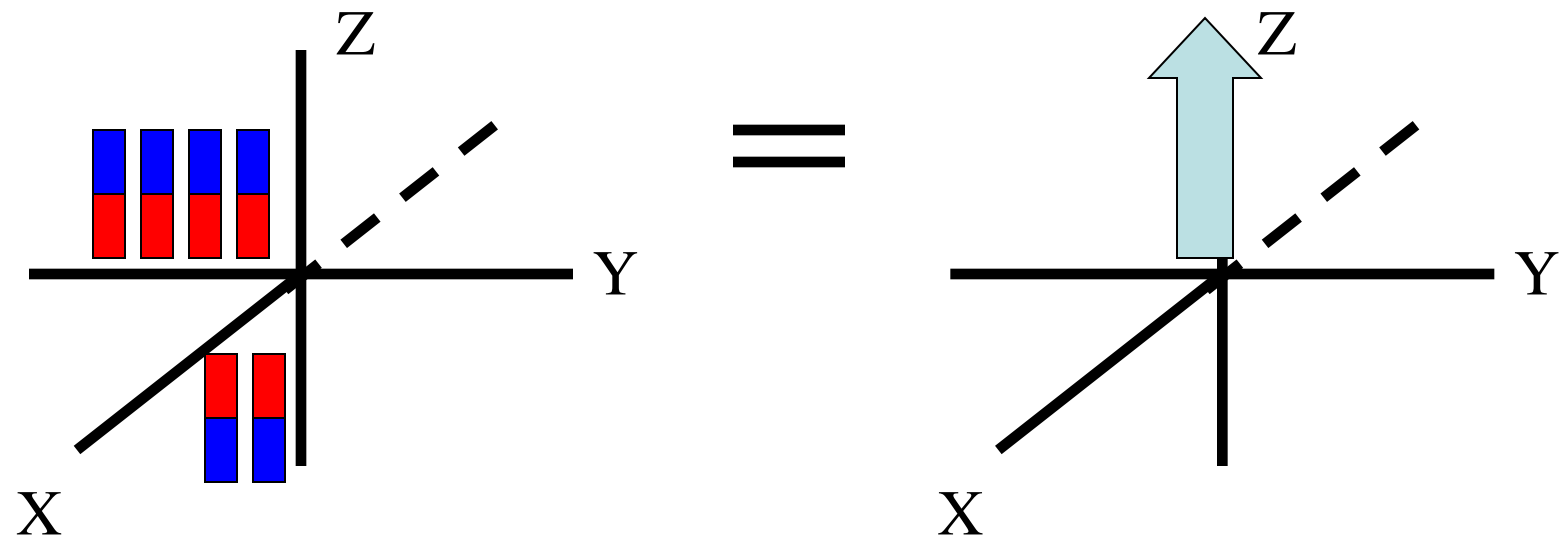
$$E = -\mu_z B_z$$

Static Magnetic Field
Oriented Along Z-Axis

Energy States (spin-1/2 nucleus)

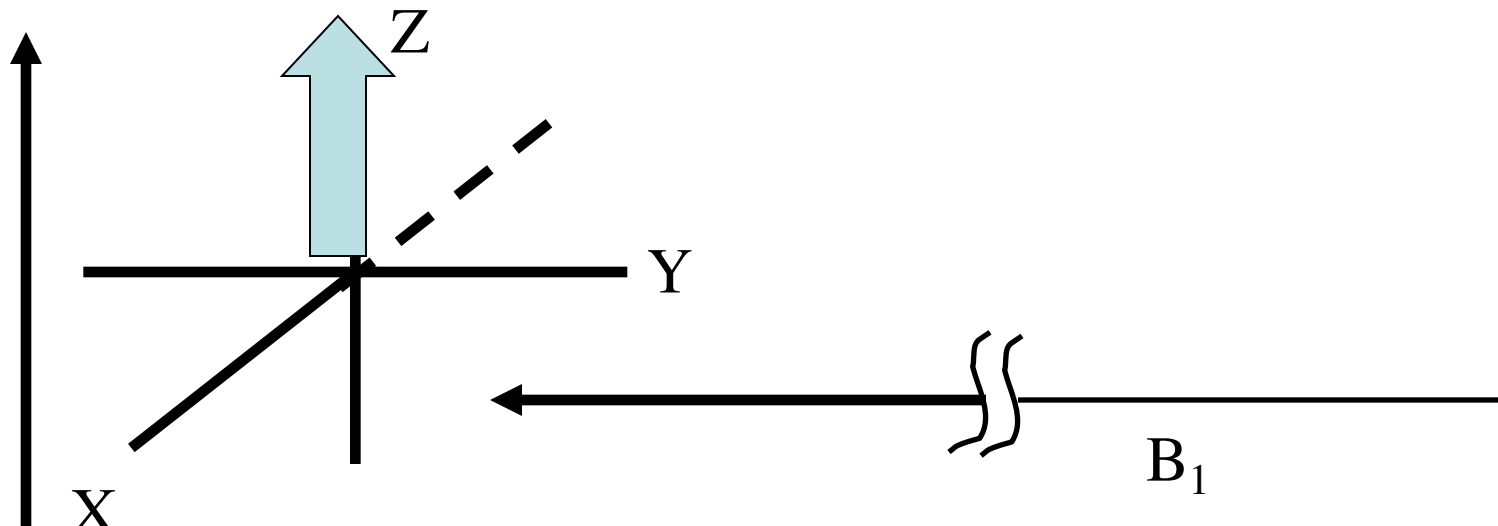


Net Magnetization along Z Axis



$$\sum_j \mu_z^j = M_z$$

Thought experiment: apply 2nd field along Y Axis

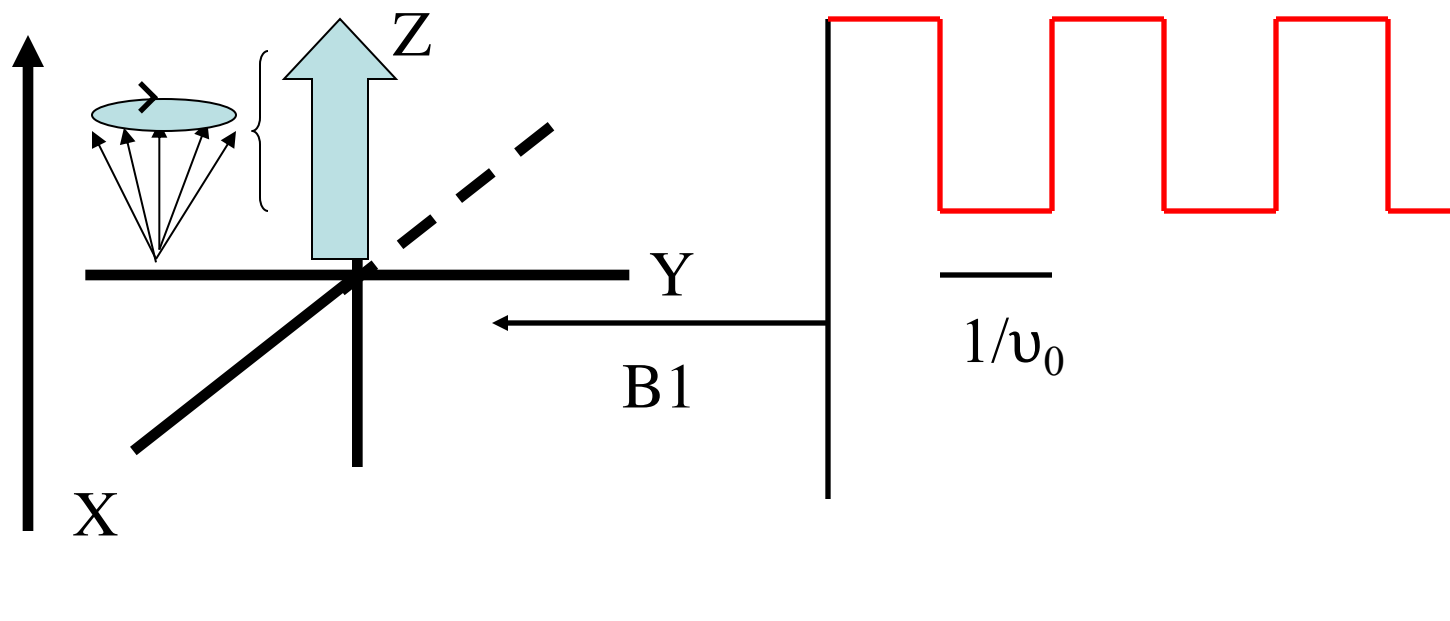


B_0

If $B_1 \gg B_0$, M_Z would rotate about B_1 .

Leave B_1 on until X axis reached ----> transverse magnetization
Approach is not practical.

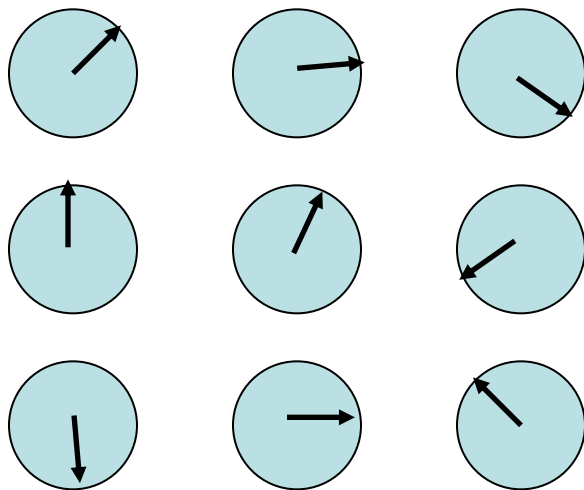
Same effect achieved with weak, resonant oscillating field



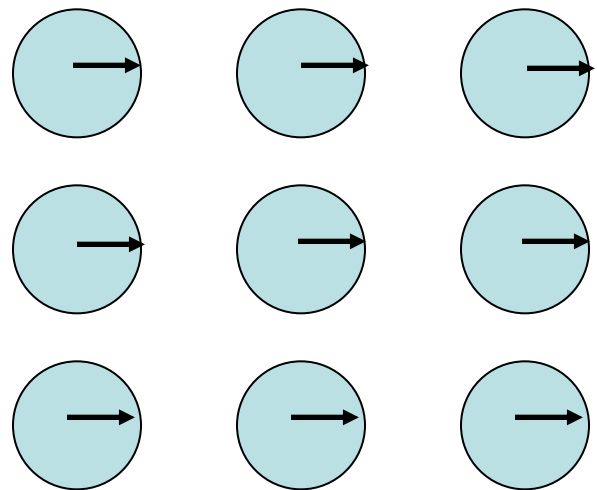
Turn B_1 on and off with a frequency matching the precessional frequency

Resonance

Ensemble of Nuclear Spins



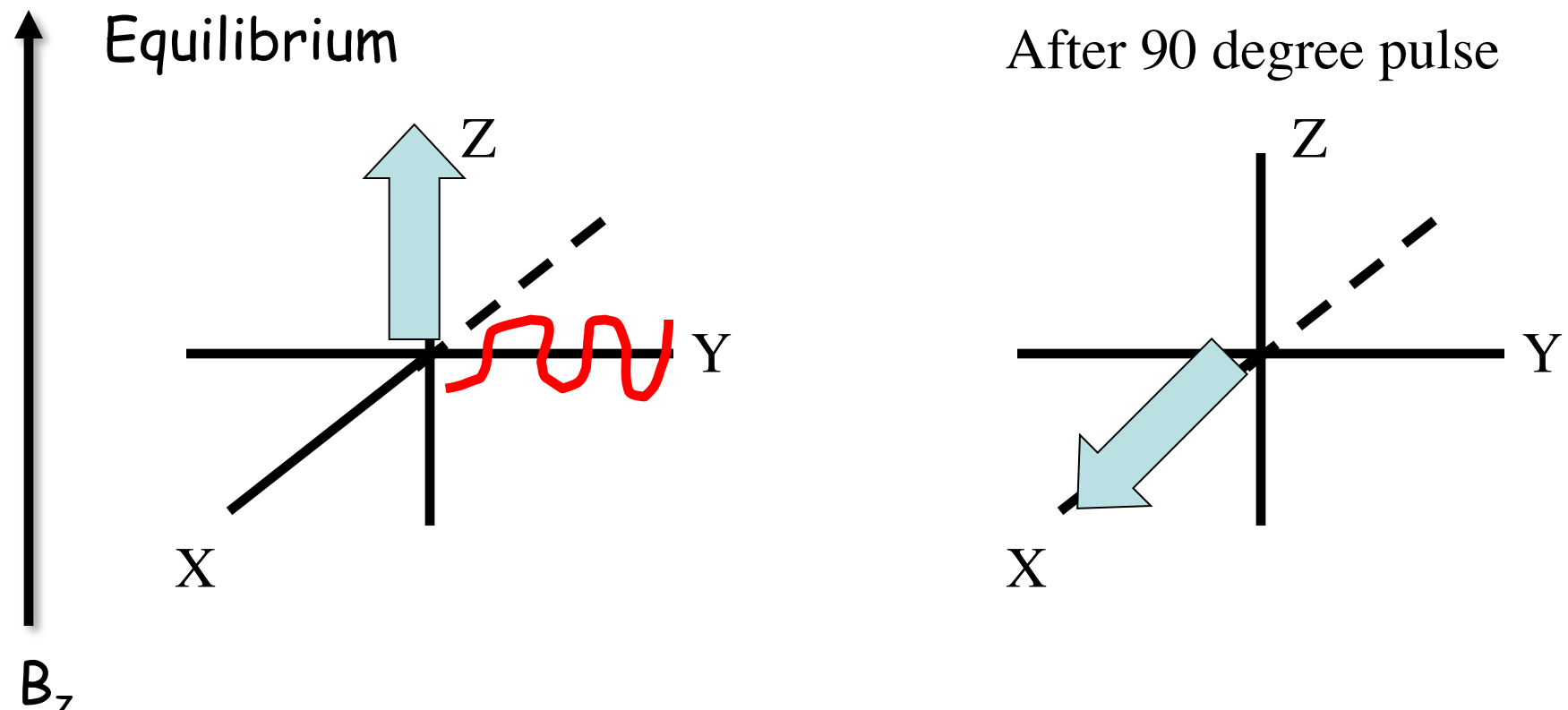
Resonant RF Field
→



Random Phase
No NMR Signal

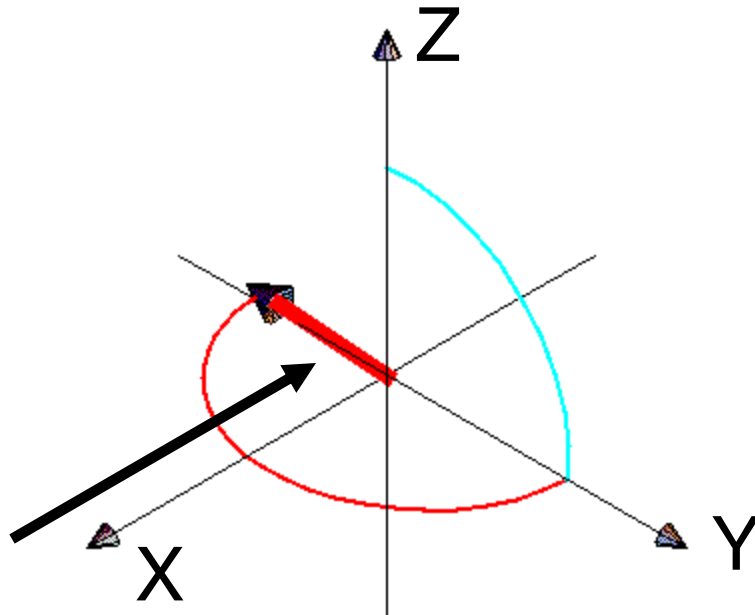
Phase Synchronization
NMR Signal!

Magnetization Vector Model



90y: Resonant 90 Degree Pulse

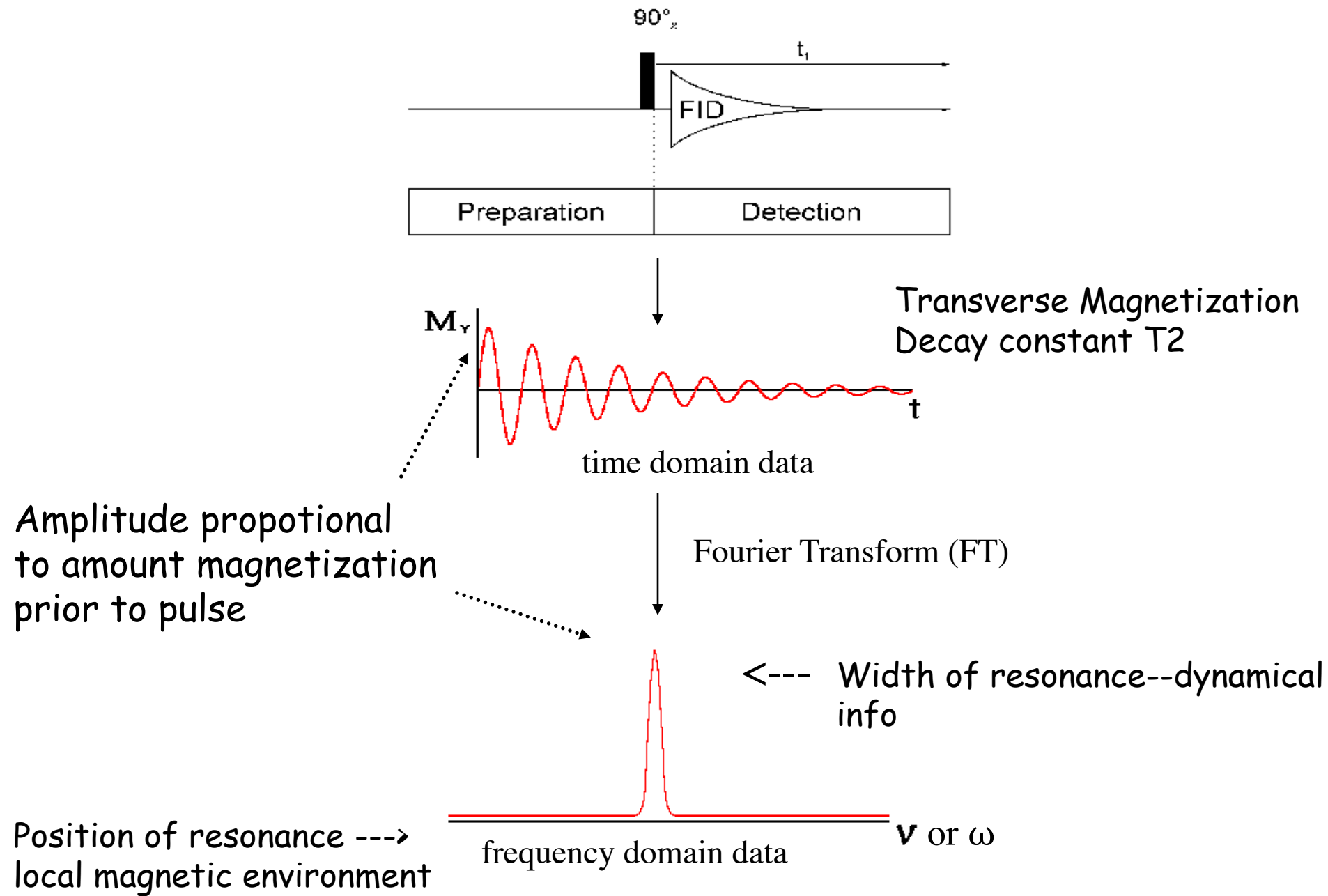
Resonant Pulse in Real Time



R.F. Field (applied at precession frequency)

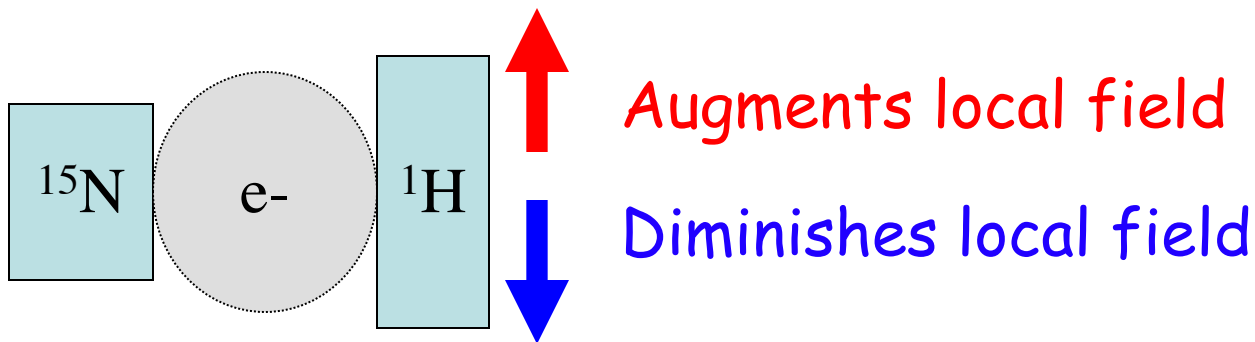
Net magnetization rotated into transverse plane
Rotates due to static and local fields

Summary of 1D Experiment



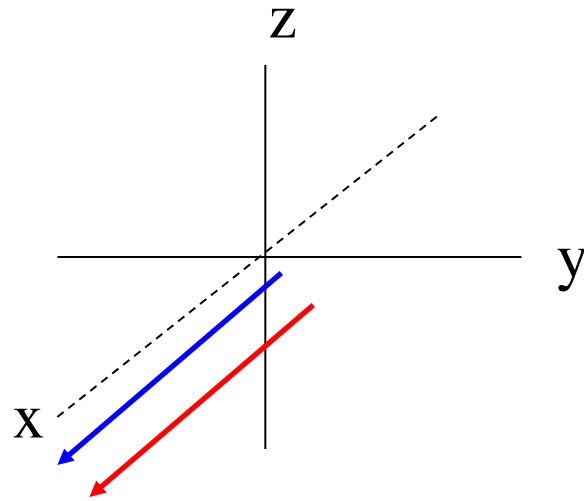
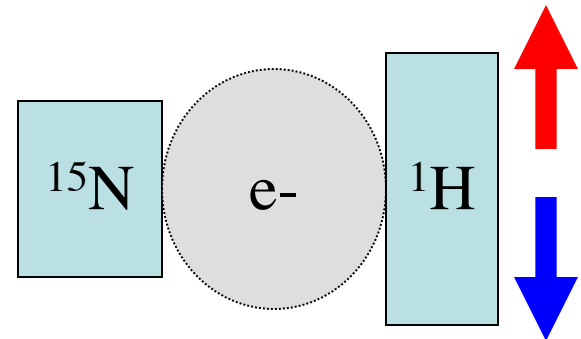
The J Coupling

Consider two spin-1/2 nuclei (ie, ^1H and ^{15}N):

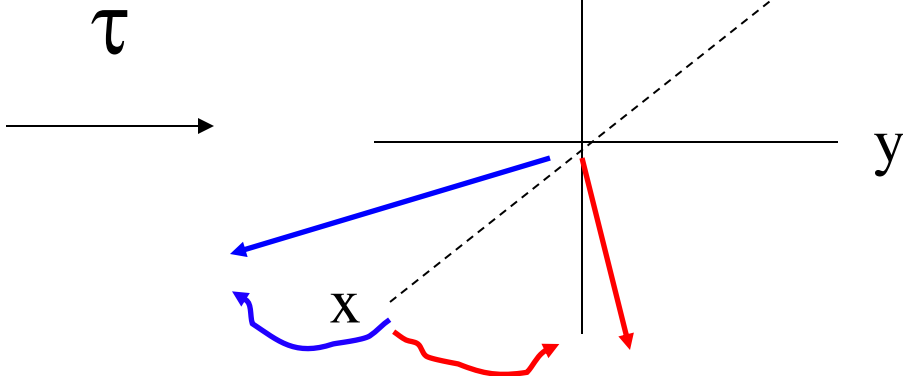


Effect transmitted through electrons in intervening bonds

Vector View

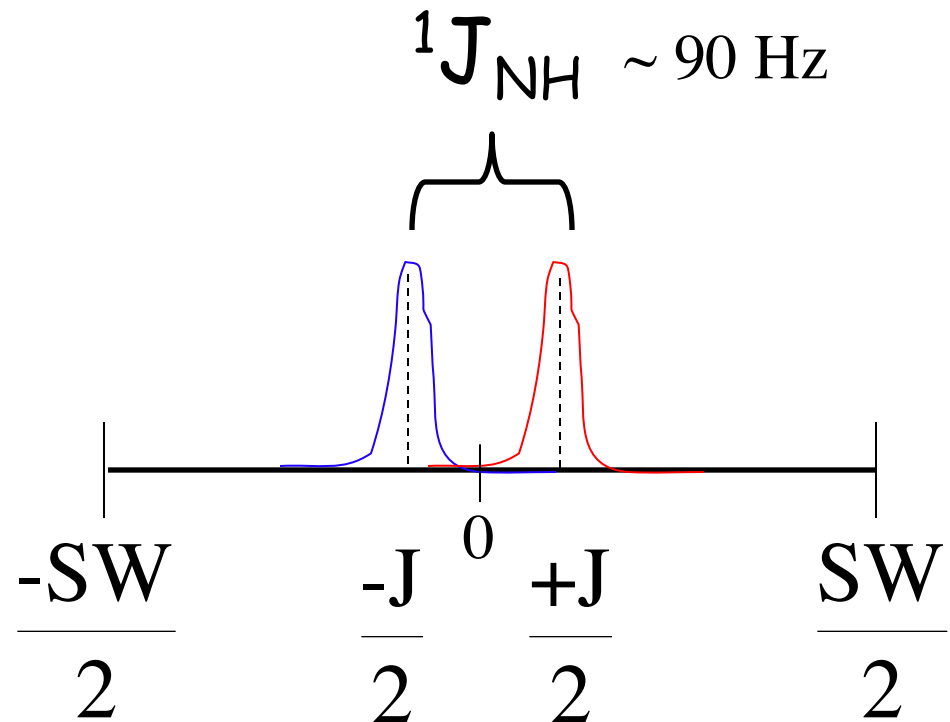


(After 90y pulse)



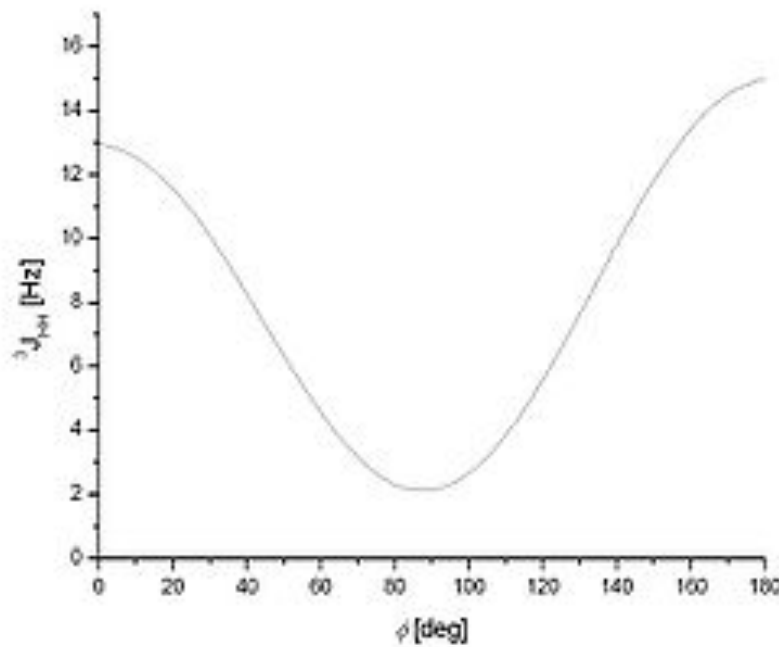
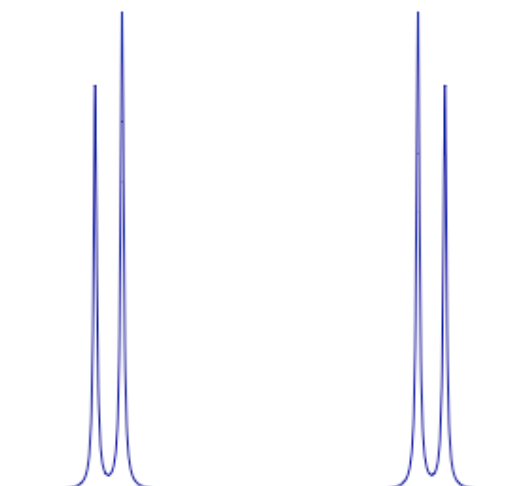
Components rotate **faster** or **slower** than rotating frame
by $\pm J/2$

Spectrum with J coupling



${}^{15}\text{N}$ Detected Spectrum

J couplings contain information on structure



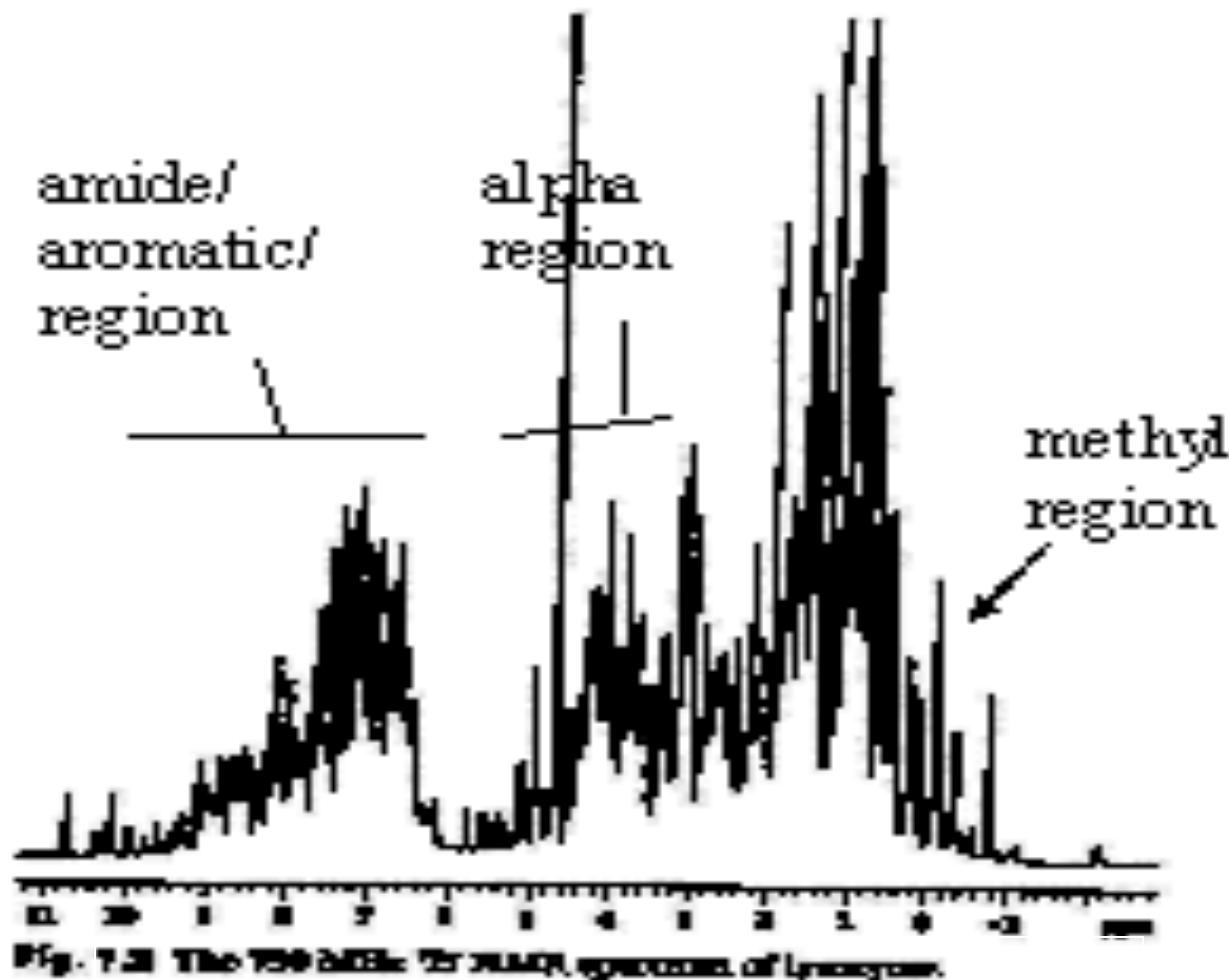
$$J(\phi) = A \cos^2 \phi + B \cos \phi + C$$

Important Observables

Chemical shift is a reporter of magnetic environment

The J coupling can inform torsion angles

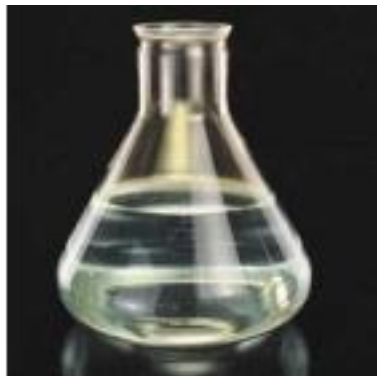
Protein NMR Spectroscopy



Periodic Table of NMR active Nuclei

IA															VIIIA				
H	IIA		Spin = $\frac{1}{2}$												He				
Li	Be		Spin > $\frac{1}{2}$																
Na	Mg	IIIIB	IVB	VB	VIB	VIIB	VIIIB		IB	IIB									
K	Ca	Sc	Ti	V	Cr	Mn	Fe	Co	Ni	Cu	Zn	Ga	Ge	As	Se	Br	Kr		
Rb	Sr	Y	Zr	Nb	Mo	Tc	Ru	Rh	Pd	Ag	Cd	In	Sn	Sb	Te	I	Xe		
Cs	Ba	La	Hf	Ta	W	Re	Os	Ir	Pt	Au	Hg	Tl	Pb	Bi	Po	At	Rn		
Fr	Rd	Ac				Ce	Pr	Nd	Pm	Sm	Eu	Gd	Tb	Dy	Ho	Er	Tm	Yb	Lu
						Th	Pa	U	Np	Pu	Am	Cm	Bk	Cf	Es	Fm	Md	No	Lr

Isotopic Labeling Proteins for NMR



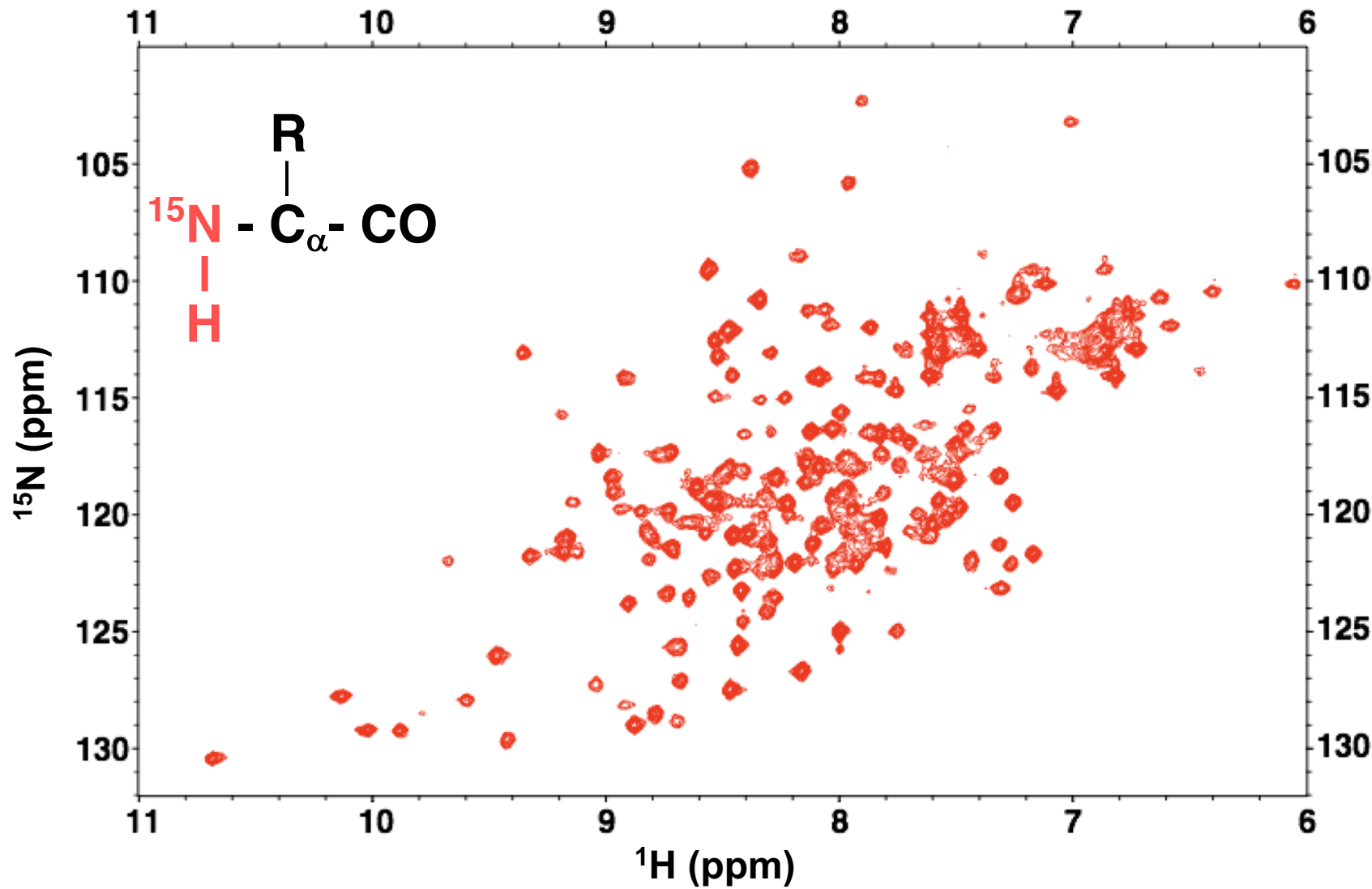
Bacterial expression:
Minimal media, ^{15}N NH_4Cl or
 ^{13}C glucose as sole nitrogen and
carbon source

Amino acid-type labeling
Auxotrophic or standard strains
(ei, BL21(DE3) depending on scheme

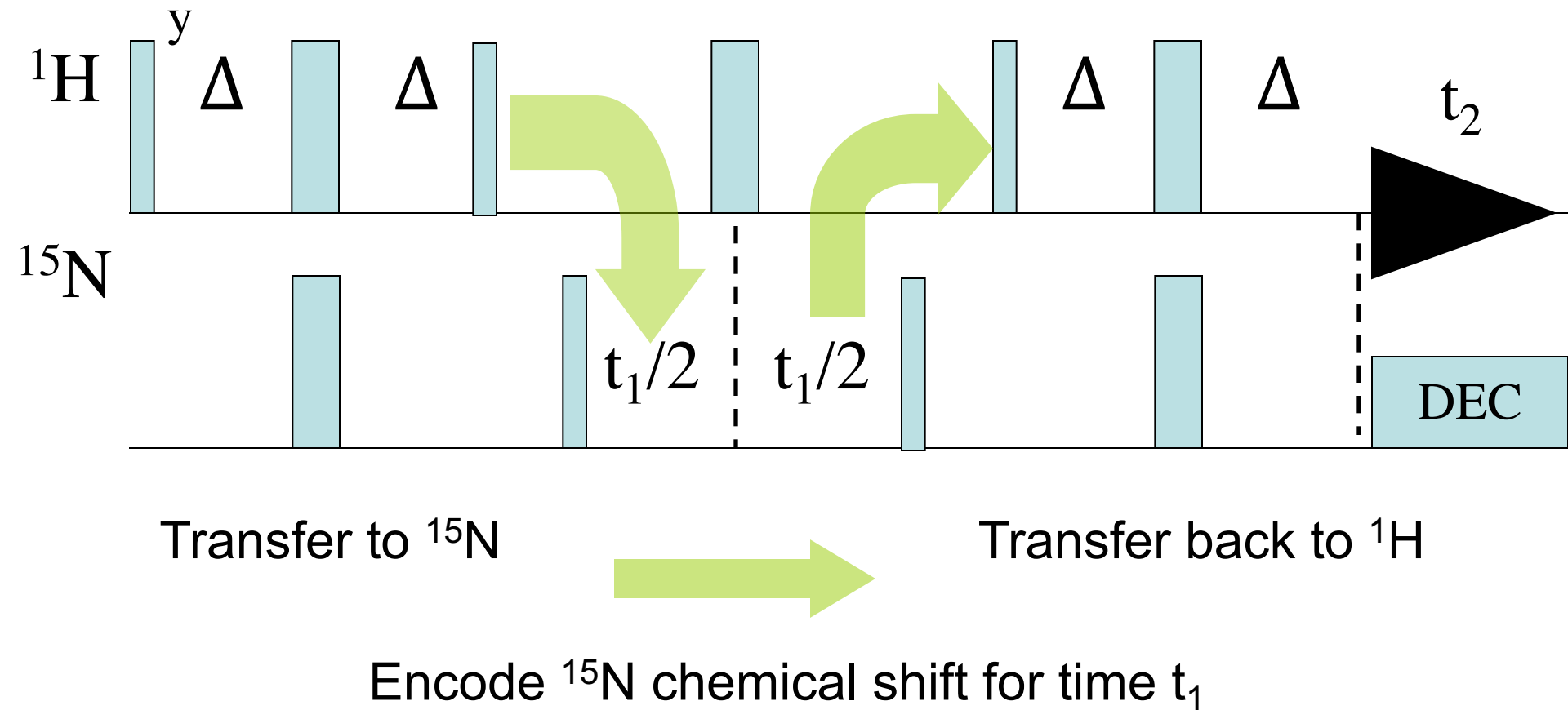
Labeling post purification ; reductive
methylation of lysines

Results in additional spin-1/2 nuclei which can be used as probes

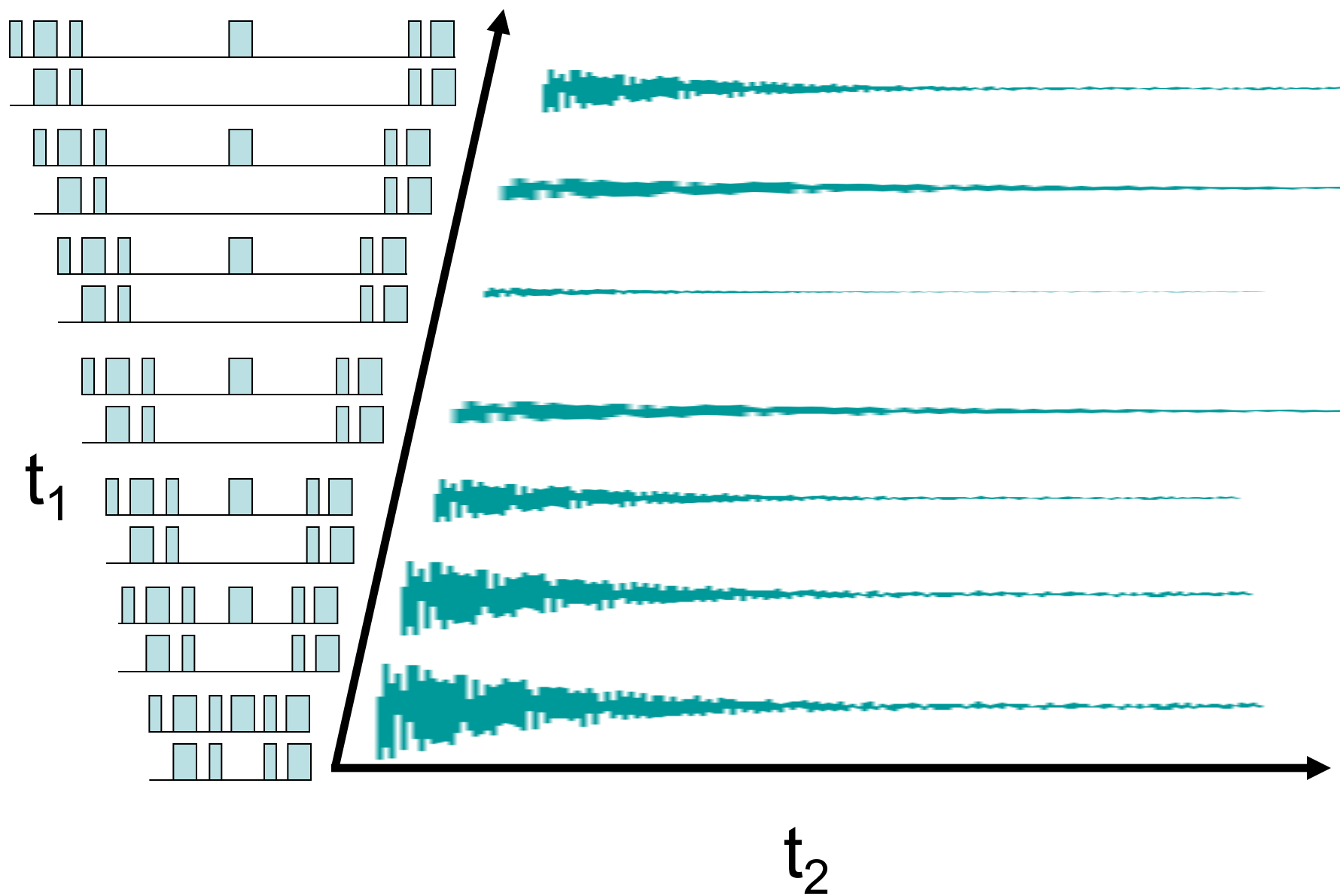
The HSQC is an NH chemical shift correlation map



An overview of the HSQC

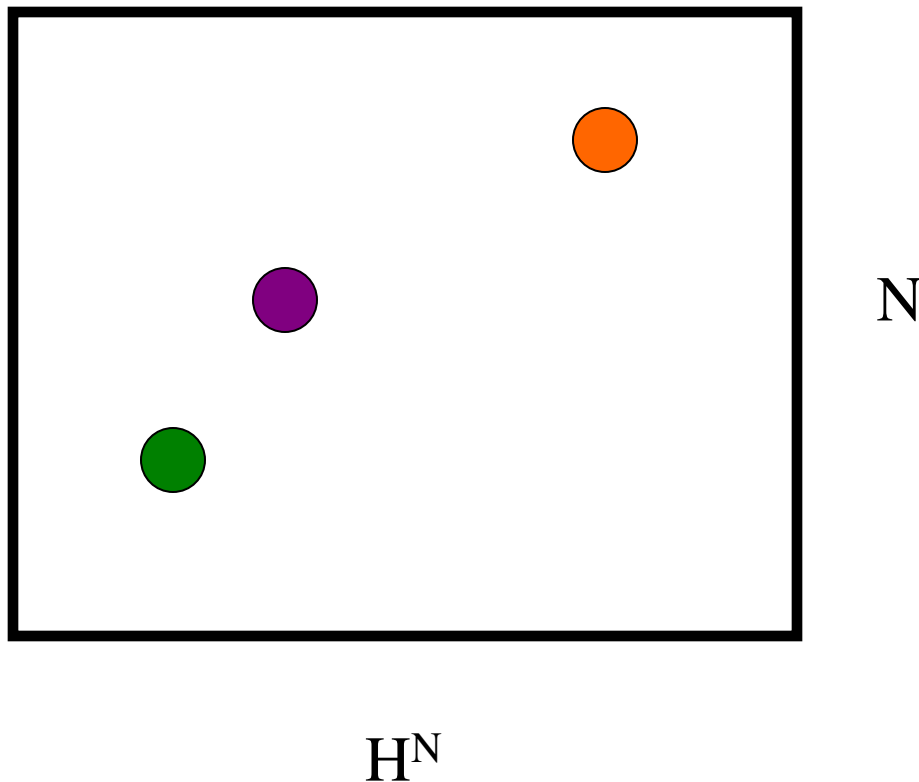


2D Time-Domain Data

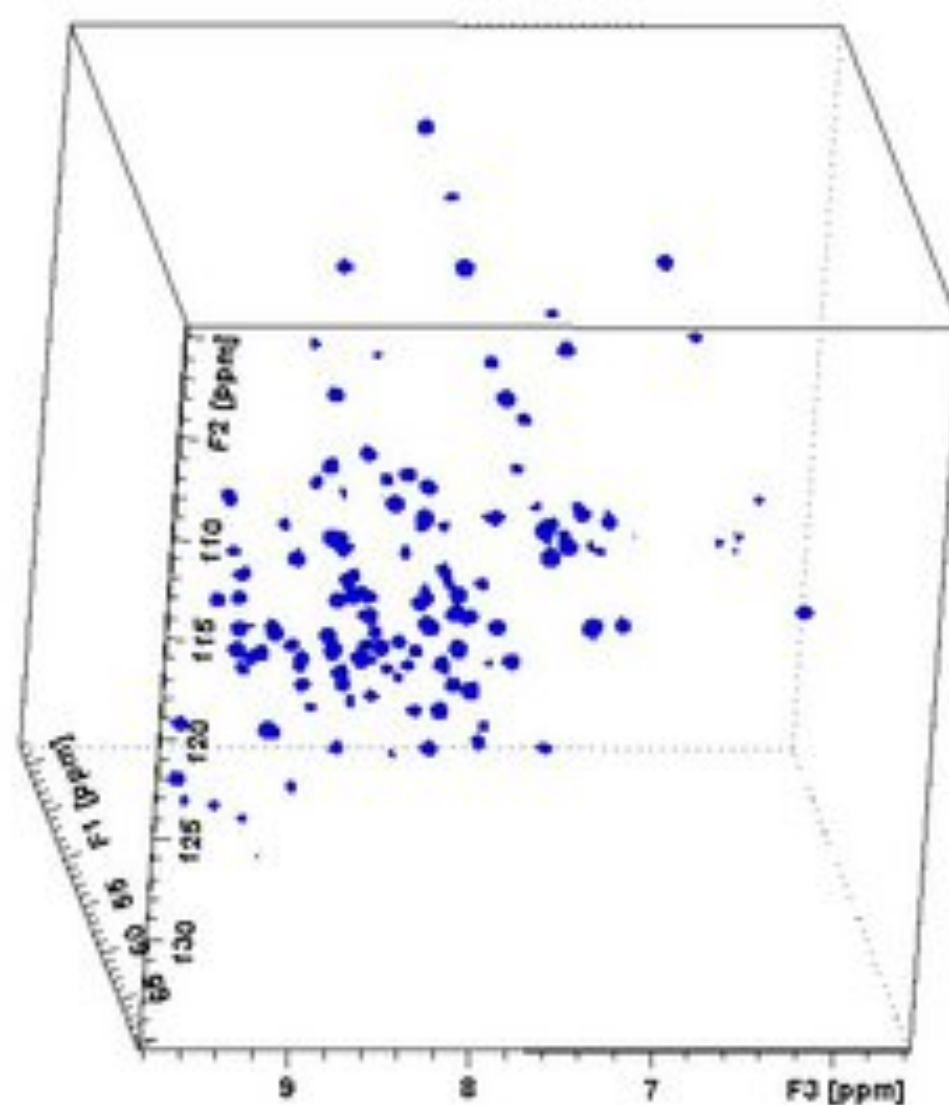


Some data shuffling then 2D FT =the HSQC Spectrum

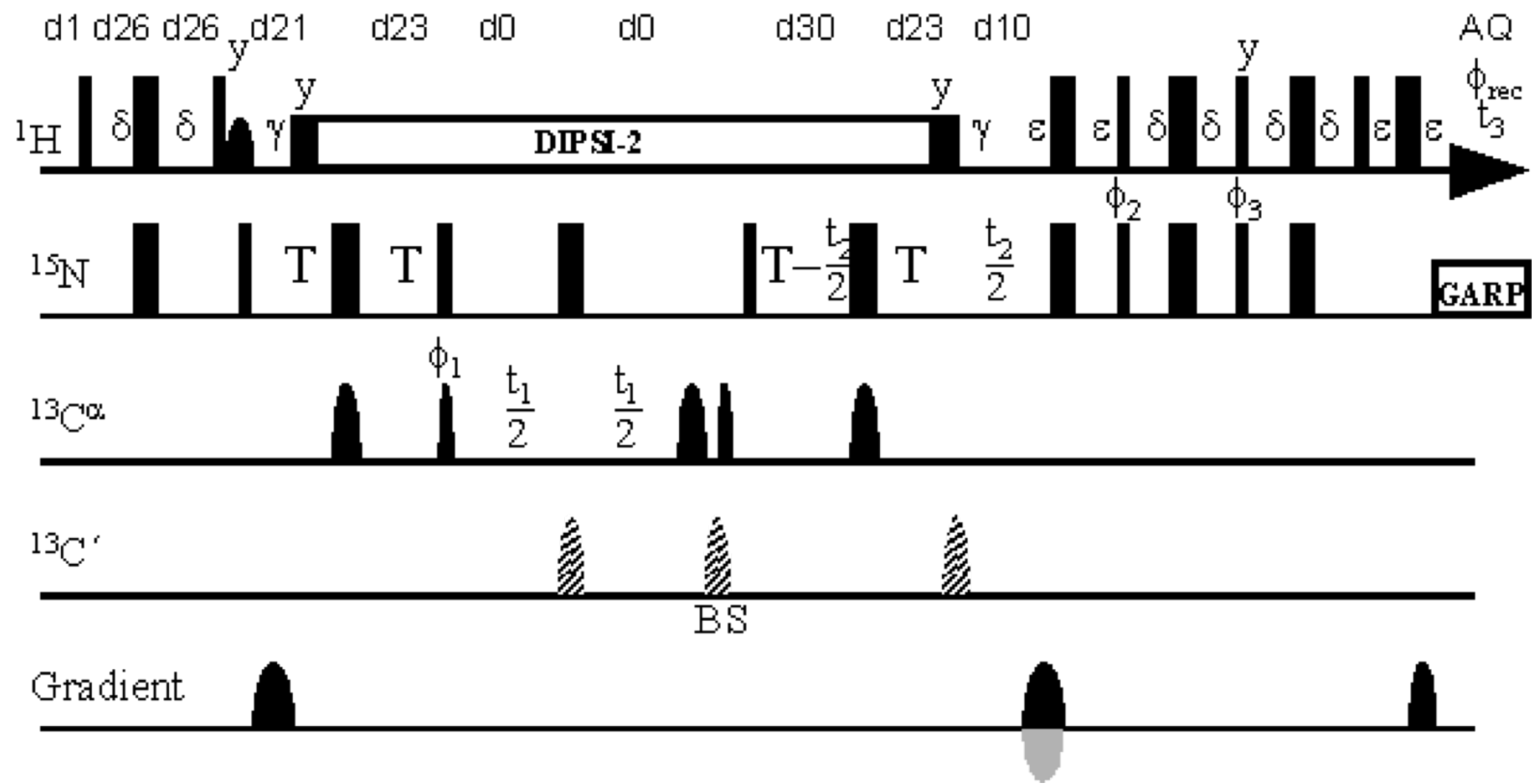
$$\text{Re} [S'(\nu_1, \nu_2)] = A_1^N A_2^H$$



3D Dimensional NMR

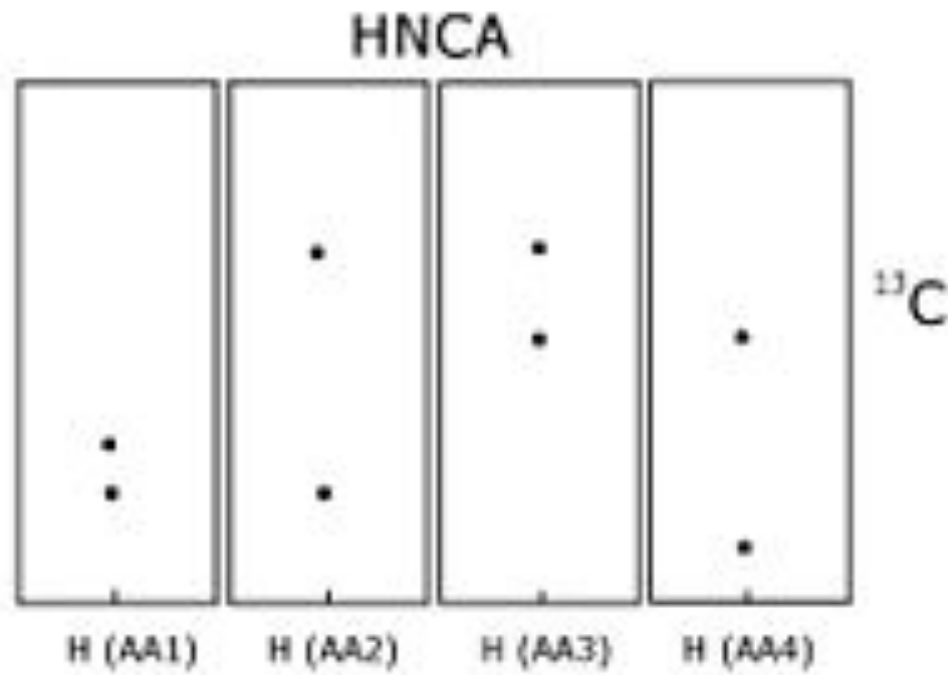
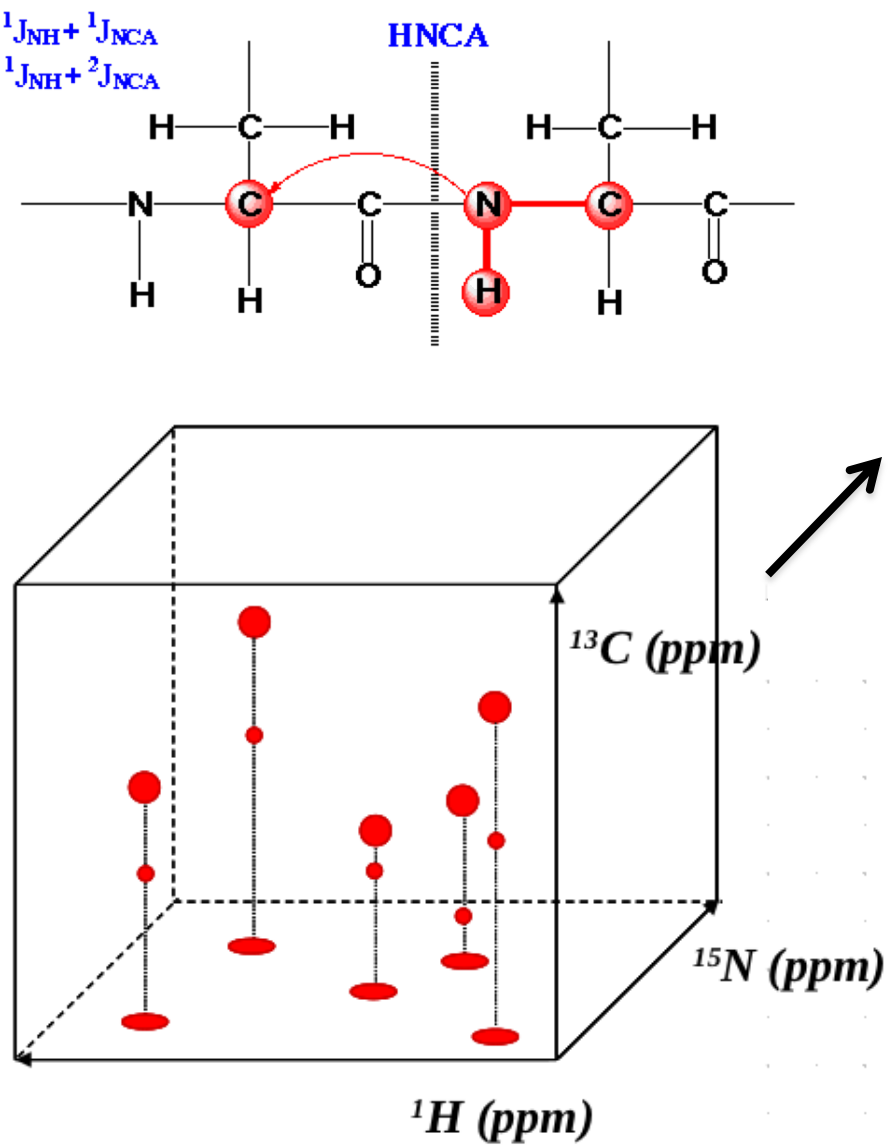


Resonance Assignments from Triple Resonance Experiments



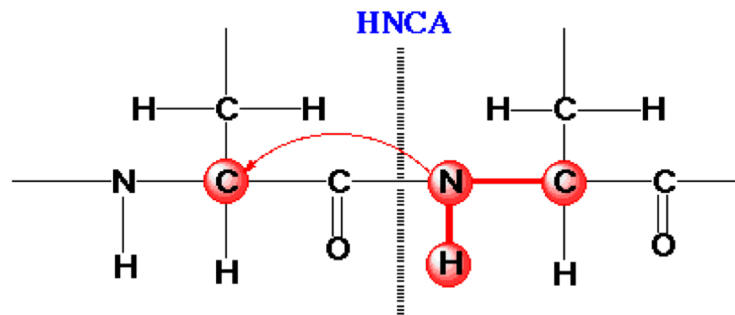
The 3D HNCA Experiment

Backbone Resonance Assignments from HNCA

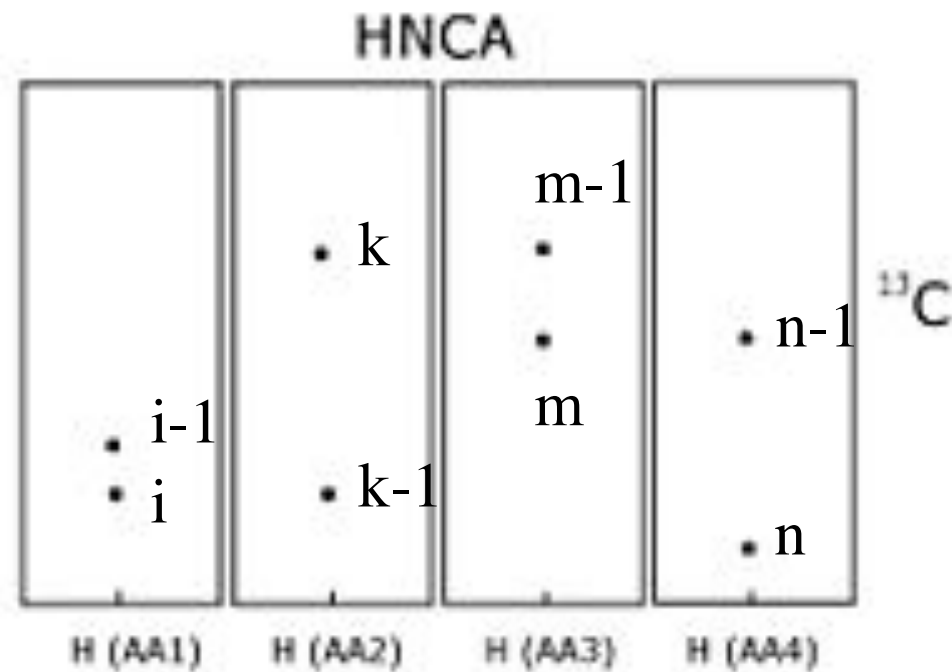


Triple Resonance Pairs

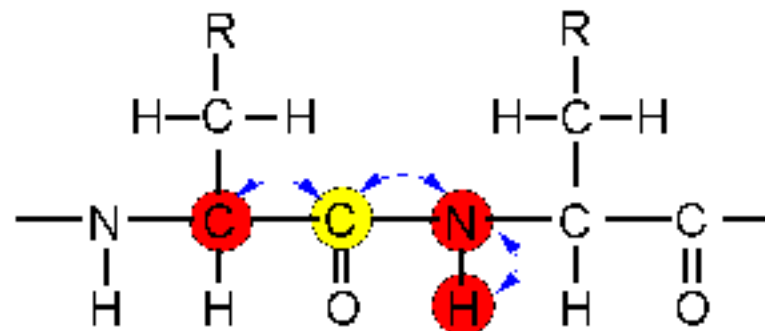
Residue i-1



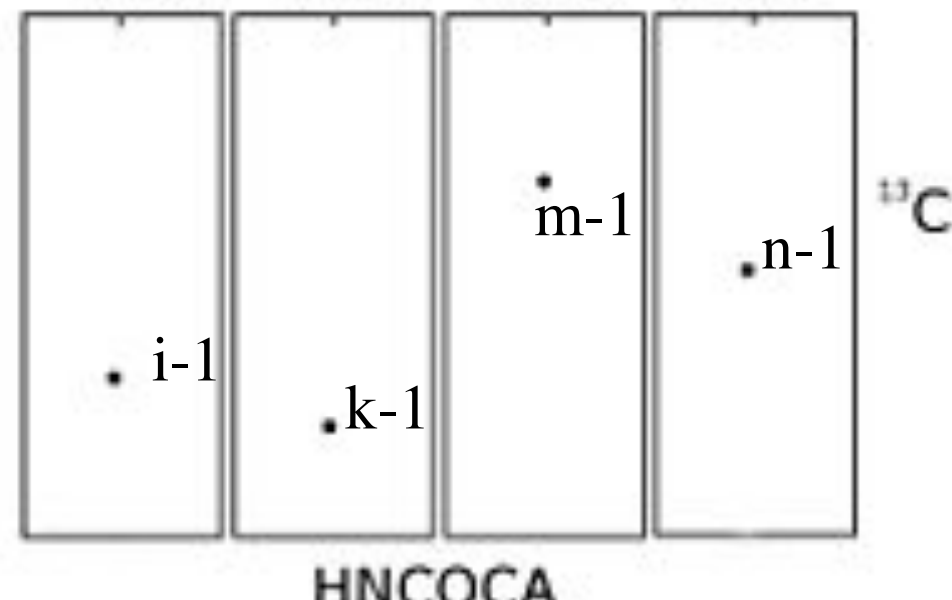
Residue i



HN(CO)CA



sequential correlation only



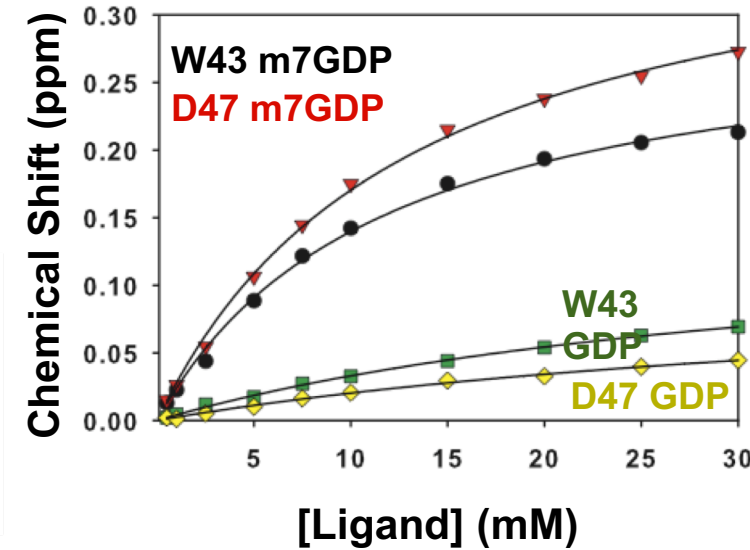
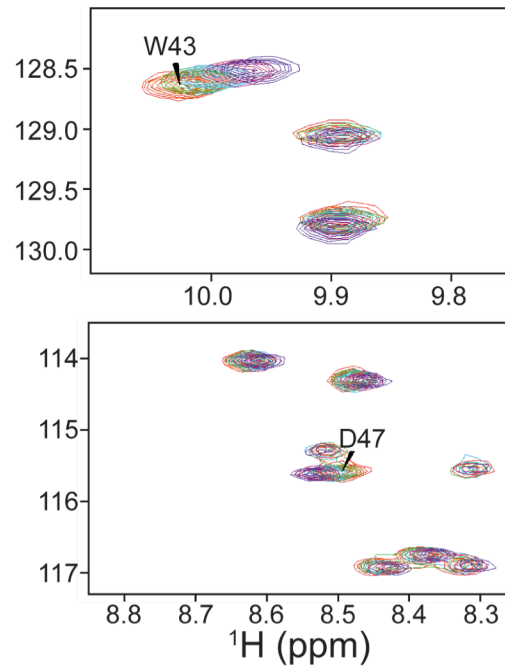
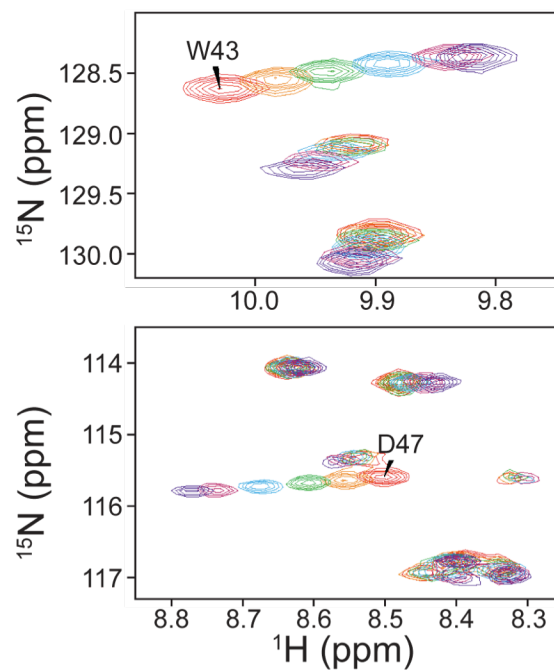
HNC(O)CA

Applications for NMR

- Mapping protein interactions
- Fragment based drug discovery, SAR-by-NMR
- Protein folding , allostery and dynamics
- TROSY: deuteration and Methyl labeling to do this on large assemblies (~1 MDa)
- Structure Determination (<40 kDa)

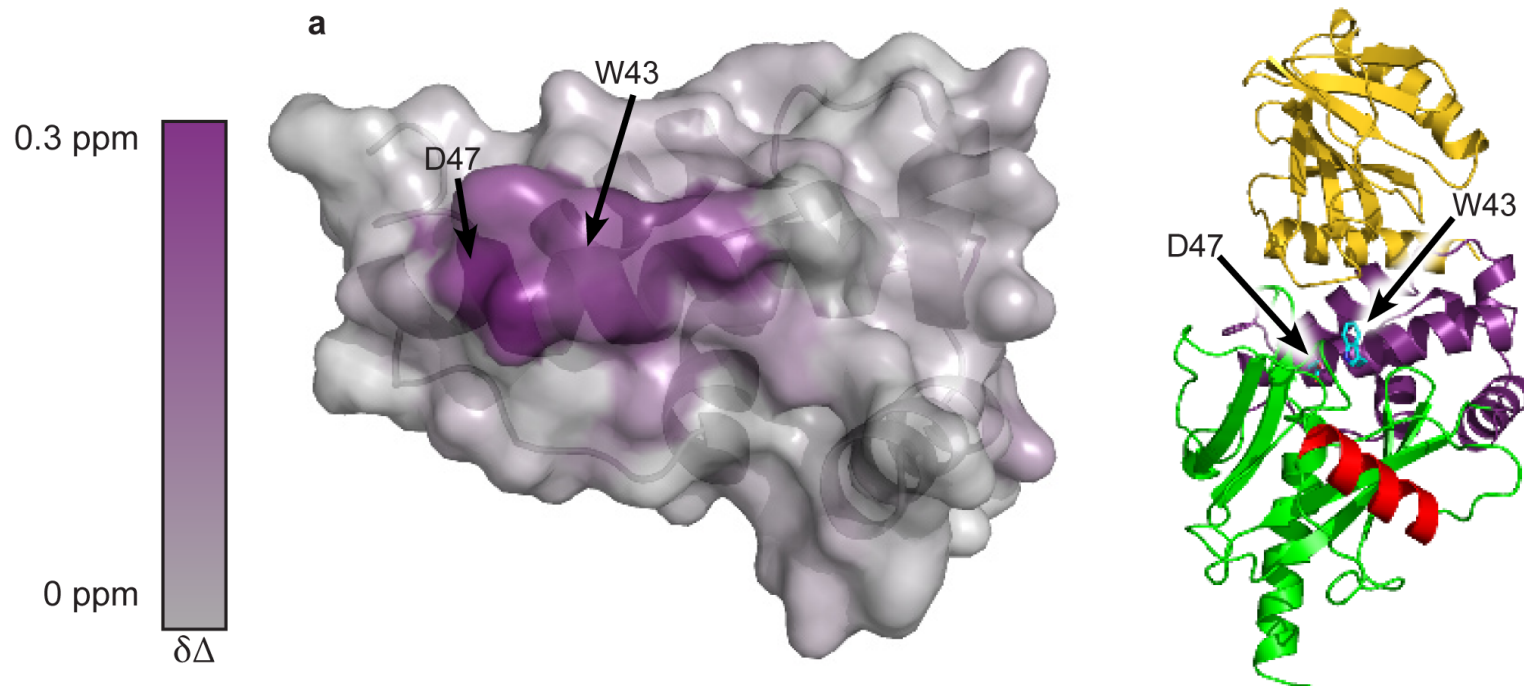
Part II:
Macromolecular Interactions
Detected by NMR

Binding of nucleotide to protein



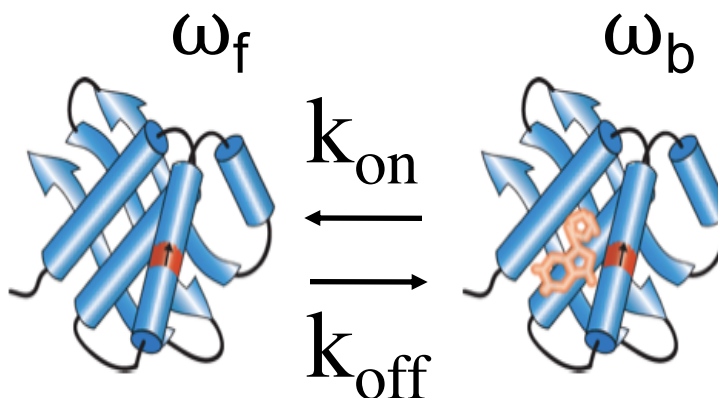
Dose dependent resonance shifts
can be fit to obtain Kd

Shifts may be color coded onto surface to identify ligand binding site



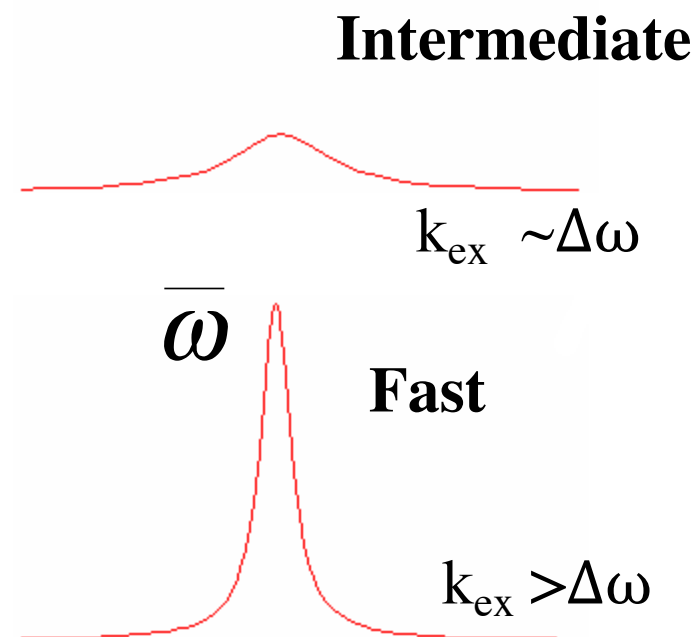
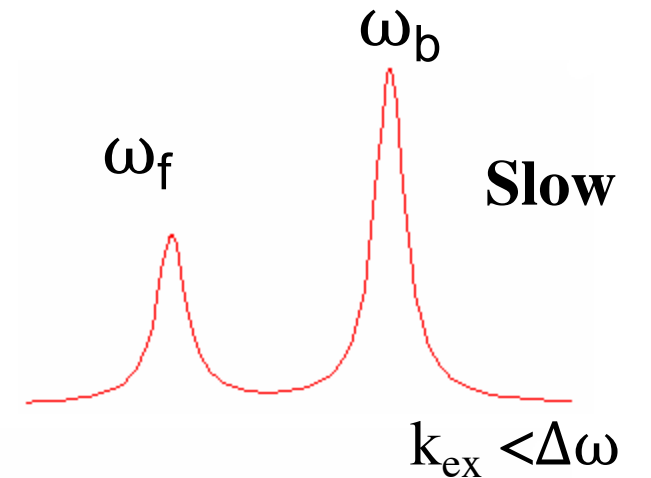
Caveats?

NMR to monitor ligand binding



$$k_{\text{ex}} = k_{\text{on}}[L] + k_{\text{off}}$$

$$\Delta\omega = \omega_f - \omega_b$$

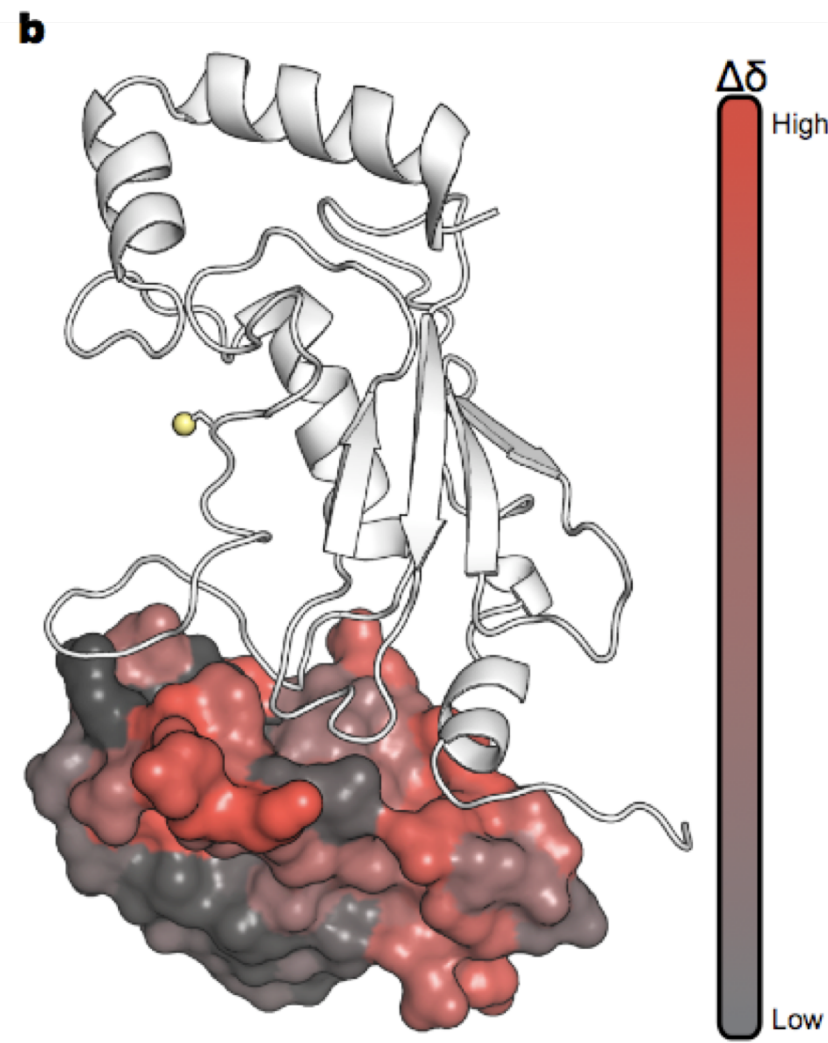
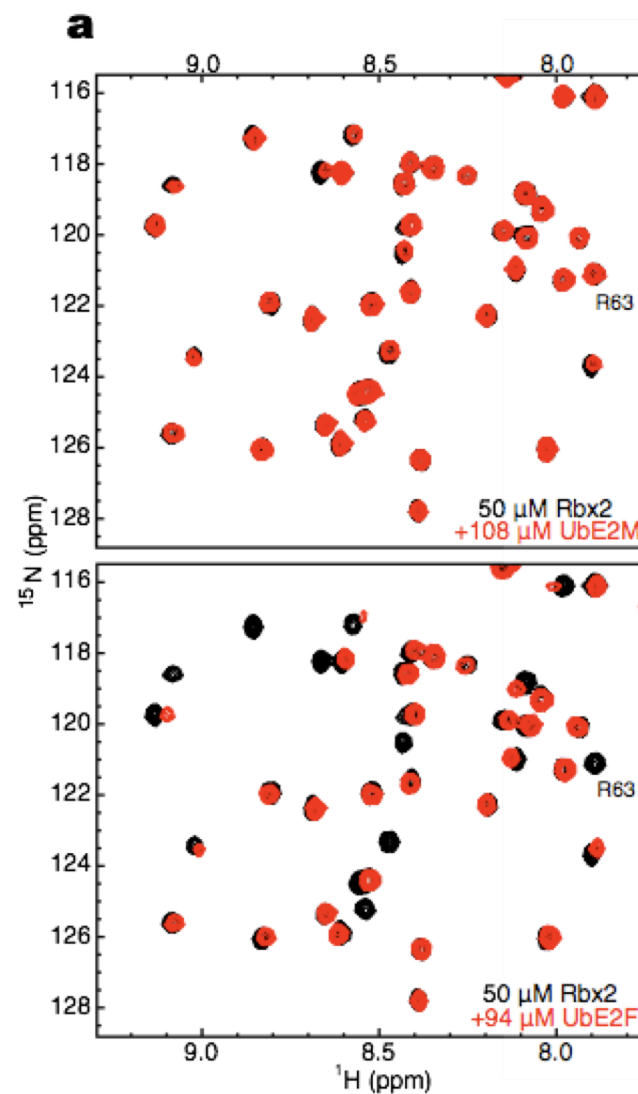


Fraction bound of labeled protein

$$P_b = \frac{\bar{\omega} - \omega_f}{\omega_b - \omega_f} = \frac{[L]}{[L] + K_d}$$

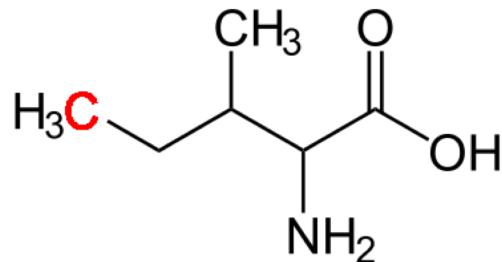
$\bar{\omega}$: observed chemical shift

Monitoring Protein/Protein Interactions by HSQC

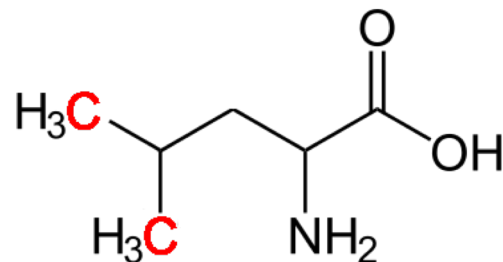


Sparse Labeling to Simplify Spectra

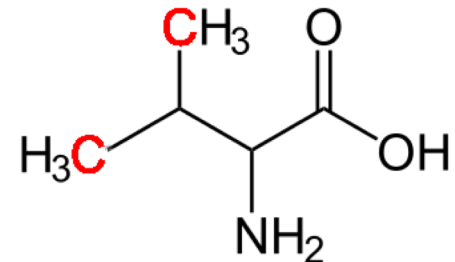
Selectively label R group methyls with C-13 (NMR visible)



Isoleucine



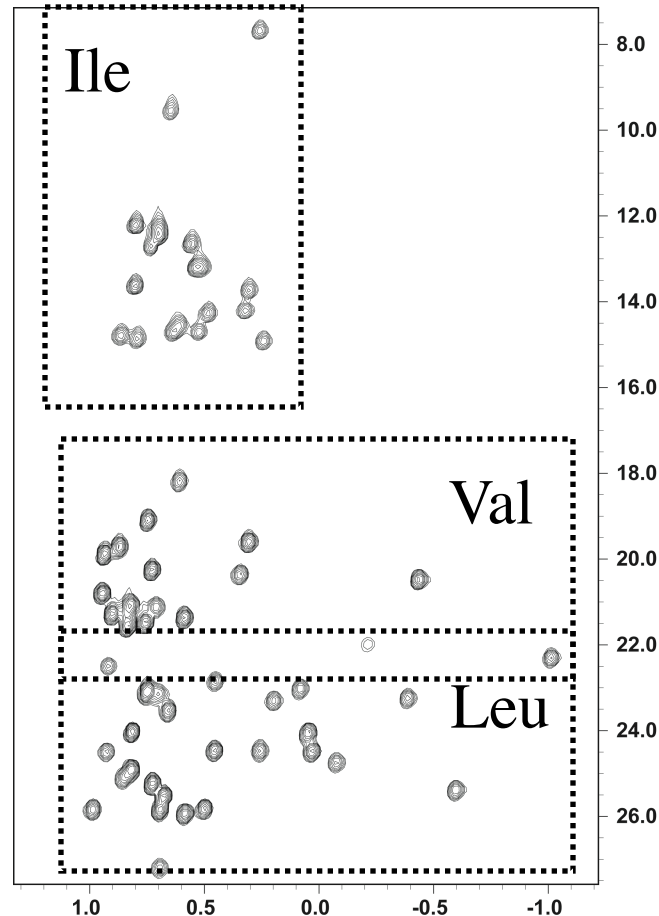
Leucine



Valine

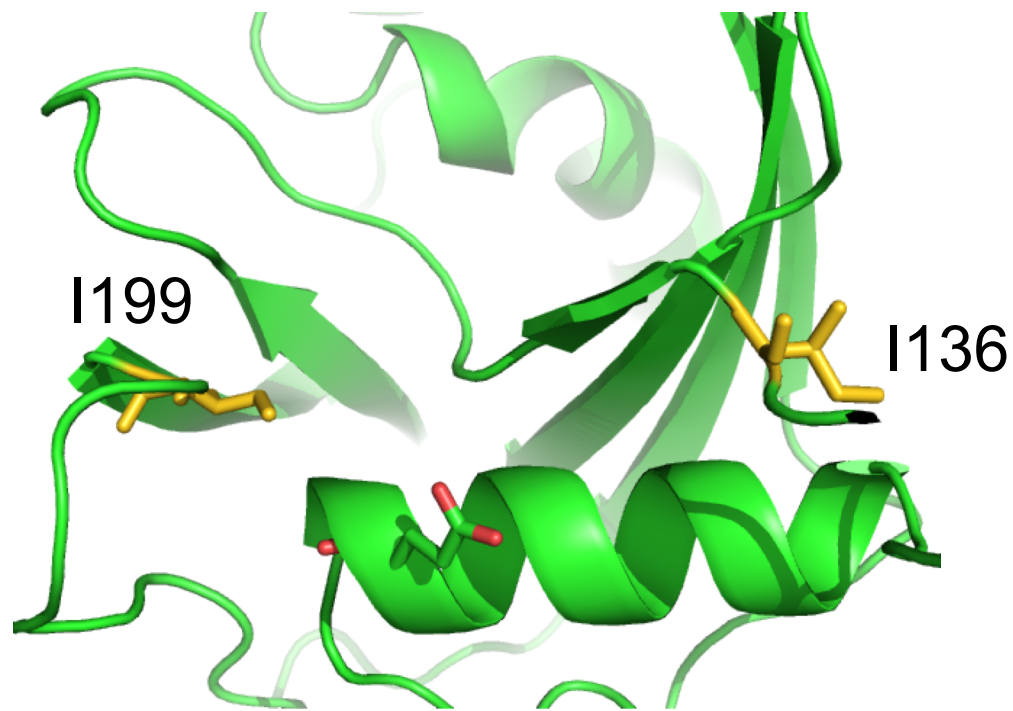
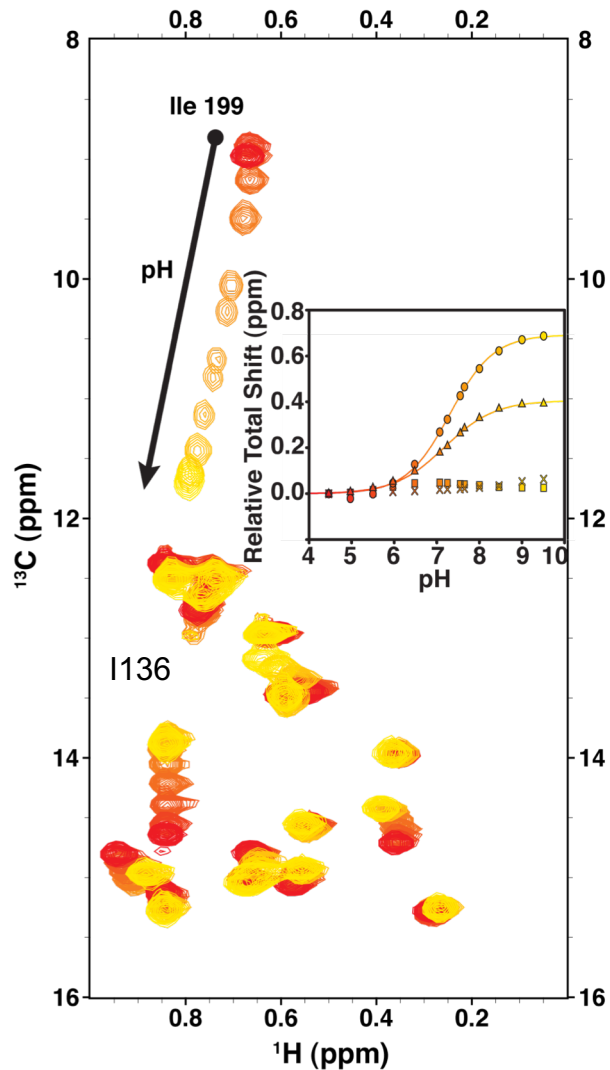
(add alpha-ketoacid precursors to ILV 30 minutes prior to induction)

^{13}C HSQC of ILV labeled protein



Measuring pKa by NMR

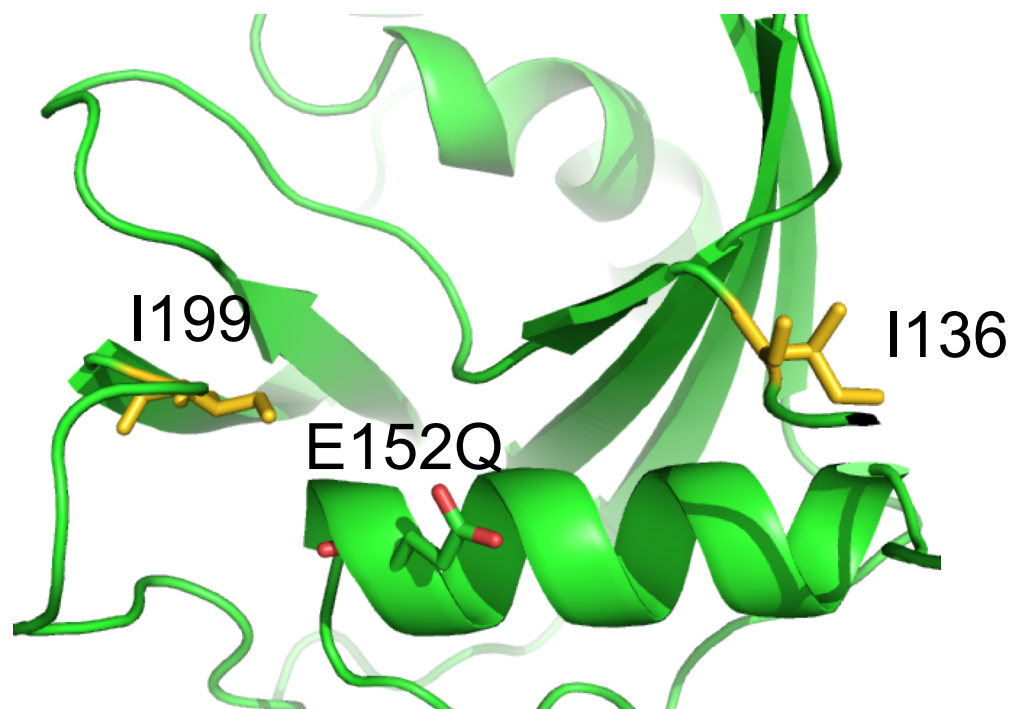
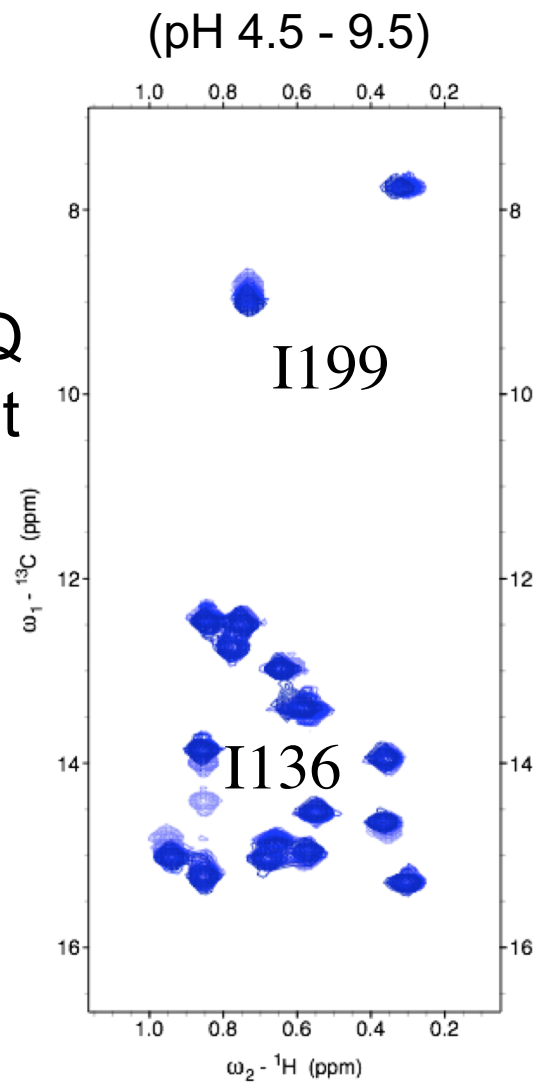
(pH 4.5 - 9.5)



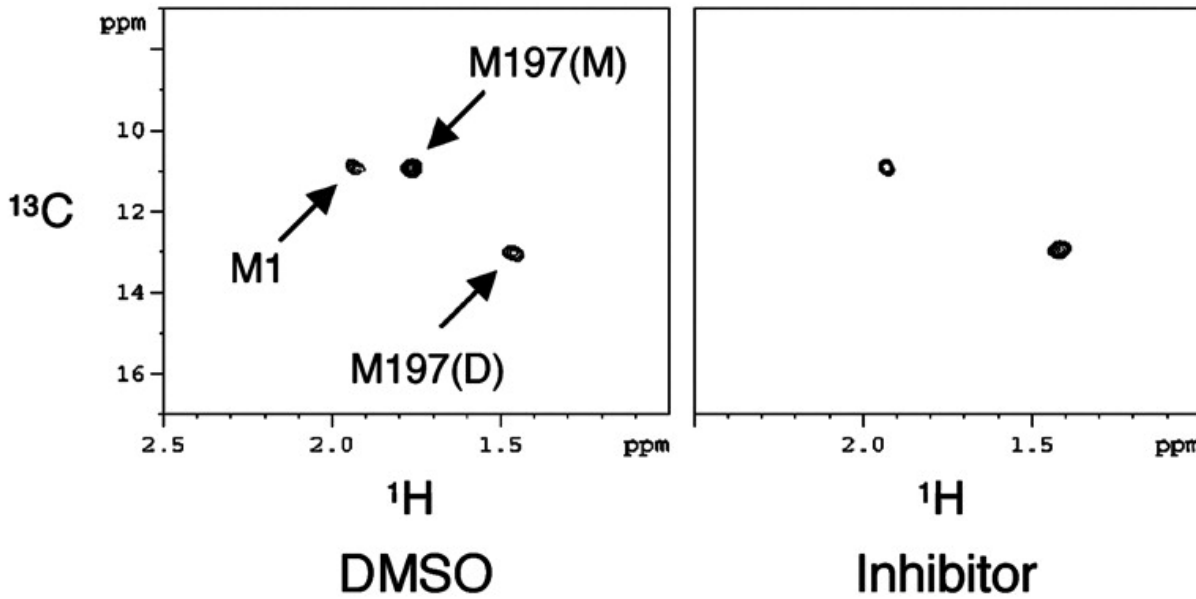
pKa of 7.2, elevated for Glu

Identification of titratable residue by site-directed mutagenesis and NMR

E152Q
mutant



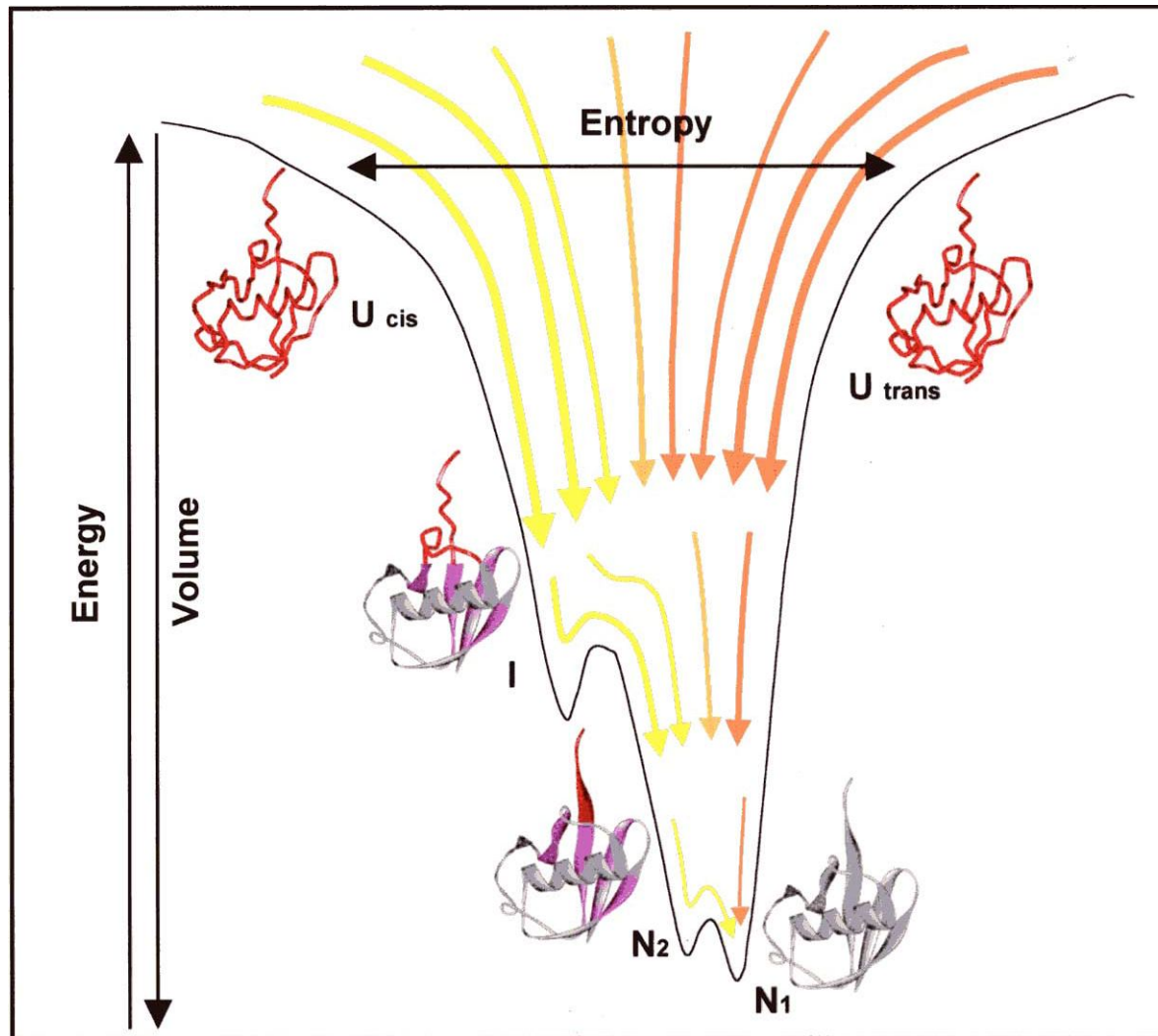
Example of slow exchange: monomer-dimer equilibrium



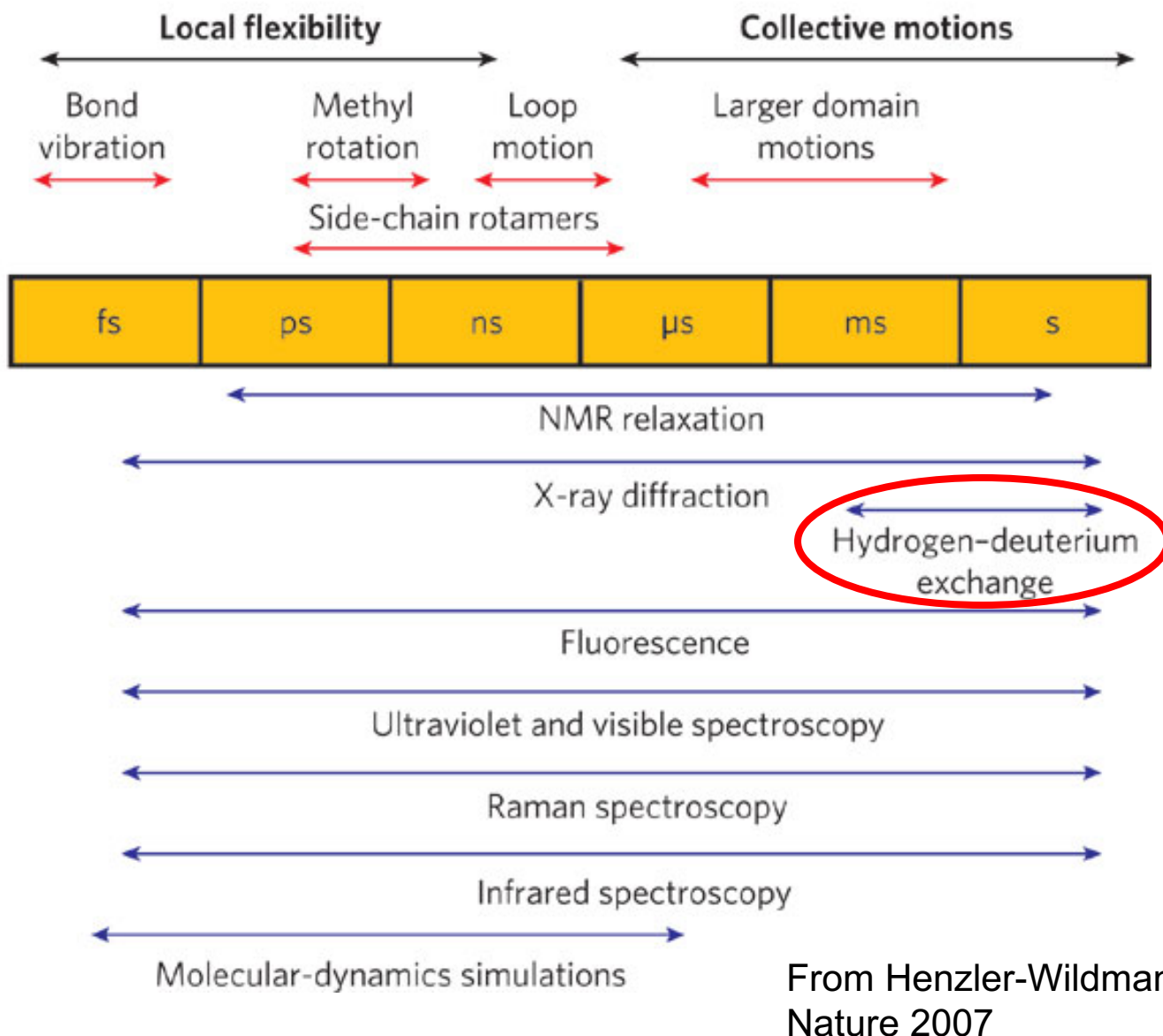
Inhibition of KSHV Pr
stabilizes
the dimeric conformation

Methionine specific labeling simplifies analysis

Part III: Dynamics by NMR

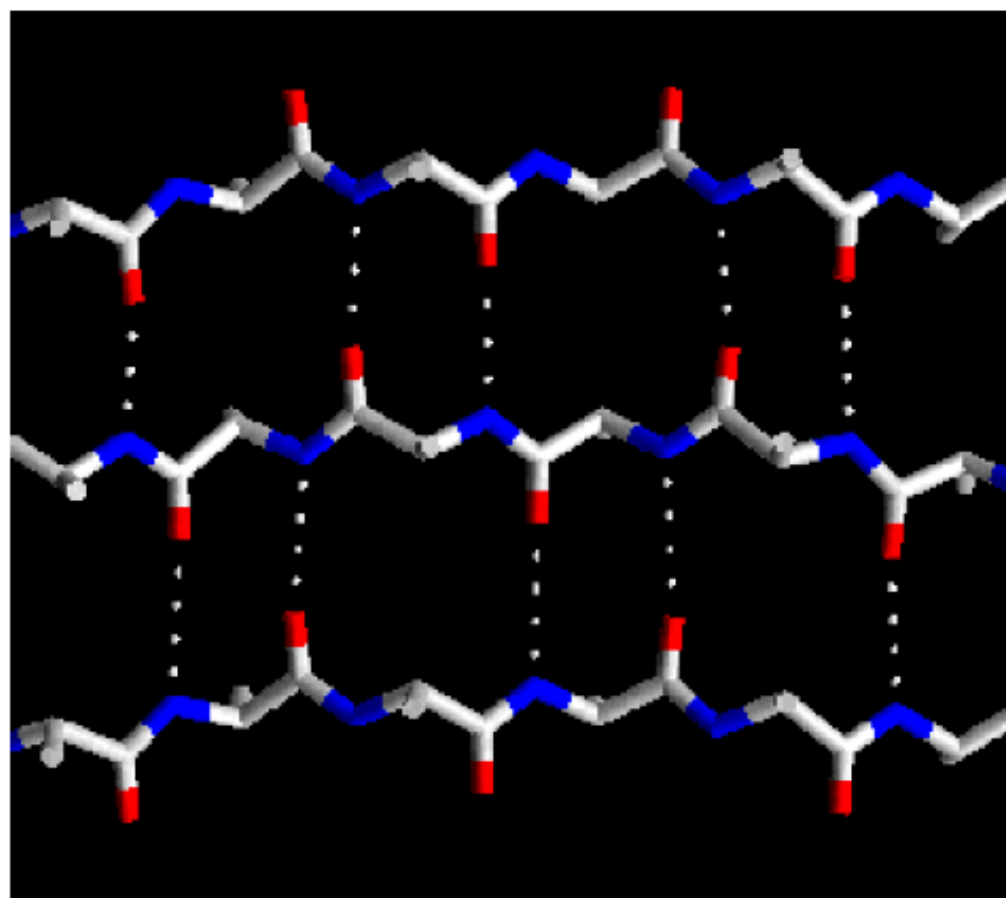
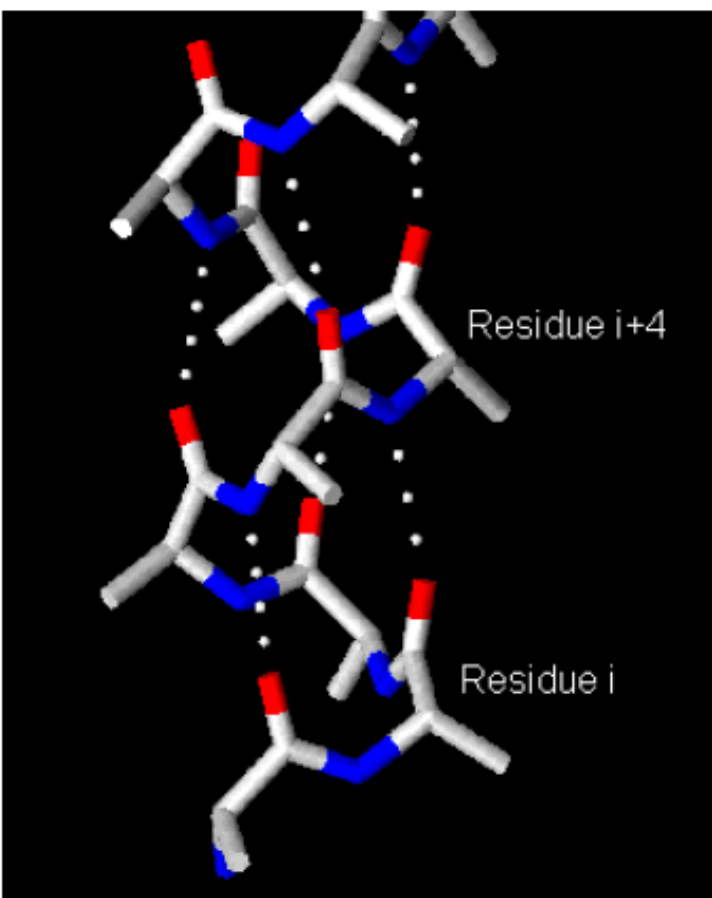


Timescales of Protein Dynamics

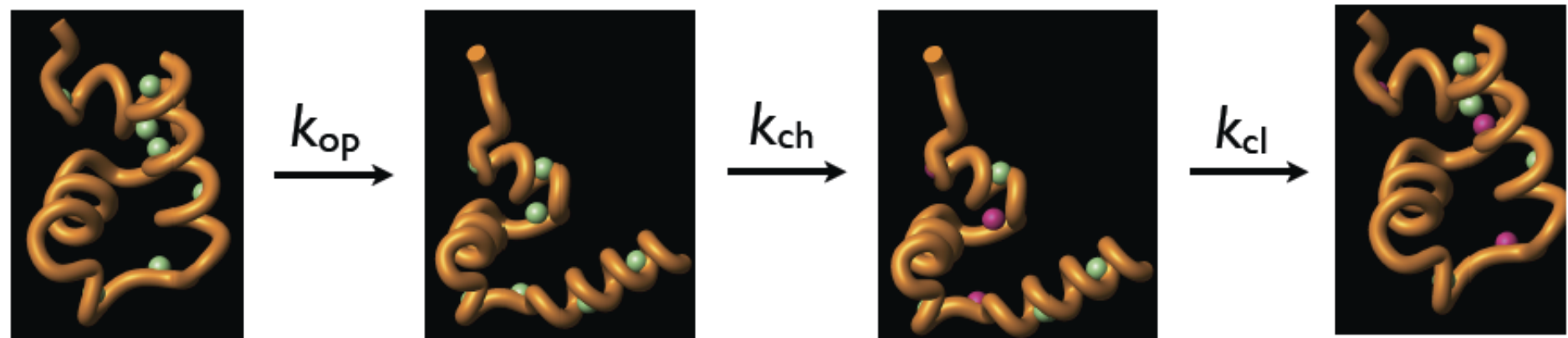


H/D exchange for measuring stability of H-bonds

Long lasting hydrogen bonds in proteins are typically part of secondary structure



Exchange of protons in the open conformation



EX1: $k_{ci} \ll k_{ch}$

$$k_{obs} = k_{op}$$

EX2: $k_{ci} \gg k_{ch}$

$$k_{obs} = k_{op} k_{ch} / (k_{ci}) = K_{op} k_{ch}$$

K_{op} is referred to as the protection factor, P

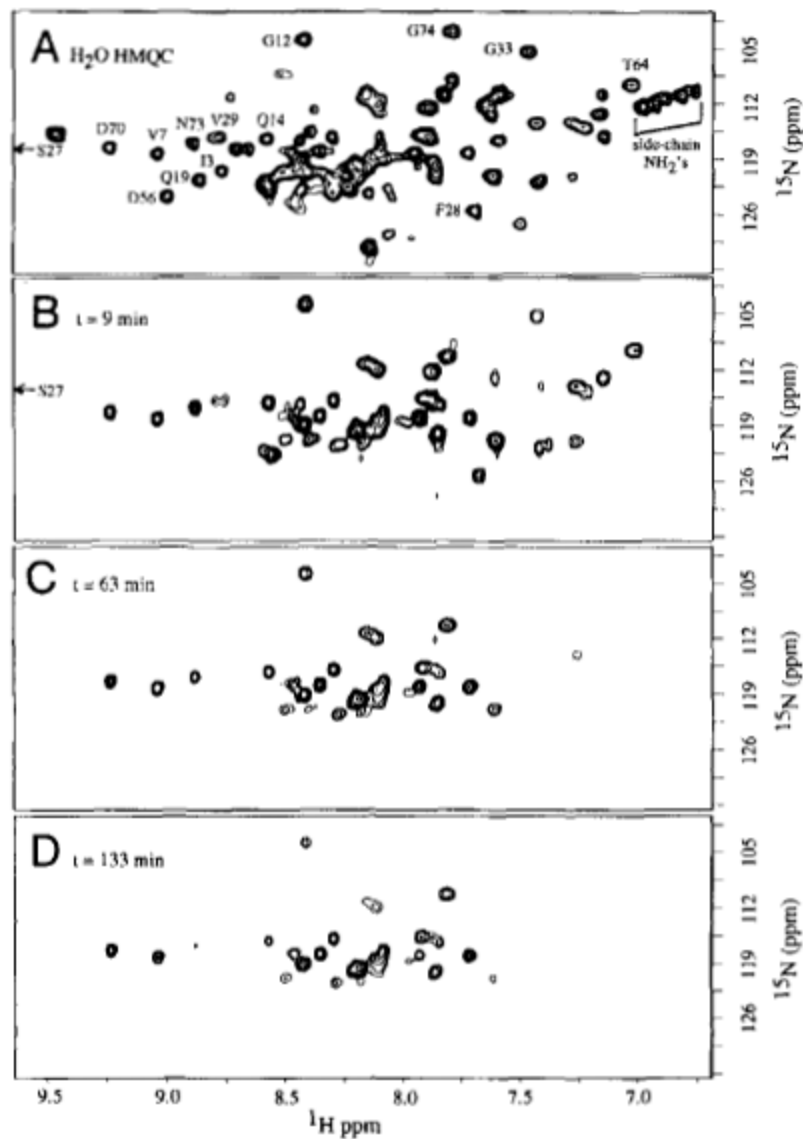
$$\Delta G_{op} = -RT \ln K_{op}$$

NMR Analysis of Protein Dynamics

Hydrogen-Deuterium Exchange

- As we saw before, slow exchanging NHs allowed us to identify NHs involved in hydrogen-bonds.
- Similarly, slow exchanging NHs are protected from the solvent and imply low dynamic regions.
- Fast exchanging NHs are accessible to the solvent and imply dynamic residues, especially if not solvent exposed.

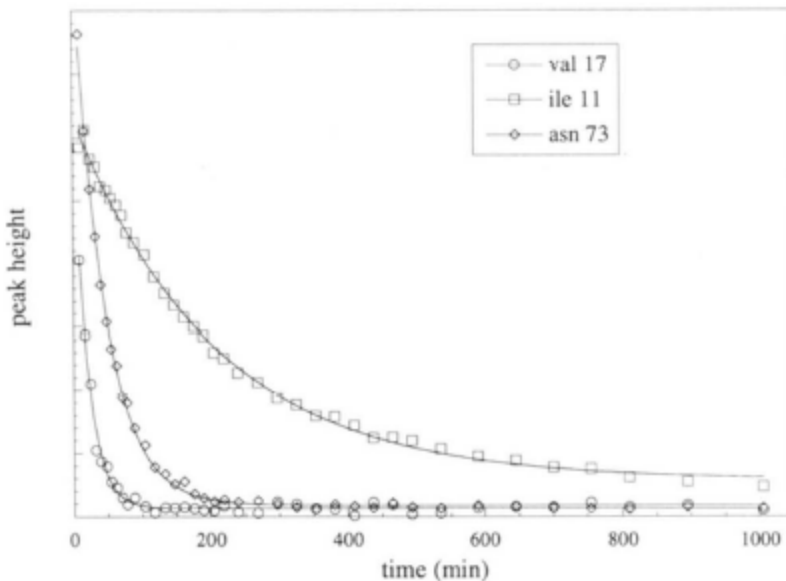
Protein sample is exchanged into D₂O and the disappearance of NHs peaks in a 2D ¹H-¹⁵NH spectra is monitored.



NMR Analysis of Protein Dynamics

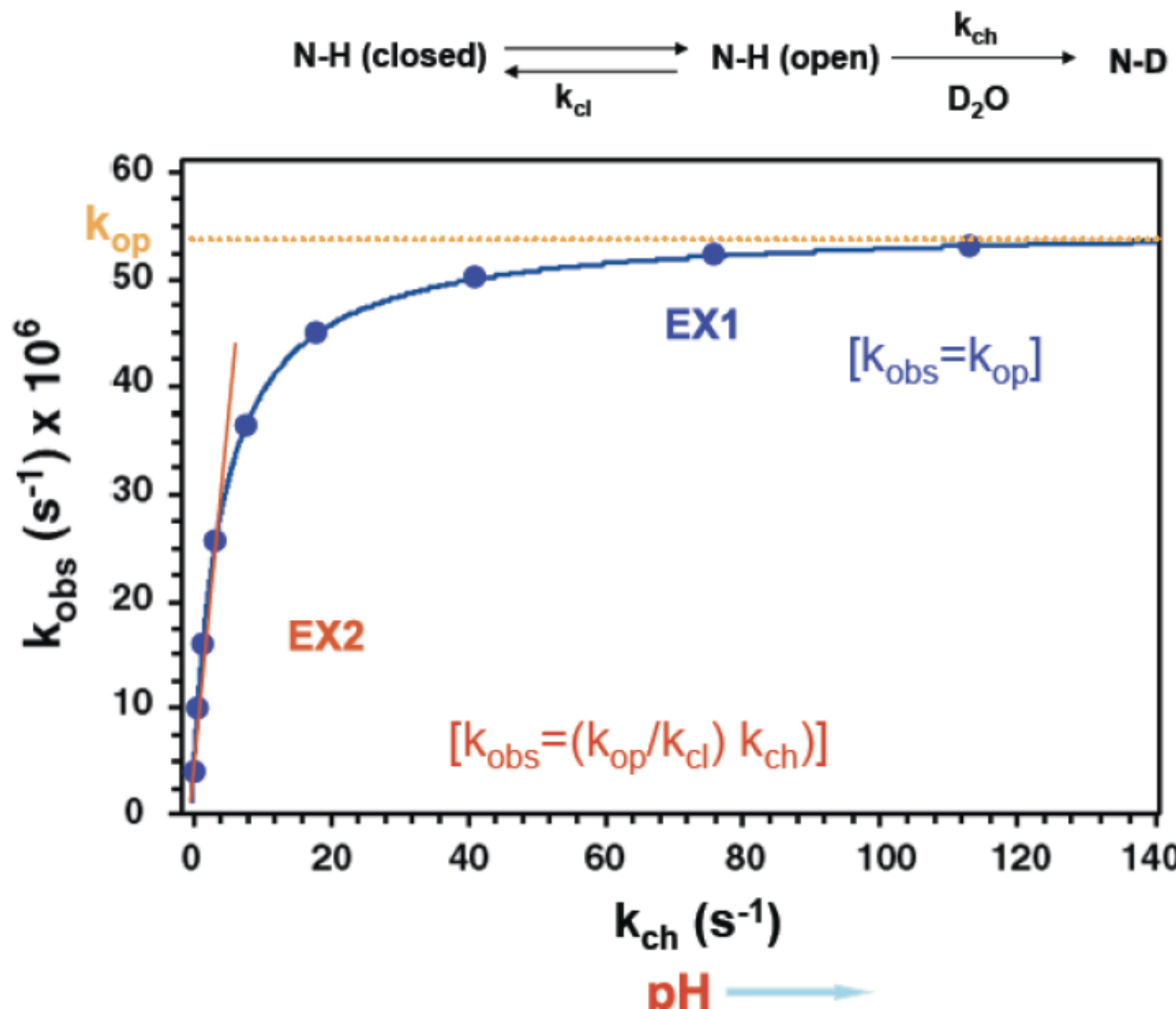
Hydrogen-Deuterium Exchange

- The observed NH intensity loss can be fit to a simple exponential to measure an exchange rate (k_{ex})
- These exchange rates may range from minutes to months!
 - NHs with long exchange rates indicate stable or low mobility regions of the protein
 - NHs with short exchange rates indicate regions of high mobility in the protein

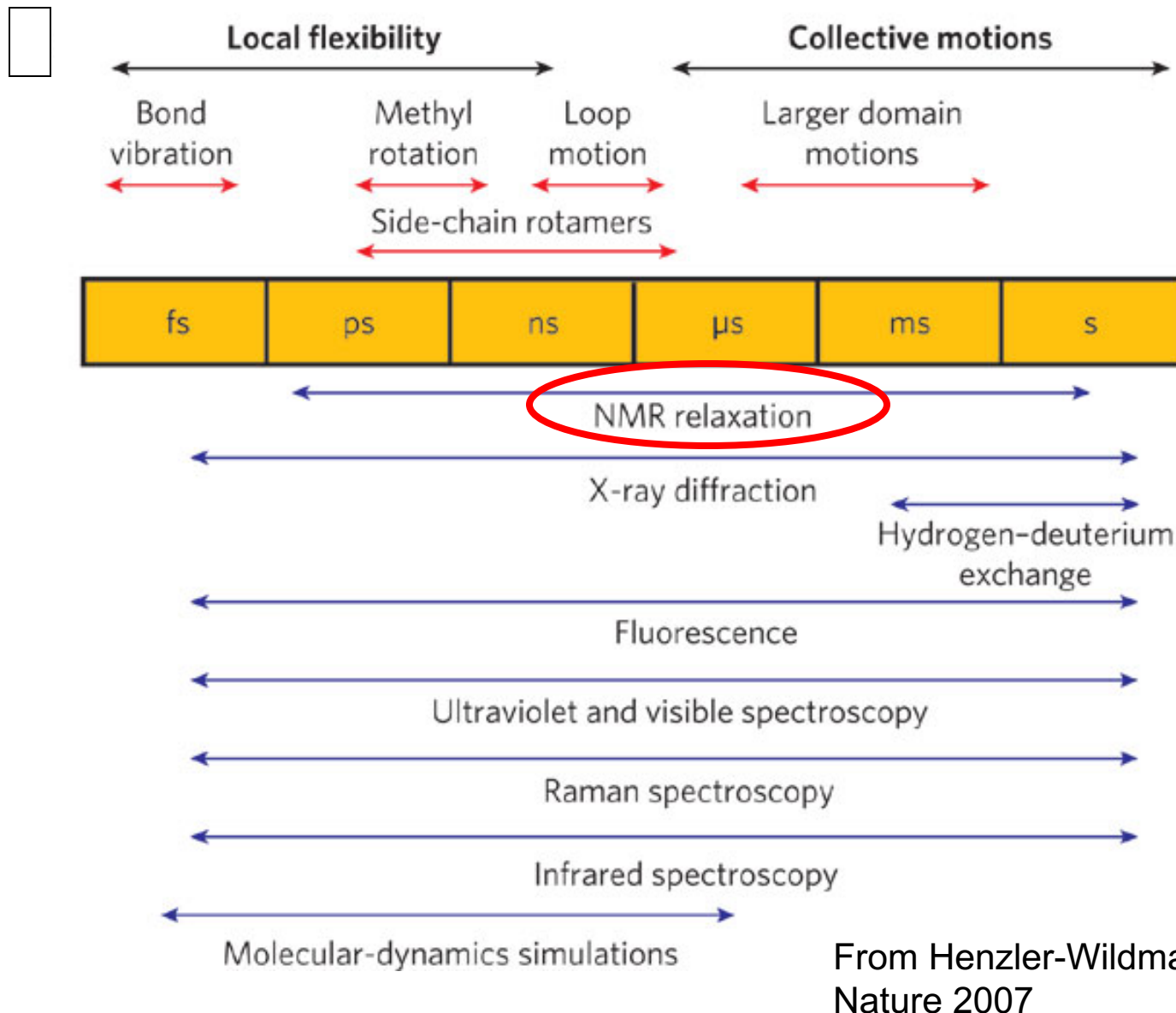


$$I = \alpha e^{-k_{\text{obs}} t}$$

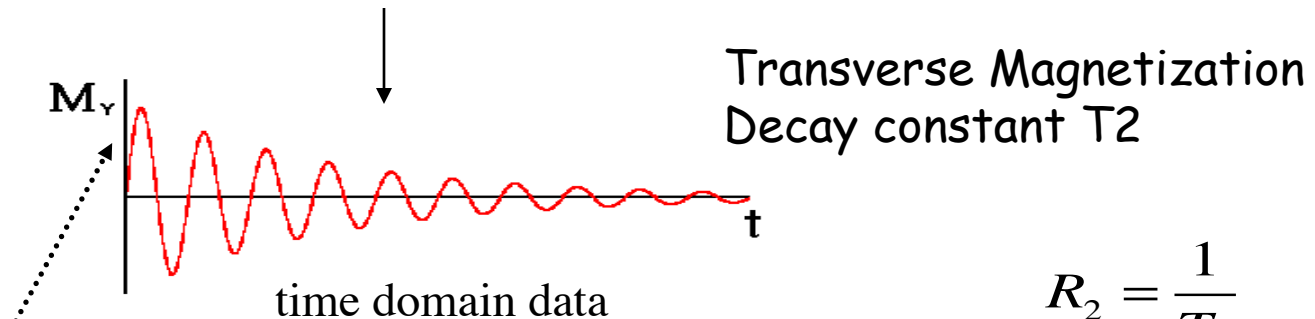
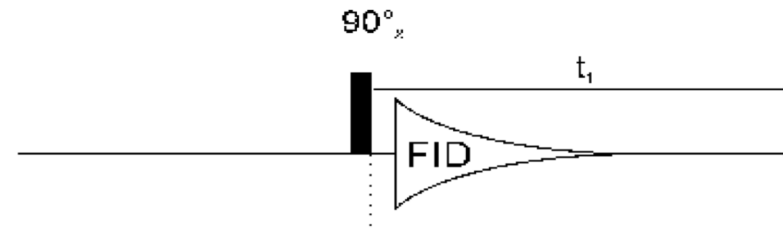
The exchange mechanism depends on pH



Timescales of Protein Dynamics



Summary of 1D Experiment



$$R_2 = \frac{1}{T_2}$$

Amplitude proportional
to amount magnetization
prior to pulse

time domain data

Fourier Transform (FT)

$$<--- FWHM = \frac{R_2}{\pi}$$

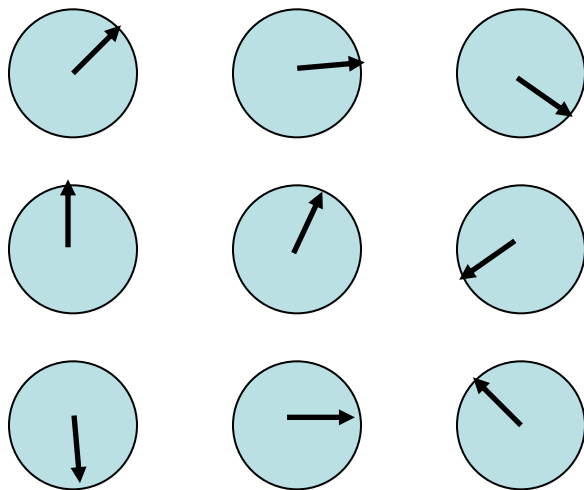
Position of resonance --->
local magnetic environment

frequency domain data

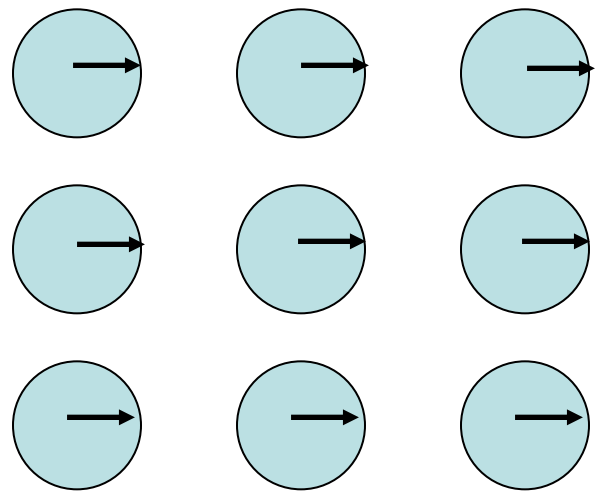
ω

R_2 is a Measure of Dephasing

Ensemble of Nuclear Spins



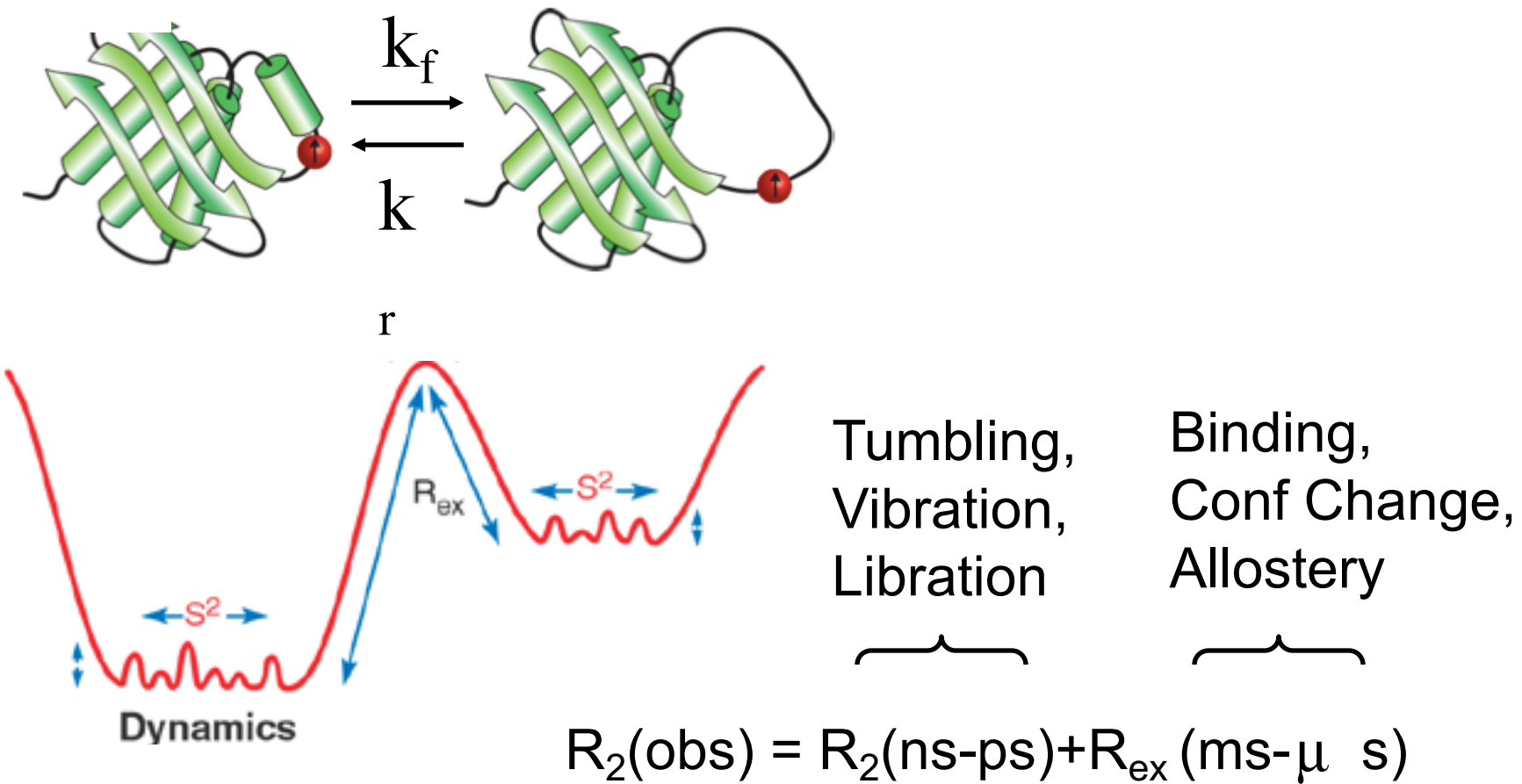
Resonant RF Field
↔
Dephasing



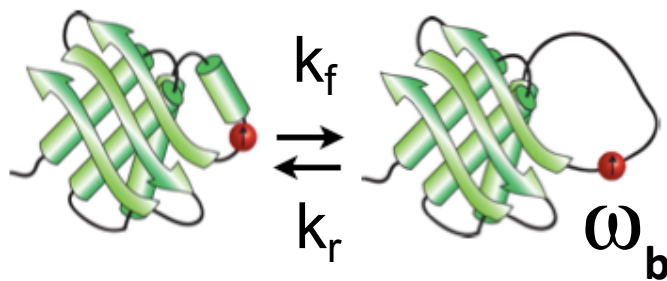
Random Phase
No NMR Signal

Phase Synchronization
NMR Signal!

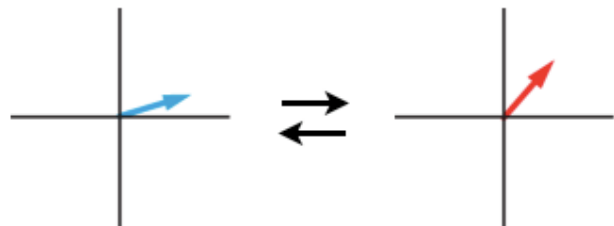
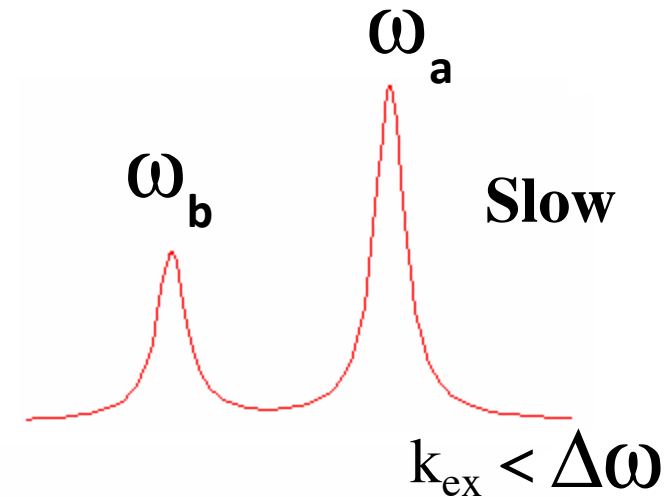
Contributions to R_2 from Conformational Dynamics on the Chemical Shift timescale



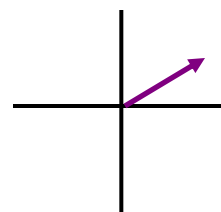
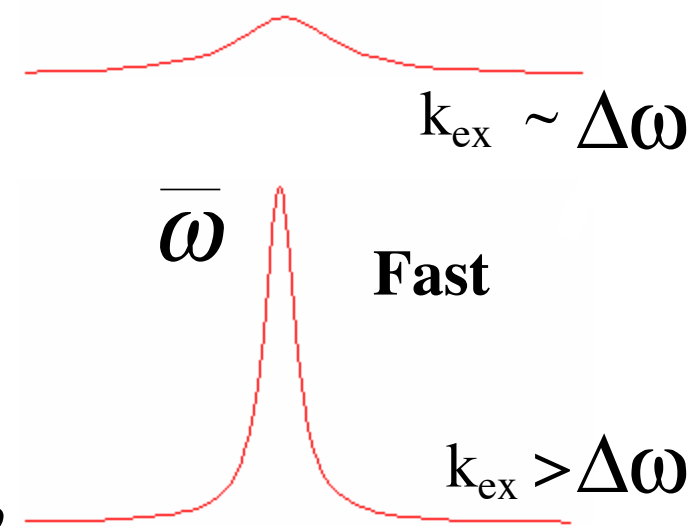
Spectral Manifestations of Exchange



$$\mathbf{k}_{\text{ex}} = \mathbf{k}_f + \mathbf{k}_r$$
$$\Delta\omega = \omega_a - \omega_b$$



Intermediate



$$\bar{\omega} = p_a \omega_a + p_b \omega_b$$

¹⁵N TYR HSQC
GB1-yDCP2-NB

7 out of 8 resonances
detected

105.0

110.0

115.0

120.0

125.0

130.0

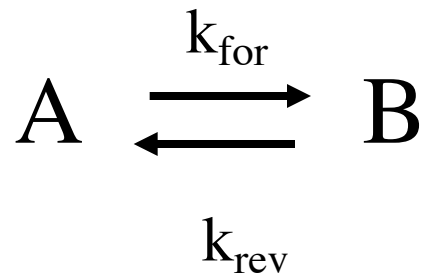
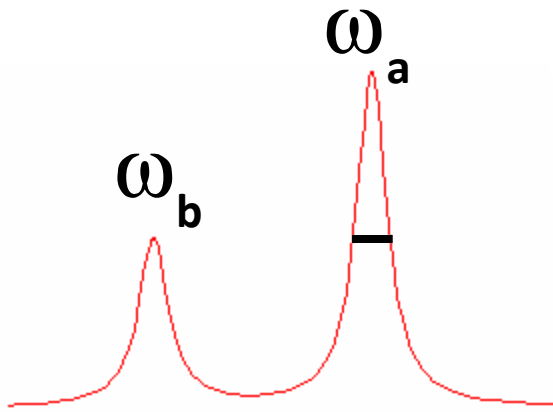
135.0

12.0

10.0

6.0

Expressions for the Linewidth in the Slow Exchange Limit ($k_{ex} < \Delta\omega$)



Populations p_a, p_b

$$R_2^a = R_2^a(ns - ps) + p_b k_{for}$$

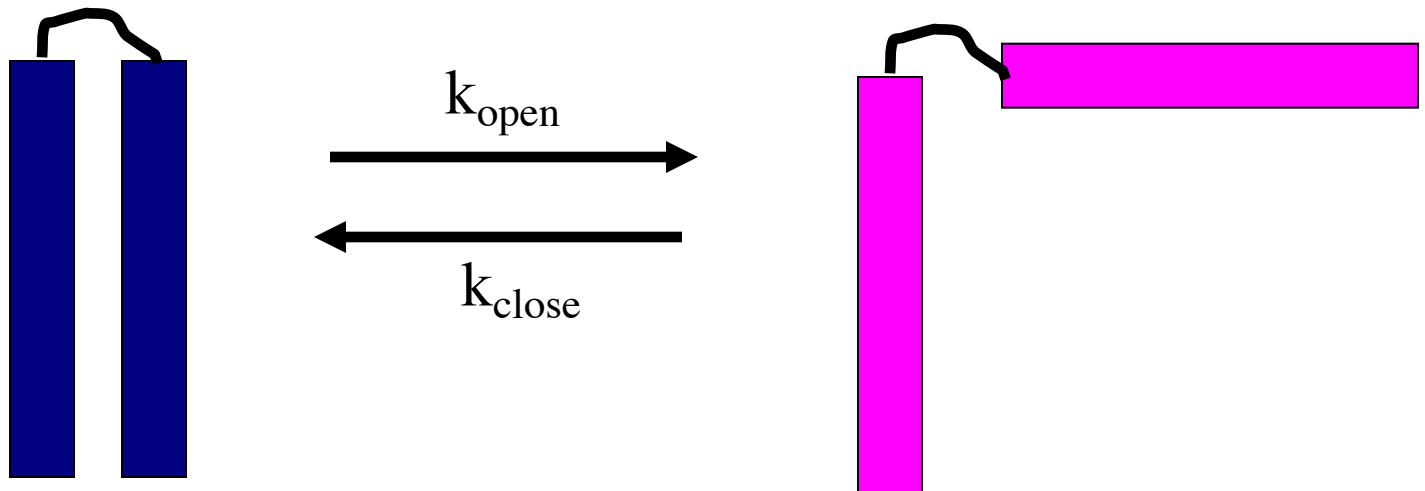
$$k_{ex} = k_{for} + k_{rev}$$

$$R_2^b = R_2^b(ns - ps) + p_a k_{rev}$$

$$\Delta\omega = \omega_a - \omega_b$$

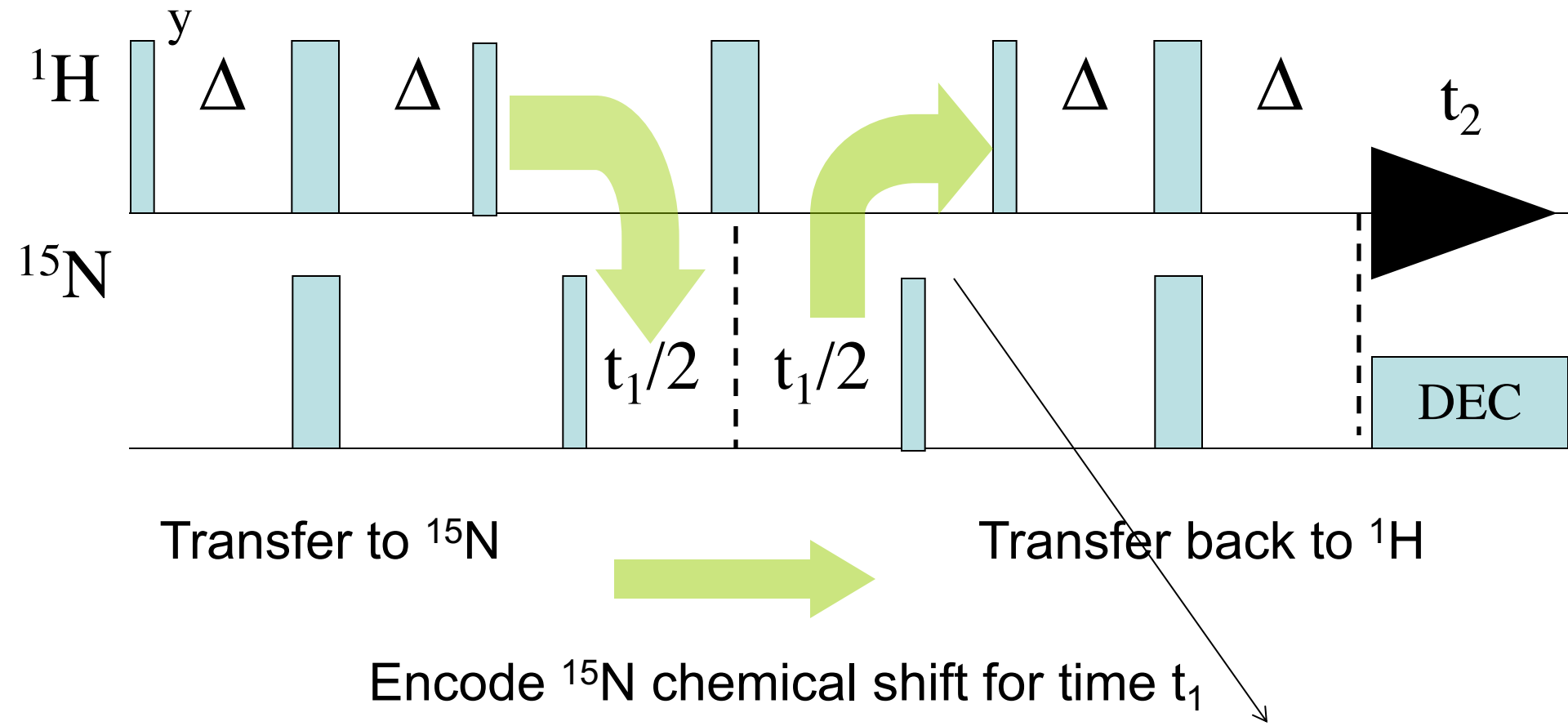
R_{ex}

Slow Exchange Between Two States



$$k_{\text{ex}} = k_{\text{open}} + k_{\text{close}}$$

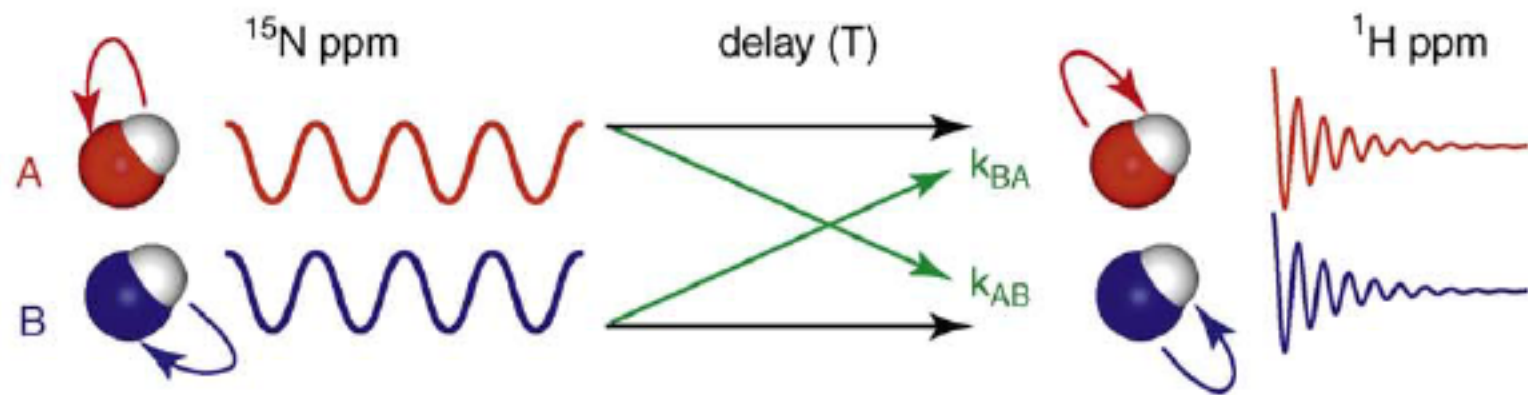
Using HSQC to measure slow exchange



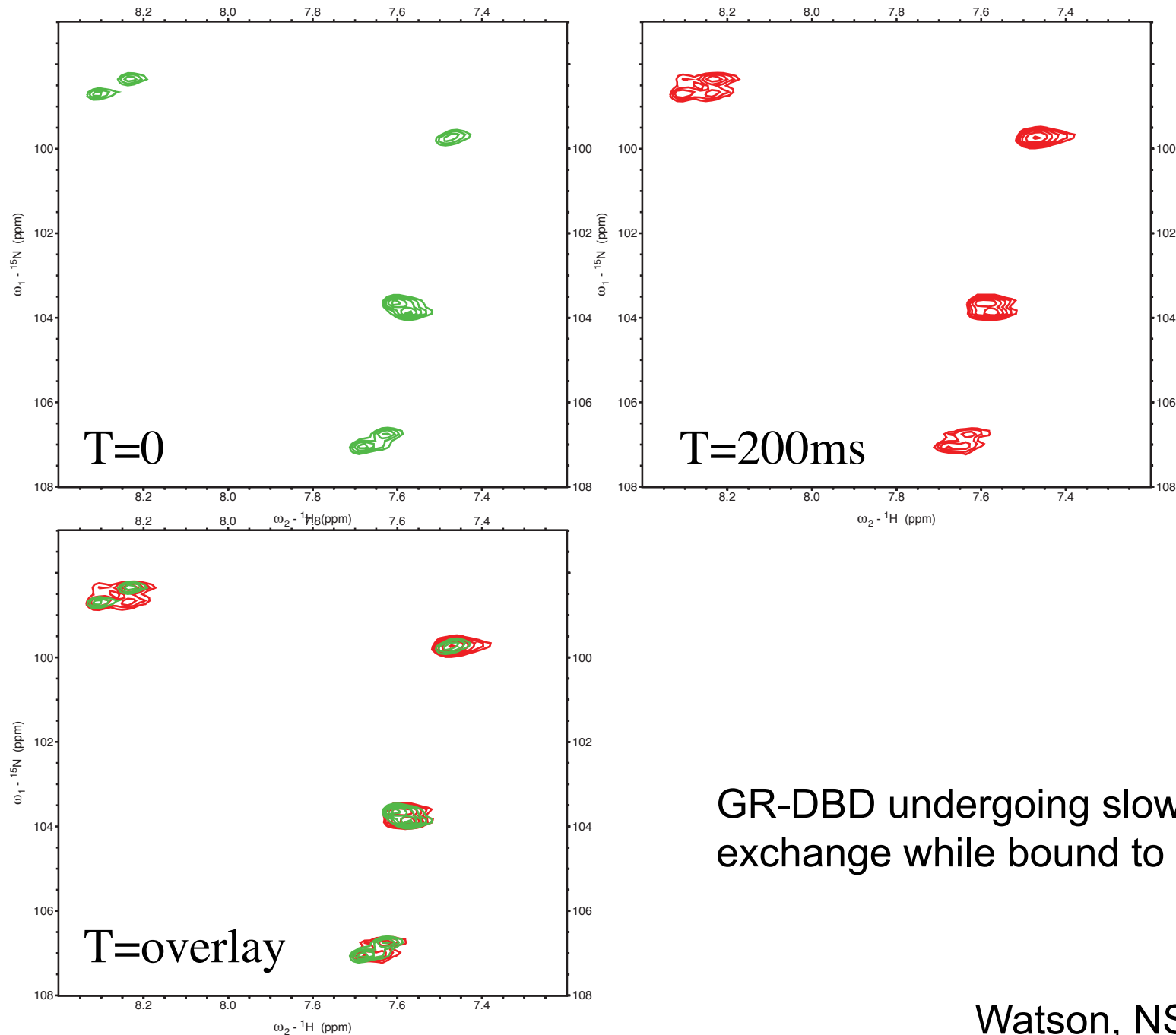
ZZ-exchange, Montelione and Wagner

Insert delay
to allow
exchange

Exchange Cross-Peaks

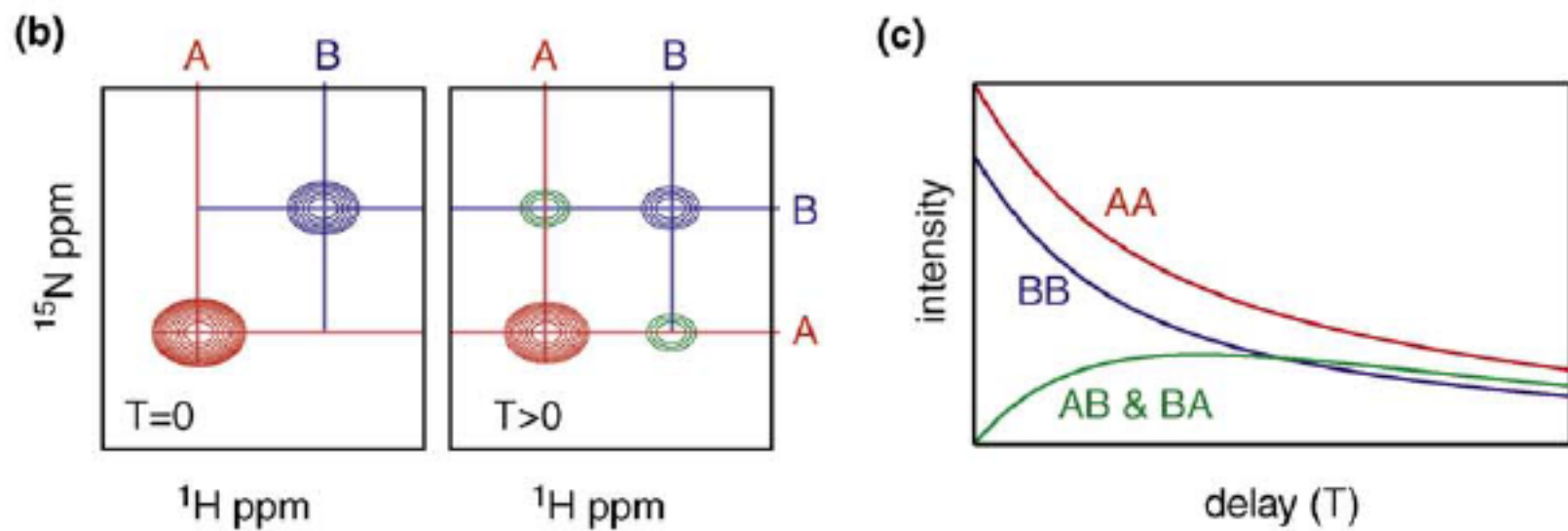


Cross-peaks from a conformational change during delay
e.i.-red to blue



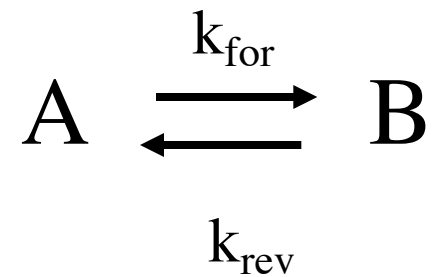
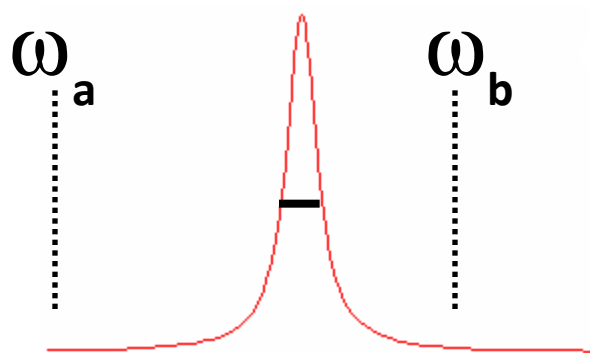
GR-DBD undergoing slow exchange while bound to DNA

ZZ-exchange peak intensity dependence on delay



Fit to obtain populations and rate constants

Expressions for the linewidth in the Fast Exchange Limit ($k_{ex} > \Delta\omega$)



$$\bar{\omega} = p_a \omega_a + p_b \omega_b$$

Populations p_a, p_b

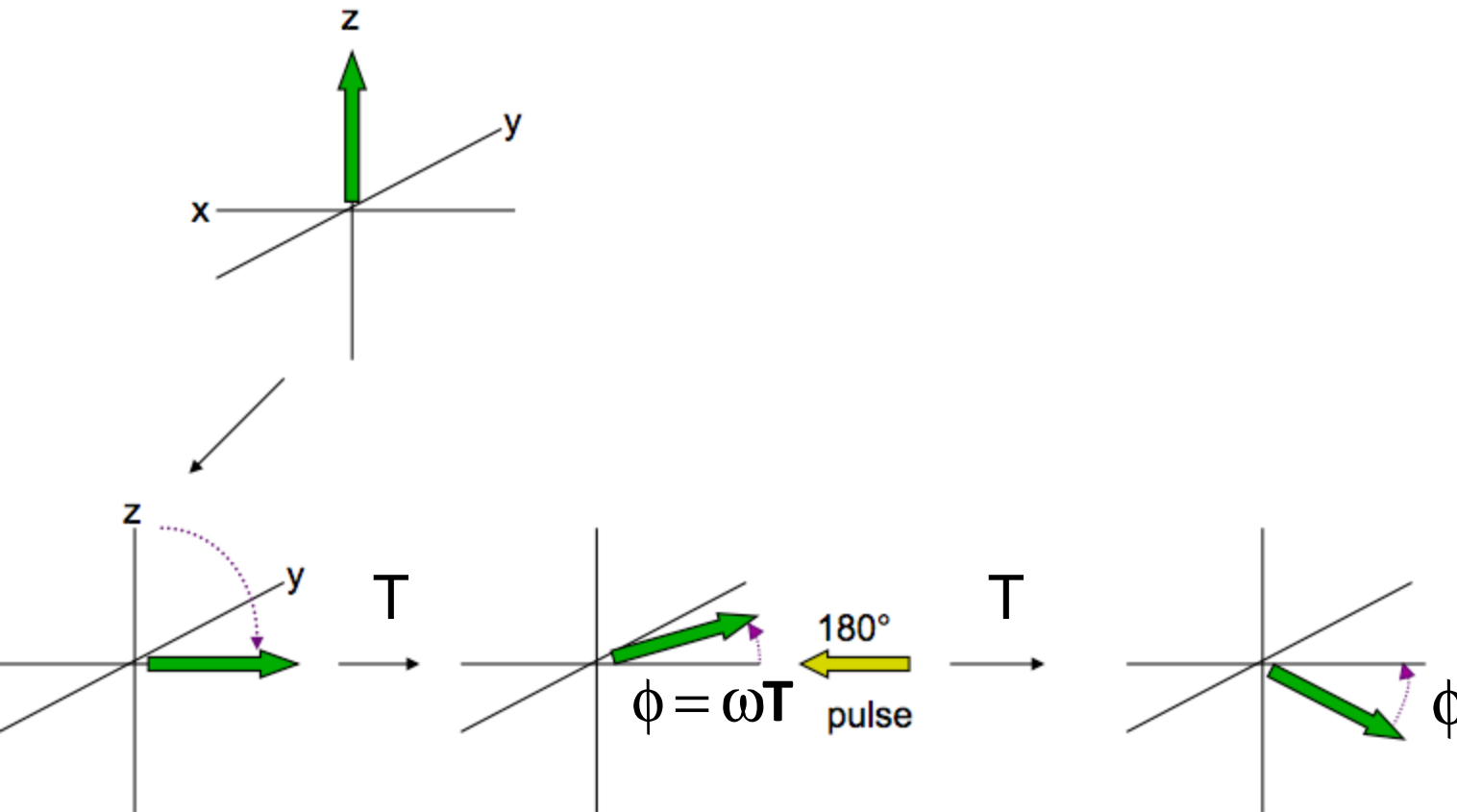
$$k_{ex} = k_{for} + k_{rev}$$

$$R_2 = \bar{R}_2 (ns - ps) + \left. \frac{p_a p_b \Delta\omega^2}{k_{ex}} \right\} R_{ex}$$

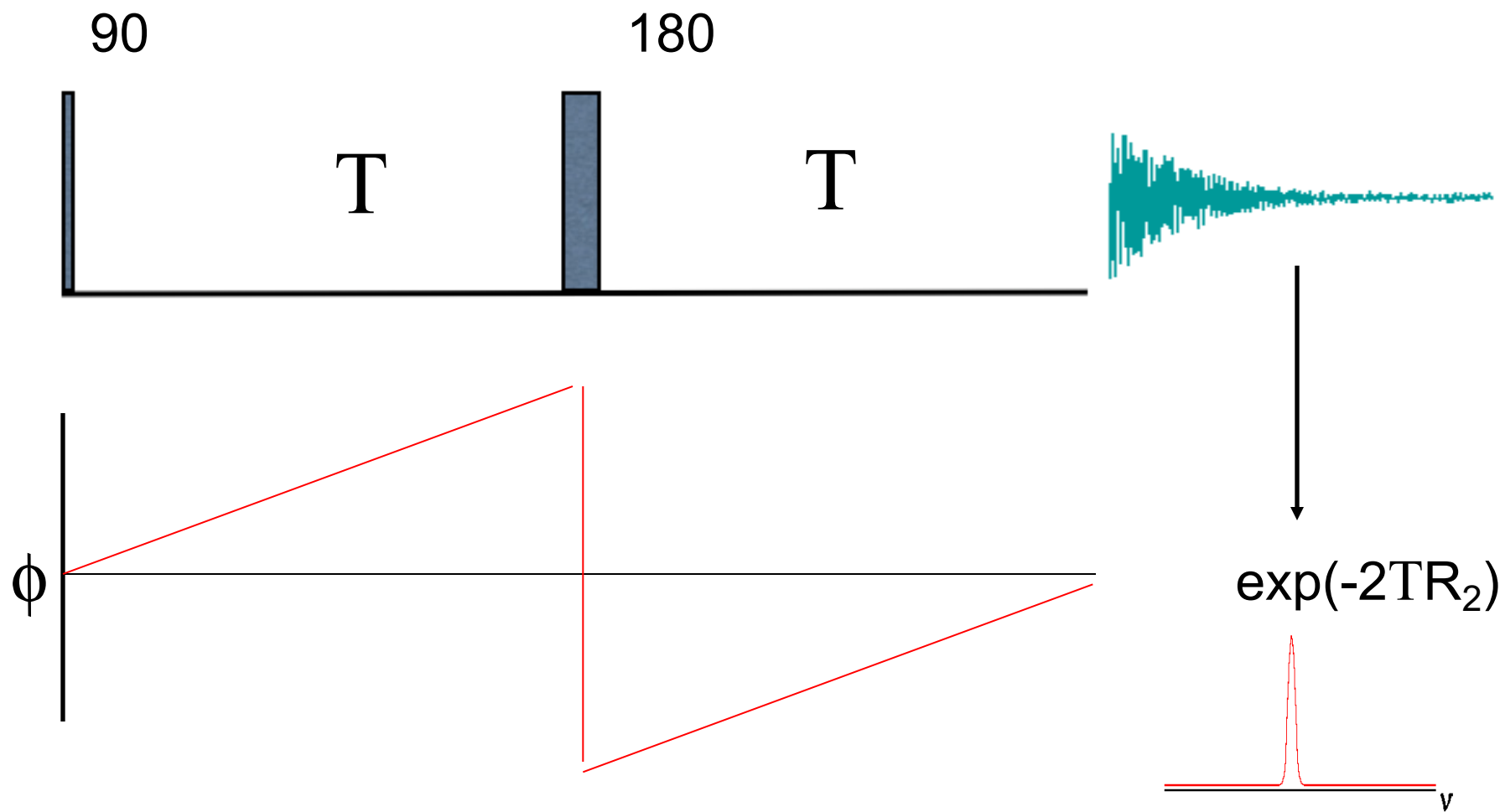
$$\Delta\omega = \omega_a - \omega_b$$

Spin Echo

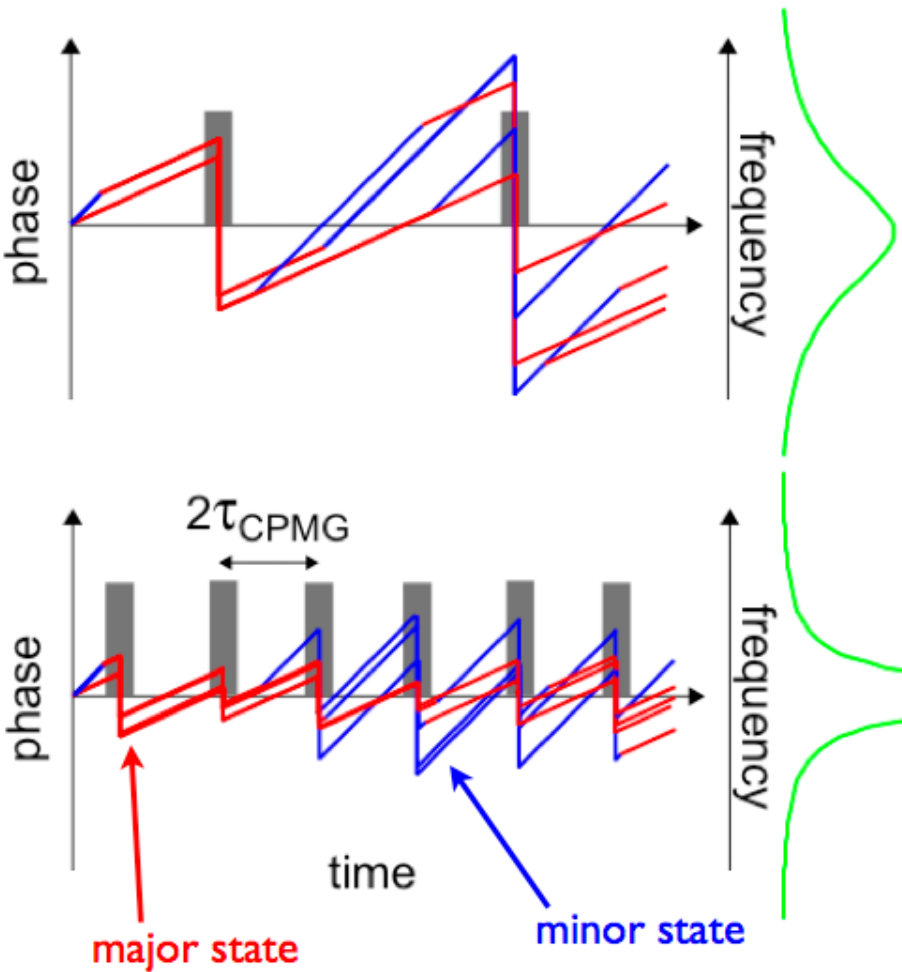
to measure ms-usec dynamics



Spin Echo to Measure R₂



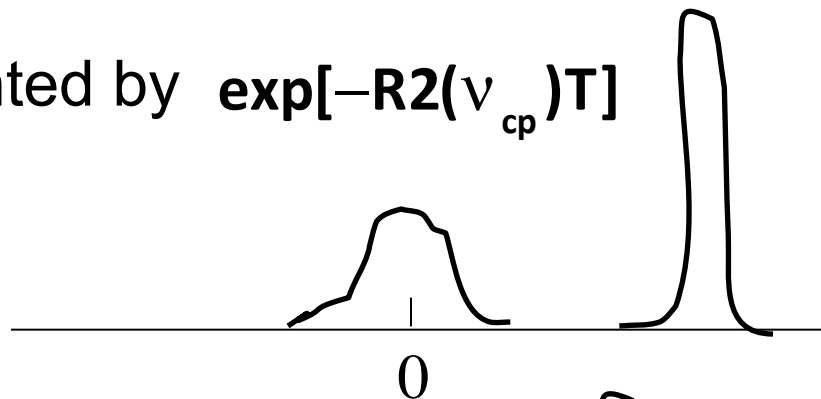
cpmg experiment



- red and blue lines = phased evolution of spins
- gray = RF pulses
 - refocus magnetization and quench effect of exchange
- R_{ex} proportional to linewidth (green)
- no exchange = perfect refocusing

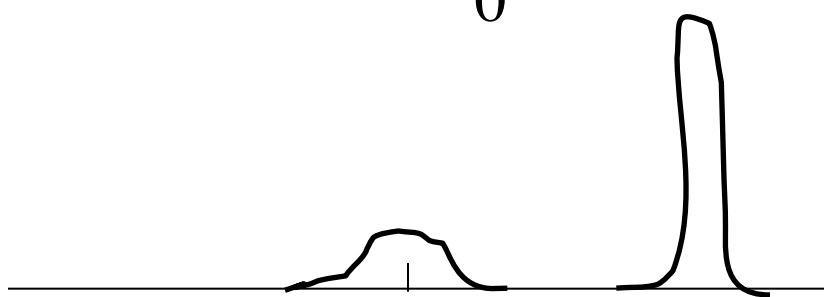
CPMG Protocol

Intensity weighted by $\exp[-R2(v_{cp})T]$

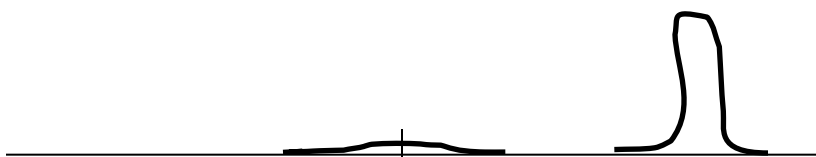


$$v_{cp} = \frac{1}{2\tau_{cp}}$$

$$v_{cp} = 1000 \text{Hz}$$

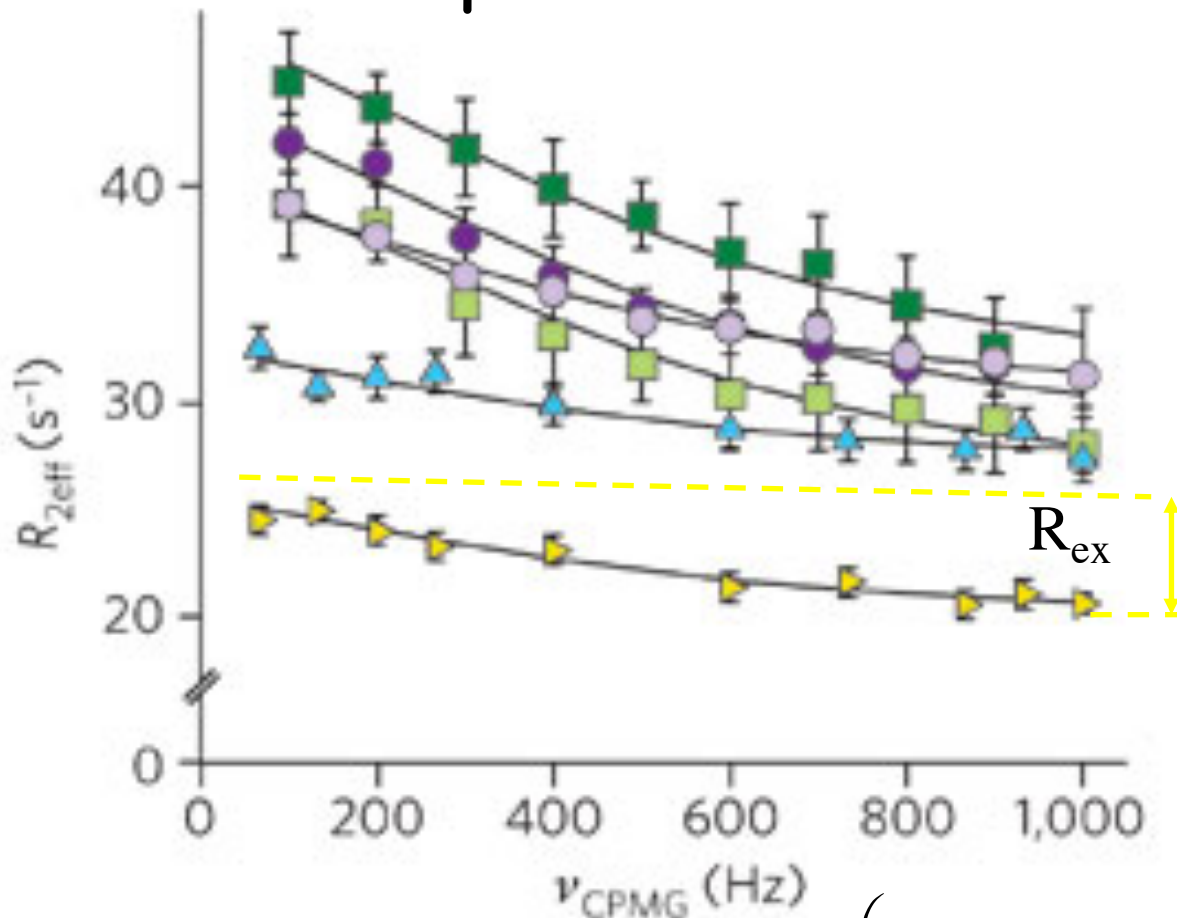


$$v_{cp} = 500 \text{Hz}$$



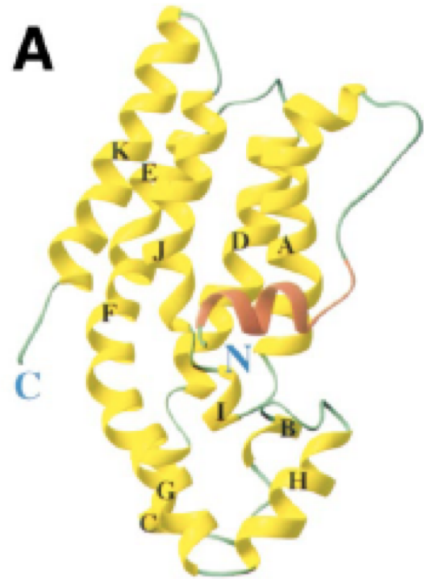
$$v_{cp} = 50 \text{Hz}$$

Dynamics Constants from Relaxation Dispersion Curves

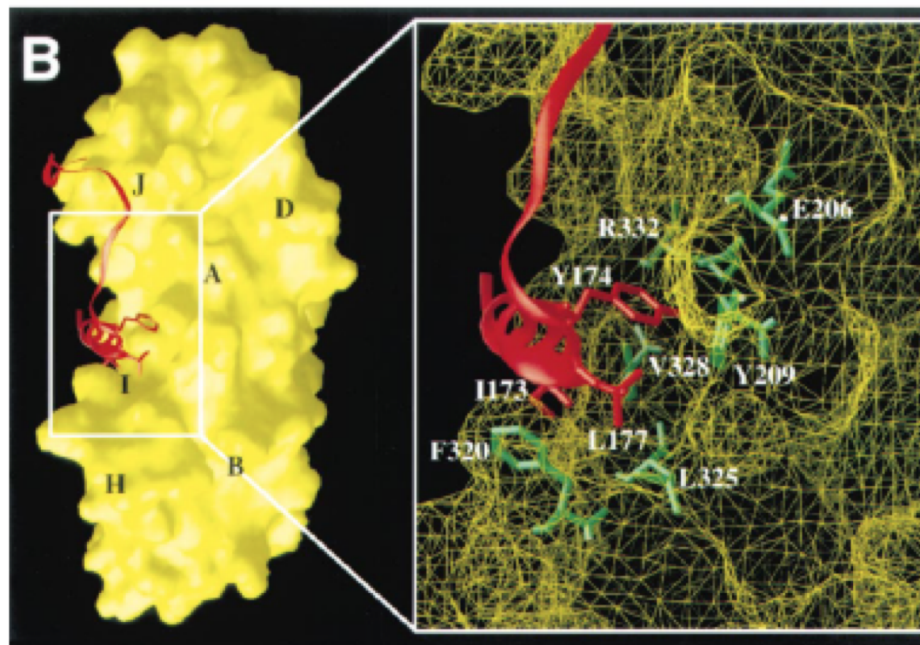


$$R_2^{\text{eff}}(\nu_{\text{CPMG}}) = R_2^a(\text{ns-ps}) + p_a p_b \frac{\Delta\omega^2}{k_{\text{ex}}} \left(1 - \frac{4\nu_{\text{CPMG}}}{k_{\text{ex}}} \tanh \frac{k_{\text{ex}}}{4\nu_{\text{CPMG}}} \right)$$

Regulation of Vav1 activity by autoinhibition



How is this GEF activated?



Example from literature

Internal dynamics control activation and activity of the autoinhibited Vav DH domain

Pilong Li^{1,3}, Ilídio R S Martins^{1–3}, Gaya K Amarasinghe^{1,3,4} & Michael K Rosen¹

Nature Structural and Molecular Biology, 15:6 (2008)

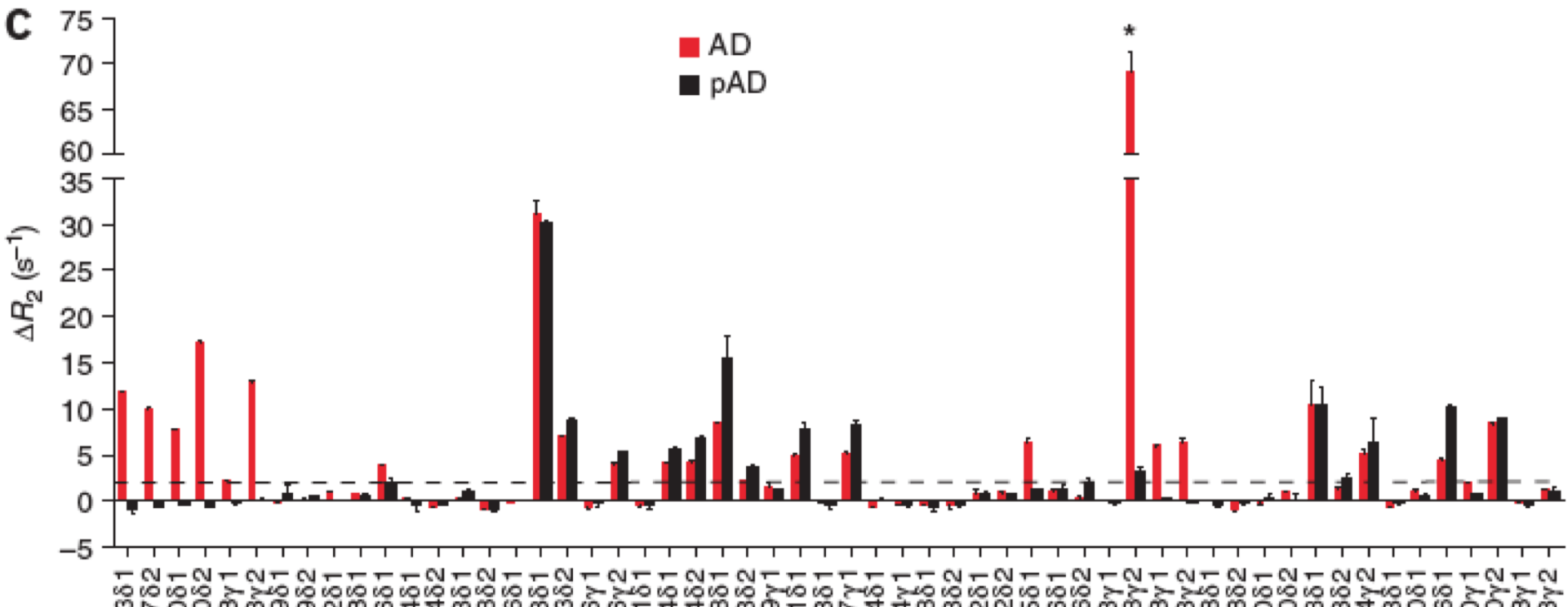
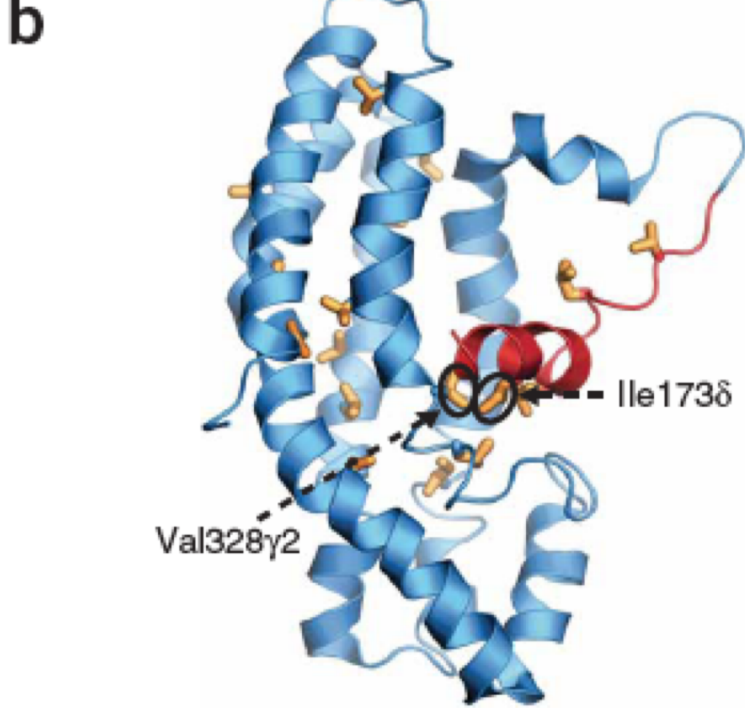
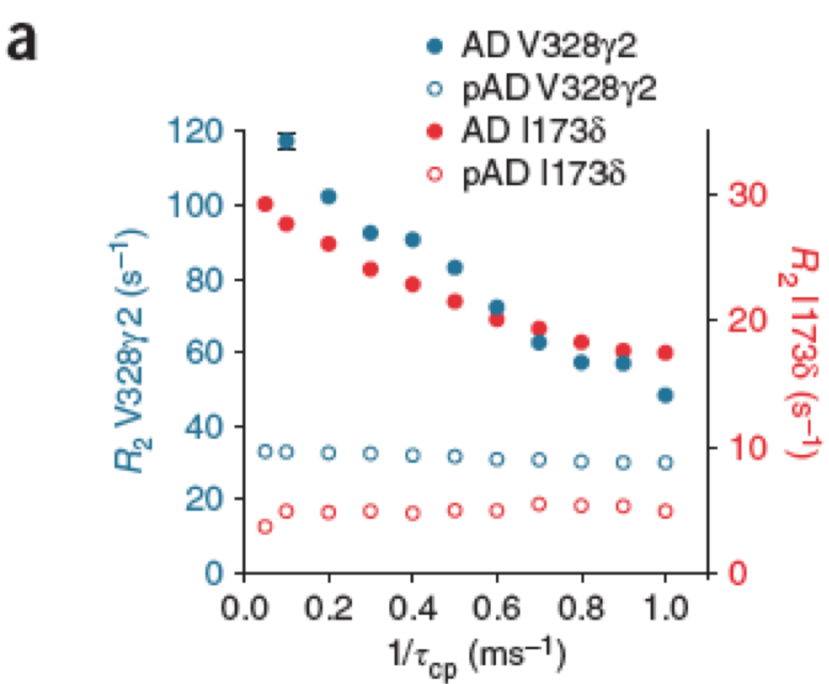
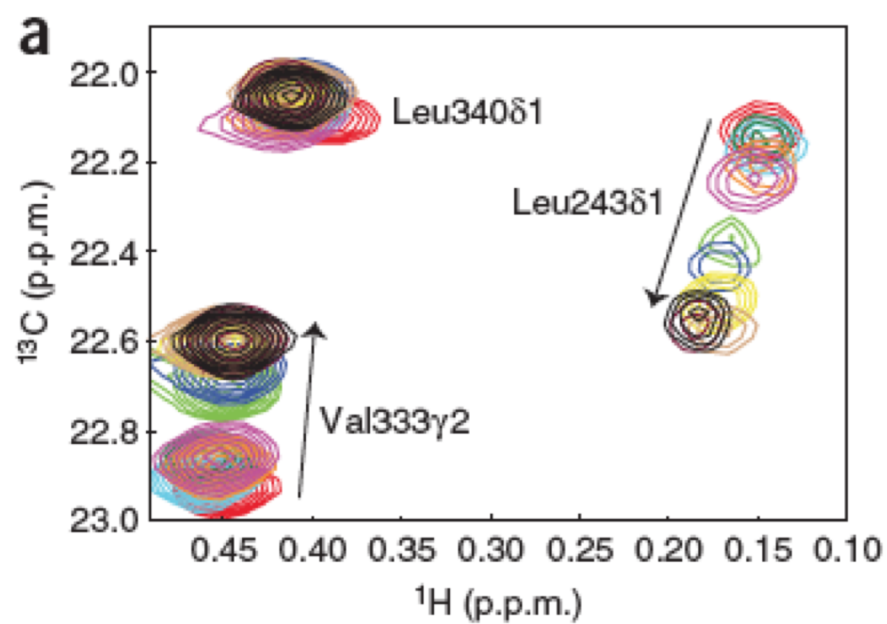


Figure 2



b

Protein	p_O
pWT	~ 1
K208E	1.00 ± 0.06
Y174F	0.99 ± 0.03
K208S	0.86 ± 0.06
K208A	0.77 ± 0.12
E169K K208A	0.64 ± 0.06
K208V	0.26 ± 0.10
E169K K208V	0.14 ± 0.08
Wild type	0.09 ± 0.03
E169K	0.05 ± 0.06
E169K E207K	~ 0

Figure 3

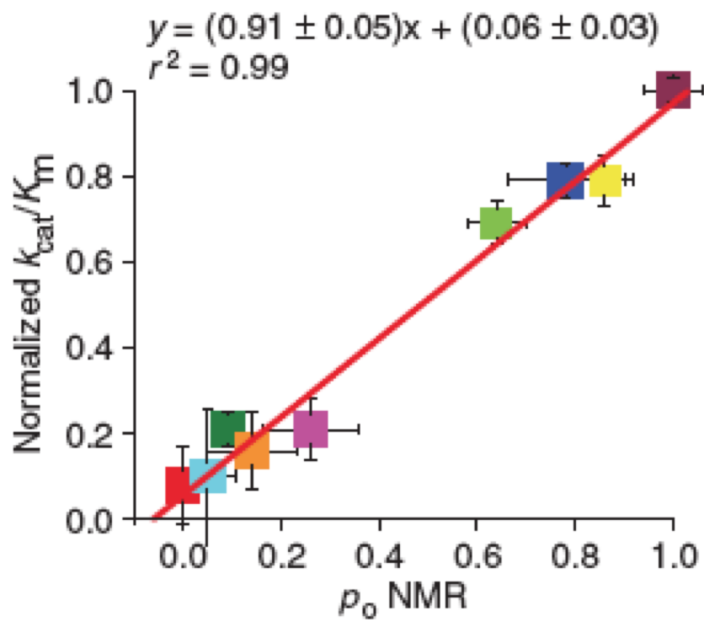
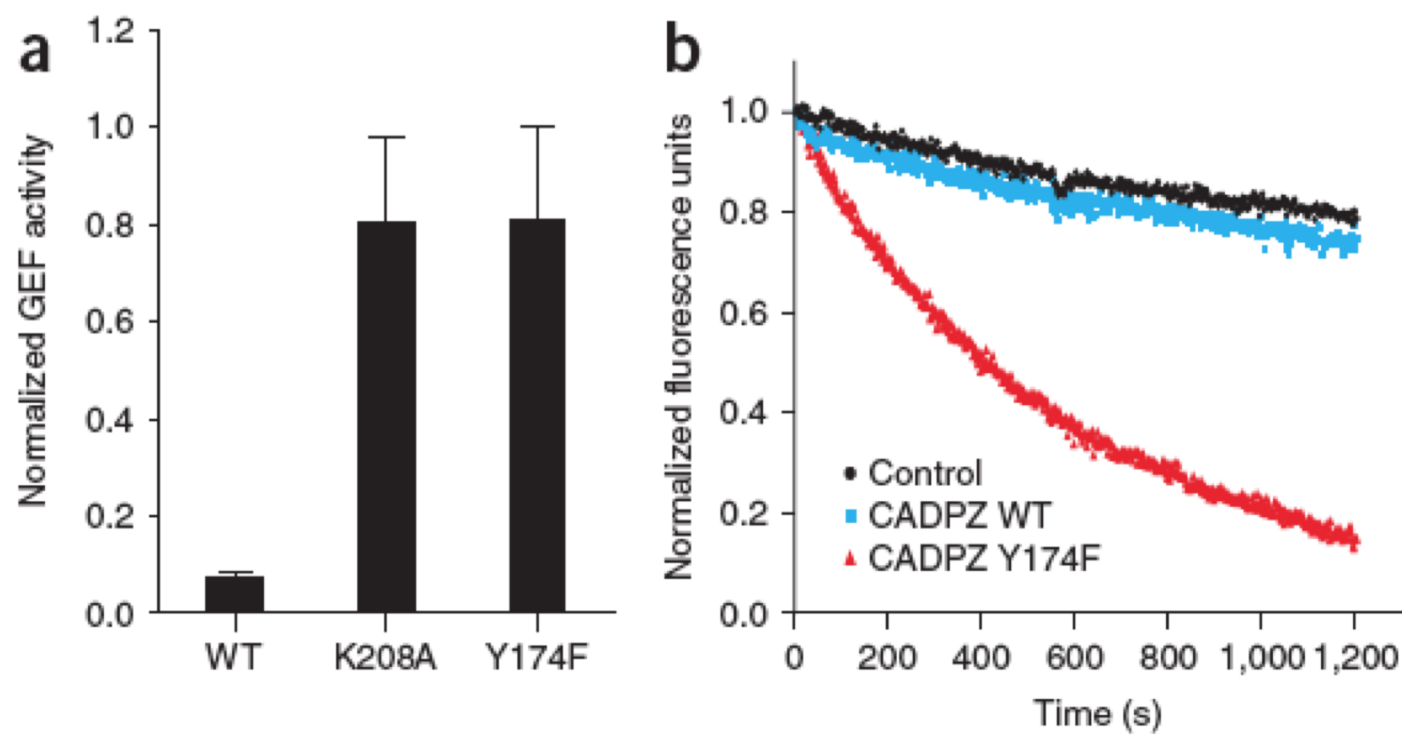
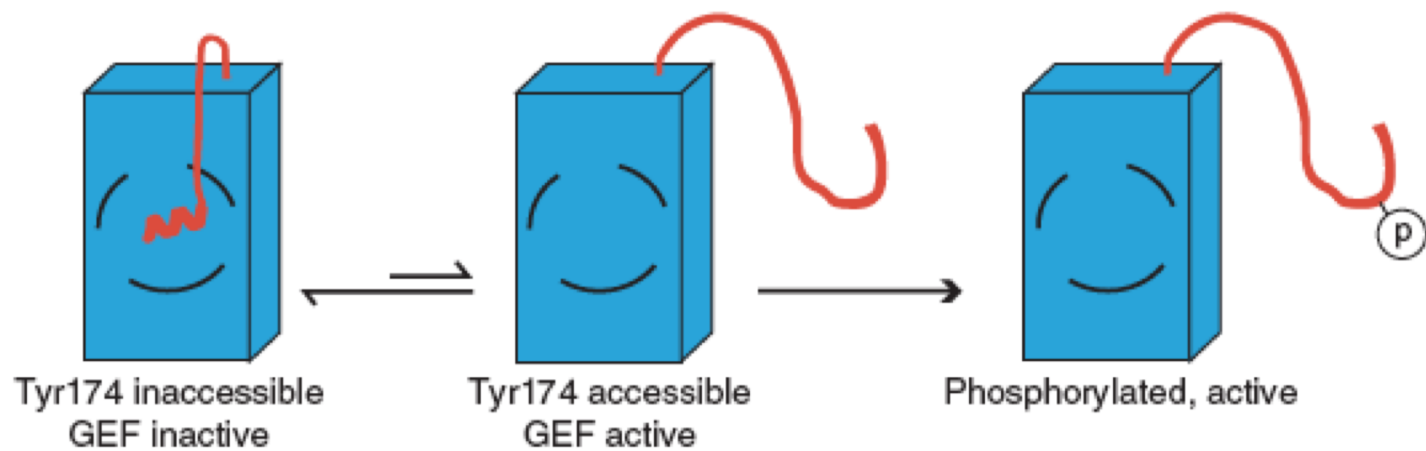


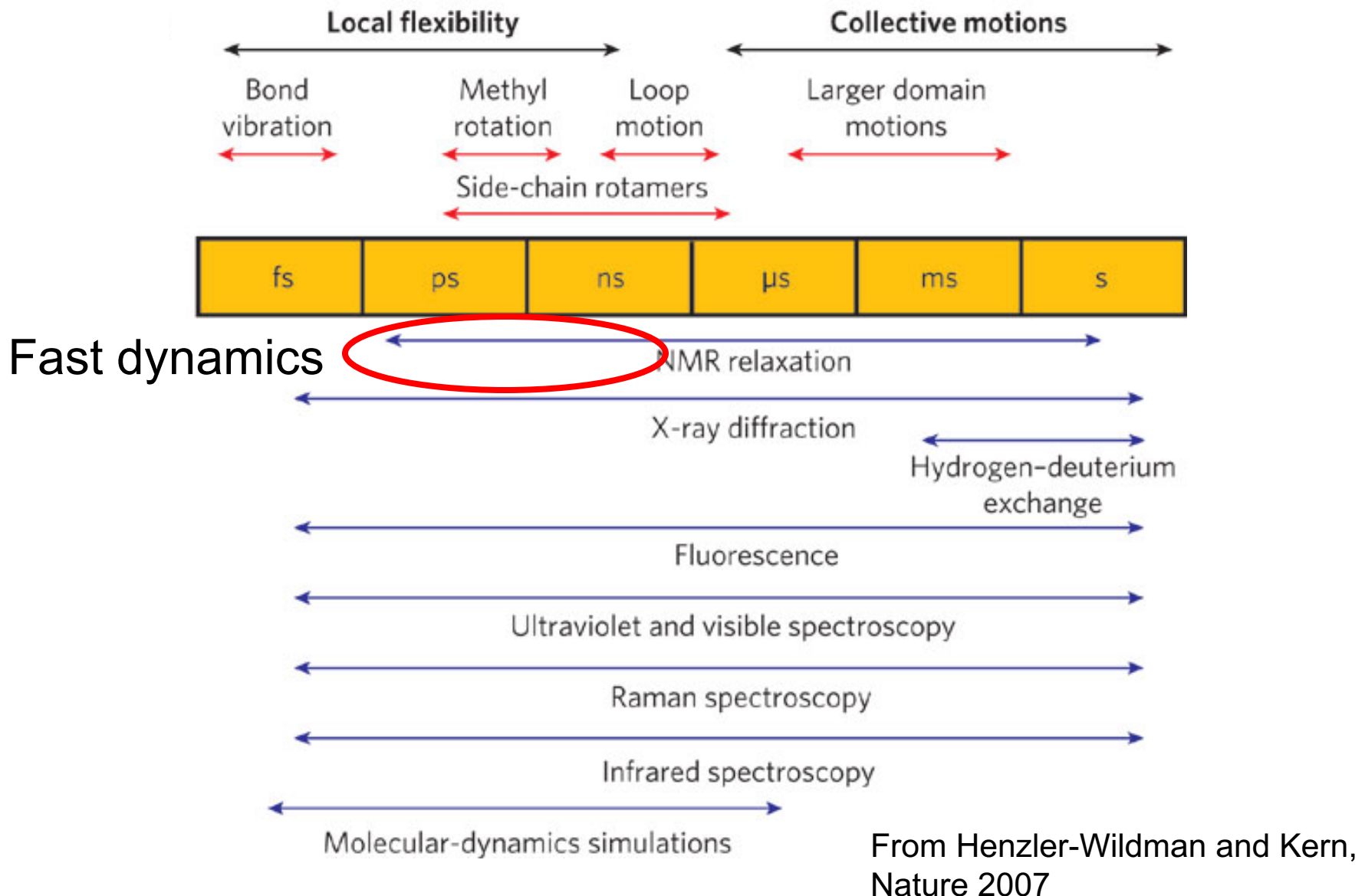
Figure 4



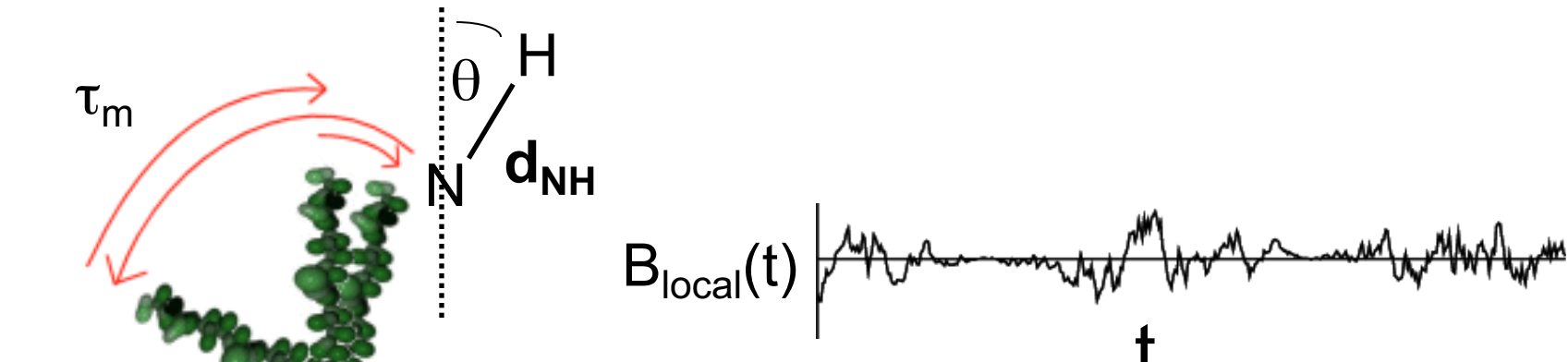
Model



Timescales of Protein Dynamics



A Major Source of Relaxation is Brownian Rotational Diffusion

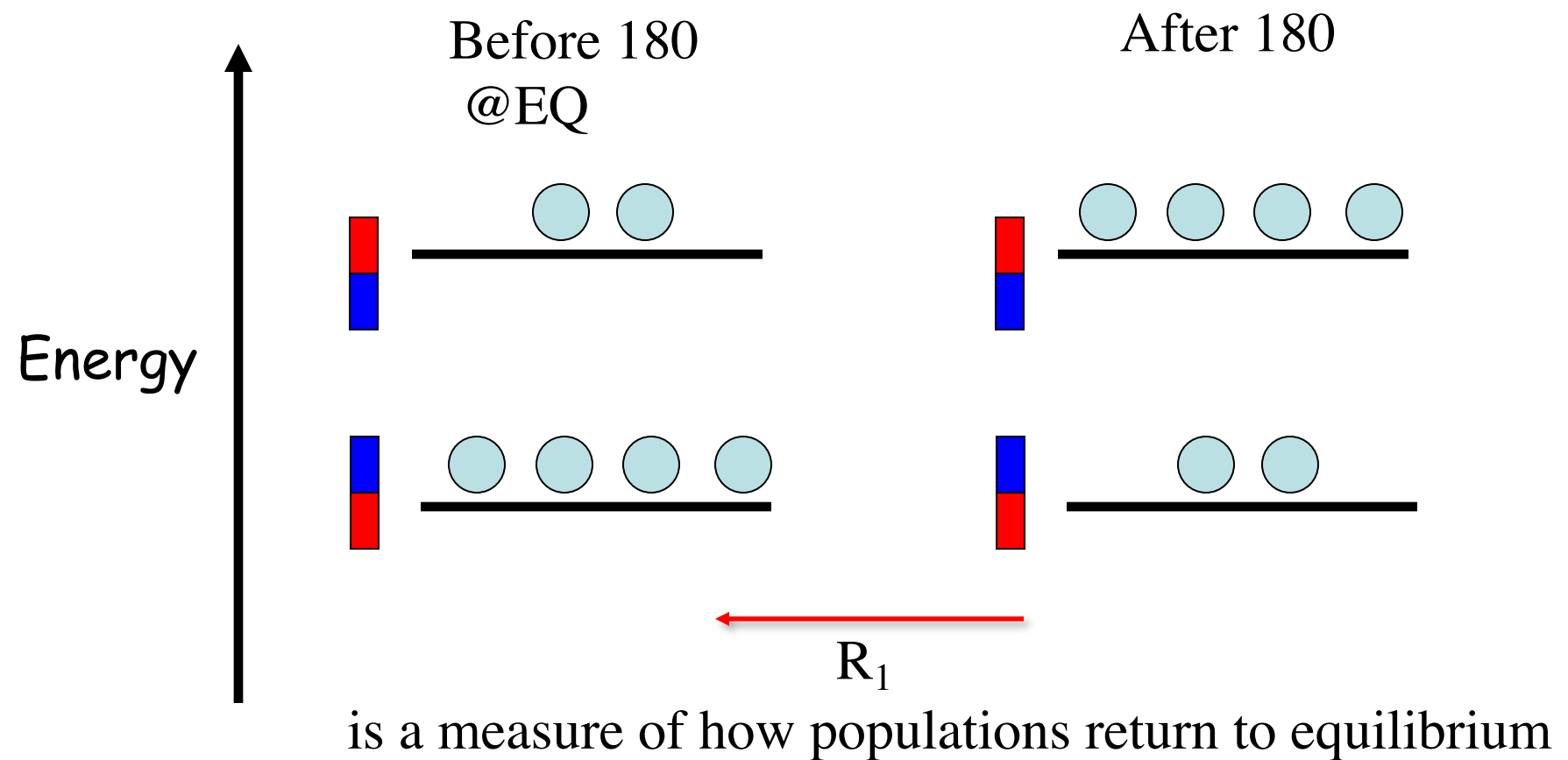


τ_m : rotational correlation time--the time to rotate through one radian.

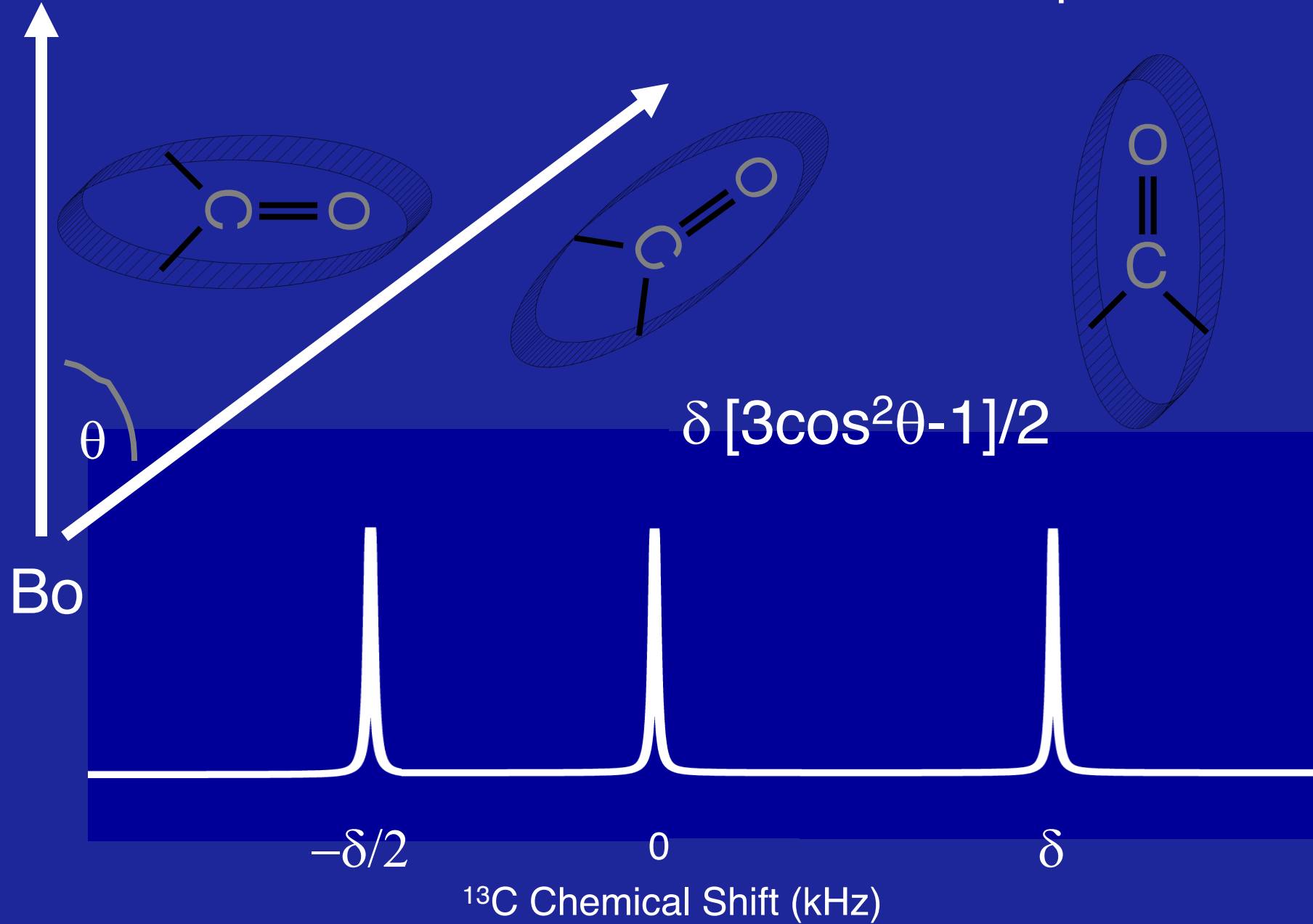
e.g. 20 ns for 40 kDa protein

B_0

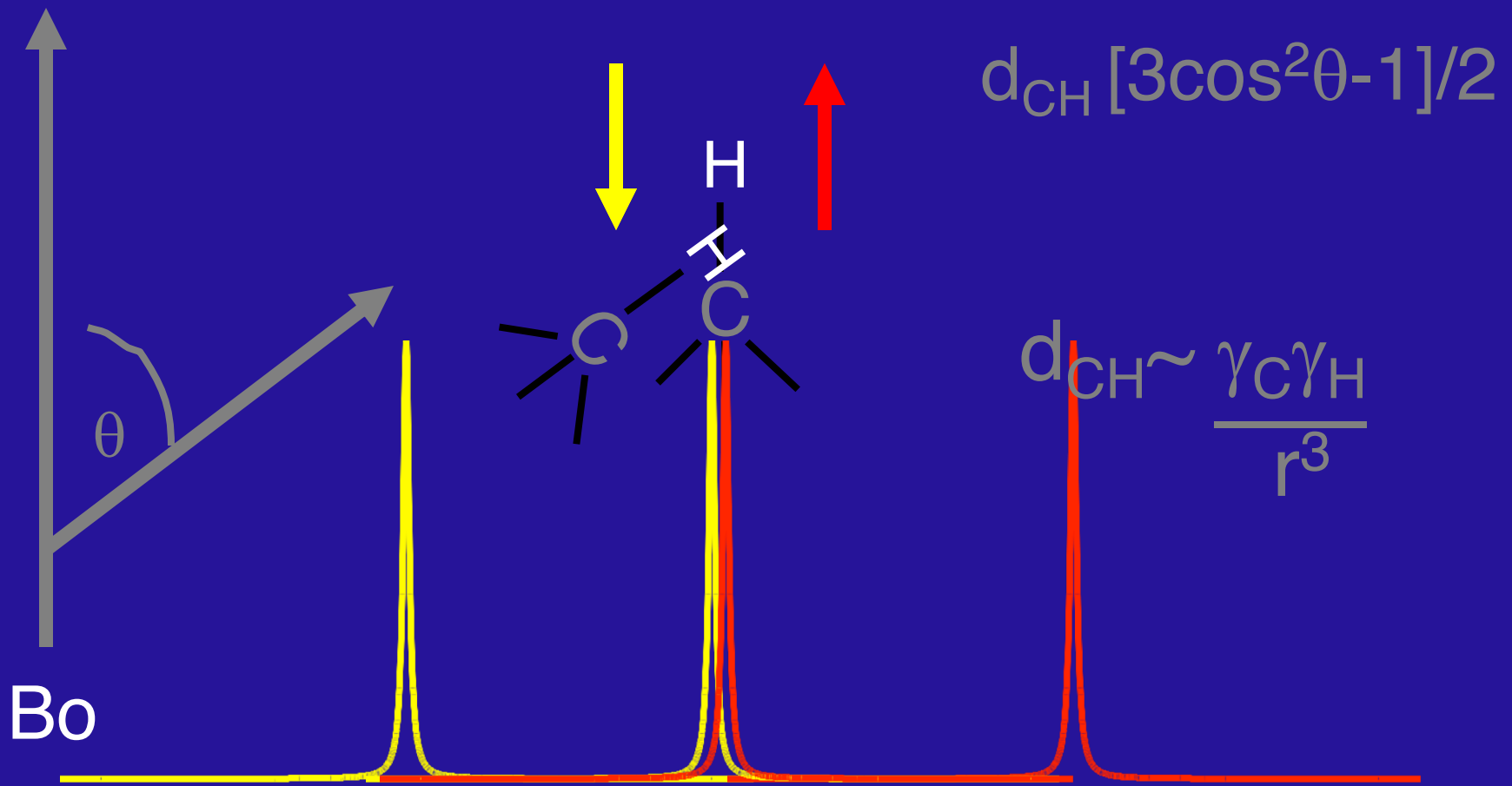
A 180 degree pulse inverts the population distribution



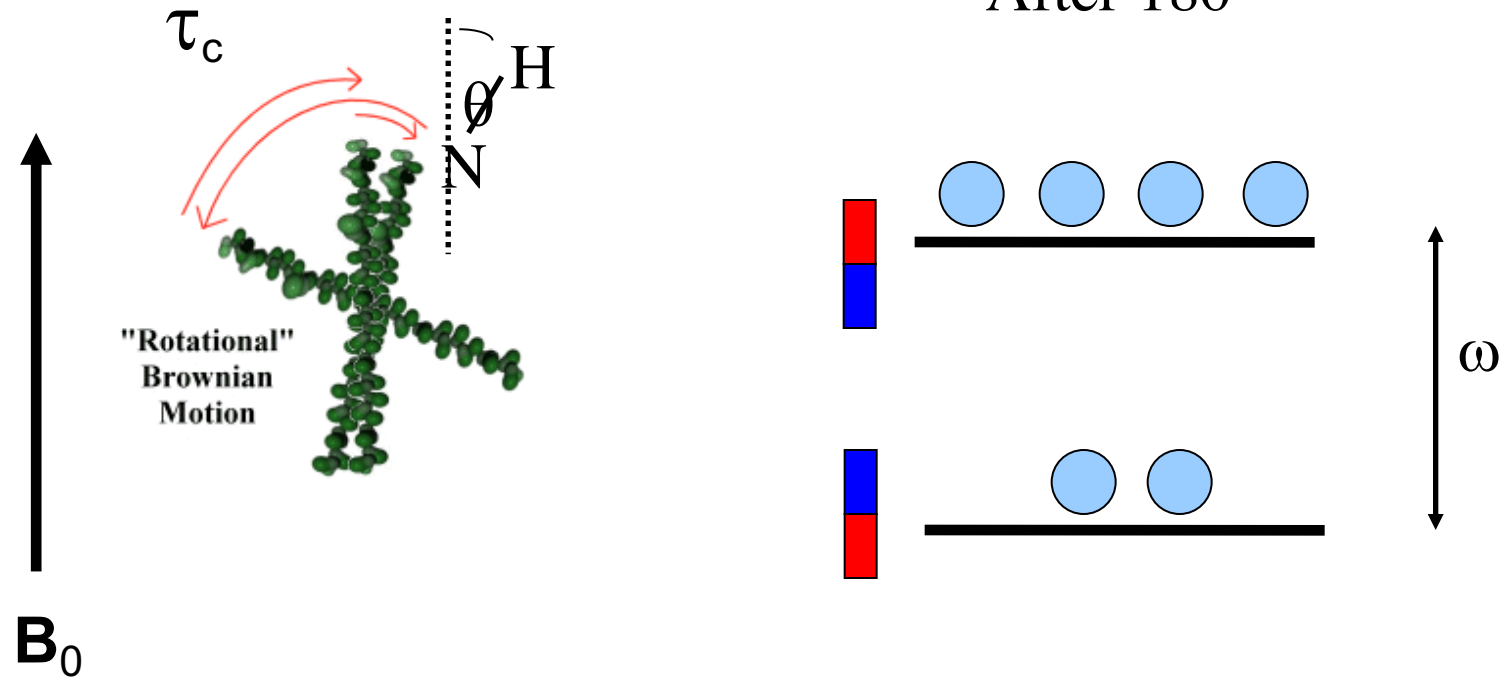
Chemical Shift Interaction is Anisotropic



Dipolar Coupling Interaction is Anisotropic



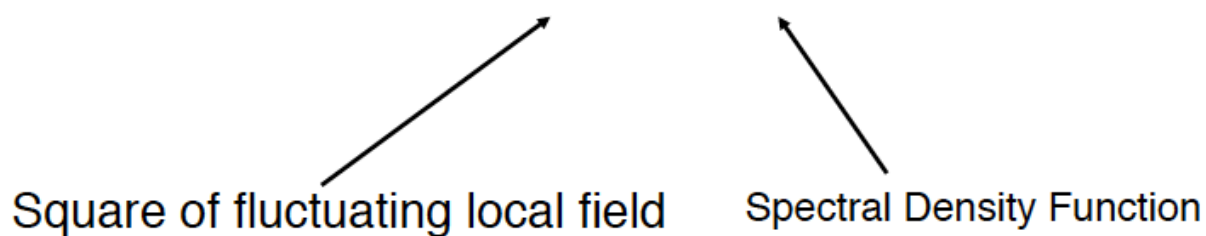
The "Frequency" Dependence of Relaxation Rates, R1 example



Efficient relaxation if $1/\tau_c = \omega$

Relaxation Rates Depend on Amplitude and Frequency of Local Field Fluctuations

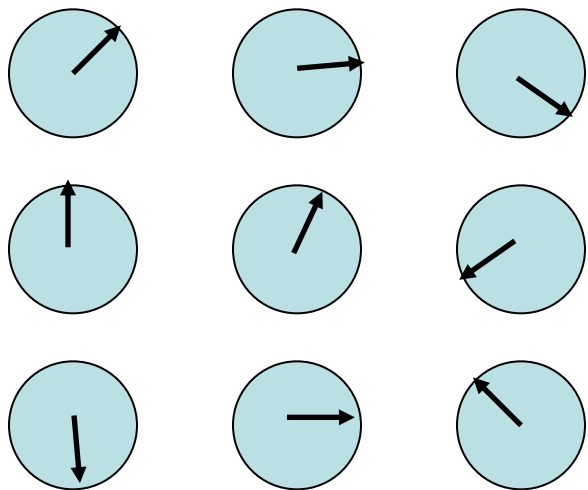
$$R_1(N) = c^2 J(\omega)$$



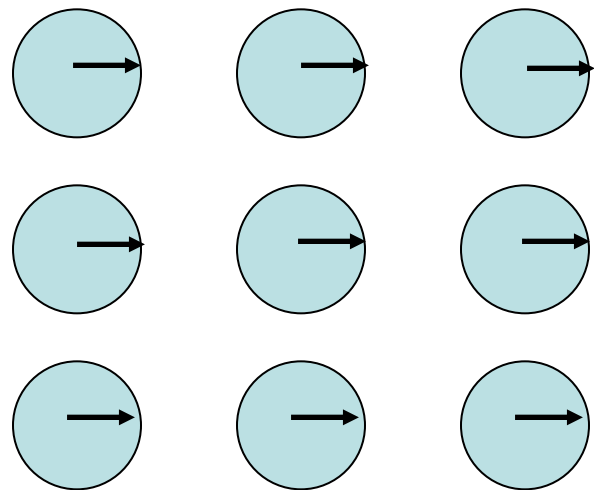
$$J(\omega) = \frac{\tau_m}{1 + (\omega\tau_m)^2}$$

Dephasing depends on ns-ps dynamics too

Ensemble of Nuclear Spins



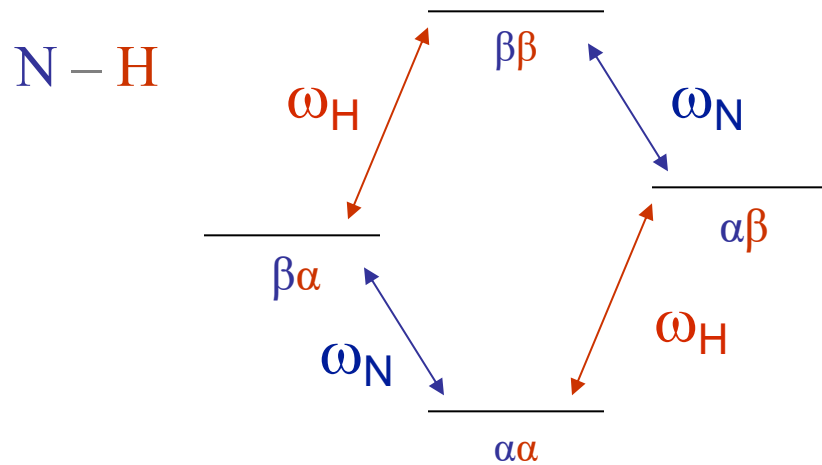
Resonant RF Field
↔
Dephasing



Random Phase
No NMR Signal

Phase Synchronization
NMR Signal!

$^{15}\text{N}-^1\text{H}$ spin pair has four states



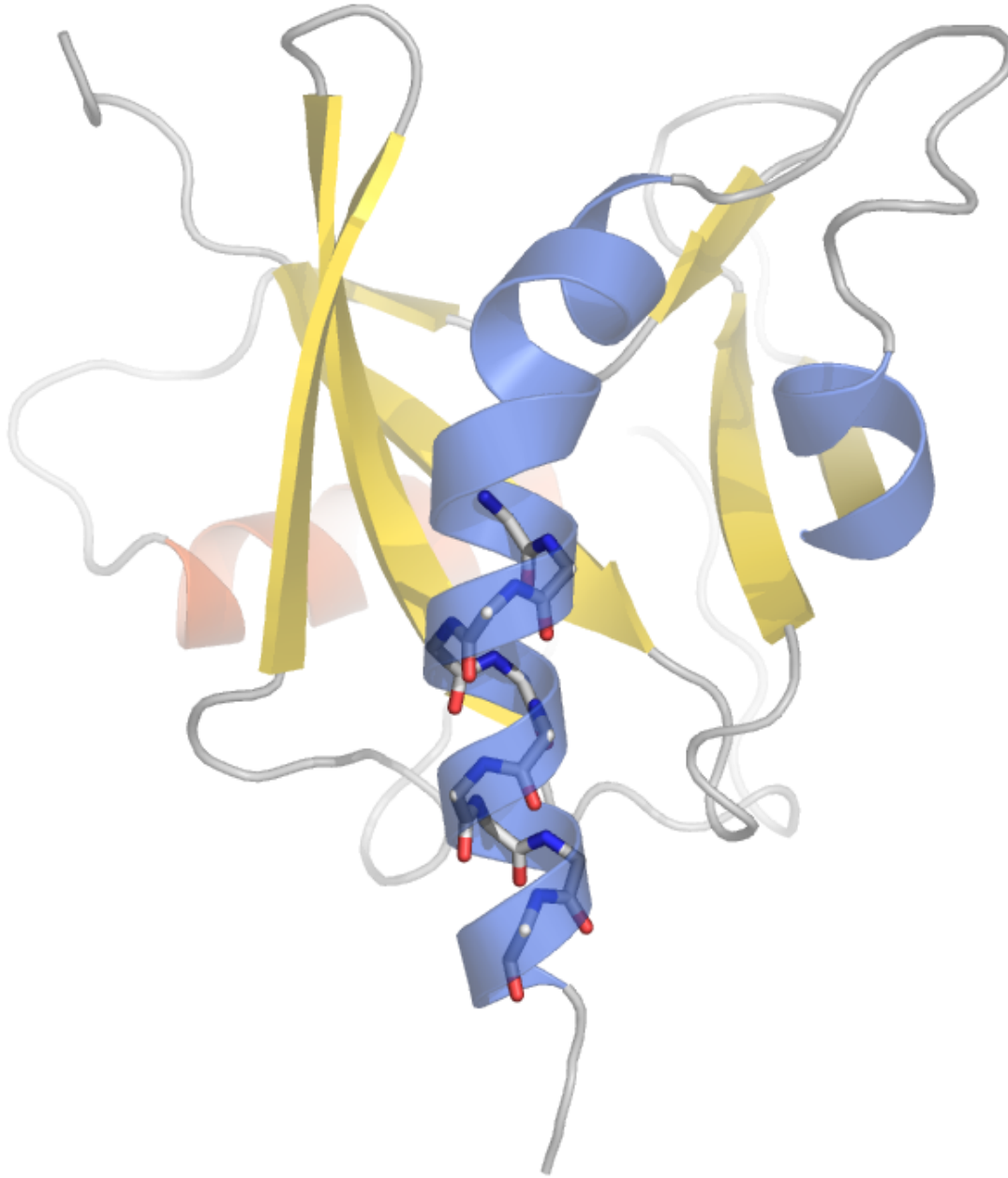
Spectral Density Functions

$$R_1 = \frac{d^2}{4} [J(\omega_H - \omega_N) + 3J(\omega_N) + 6J(\omega_H + \omega_N)] + c^2 J(\omega_N)$$

$$R_2 = \frac{d^2}{8} [4J(0) + J(\omega_H + \omega_N) + 3J(\omega_N) + 6J(\omega_H) + 6J(\omega_H - \omega_N)] \\ + \frac{c^2}{6} [3J(\omega_N) + 4J(0)]$$

where $d = \left(\frac{\mu_0 h \gamma_N \gamma_H}{8\pi^2} \right) \left\langle \frac{1}{r_{NH}^3} \right\rangle$ $c = \Delta \left(\frac{\omega_N}{\sqrt{3}} \right)$

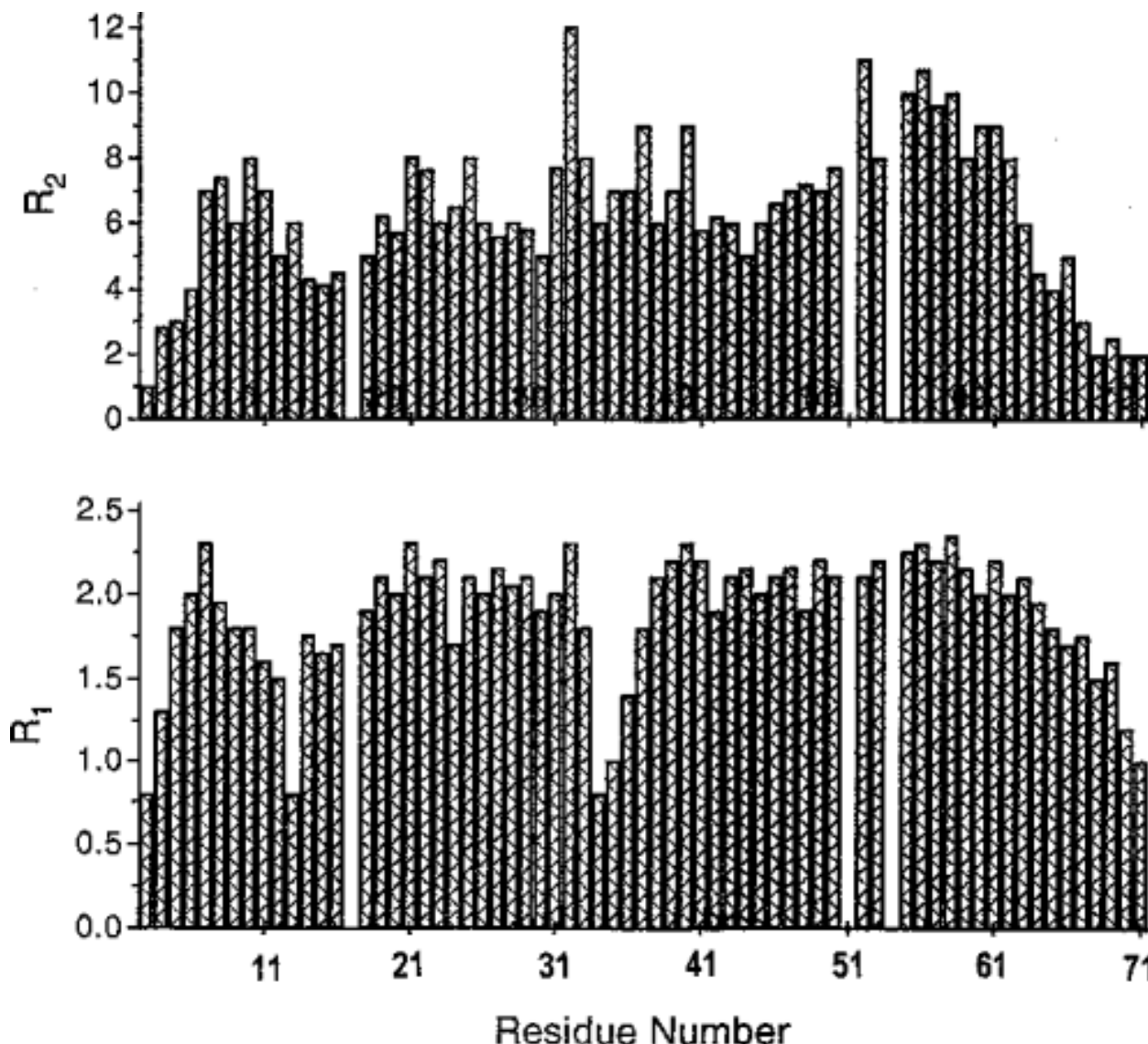
Rigid amide groups



Detecting mobile amide groups



R1 and R2 are not uniform



Model Free formalism accounts for internal motions

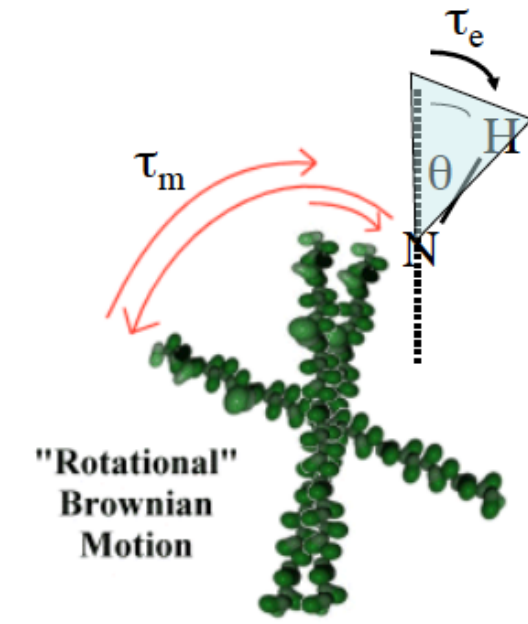
Lipari-Szabo (Model Free)

$$J(\omega) = \frac{2}{5} \left[\frac{S^2 \tau_m}{(1 + \omega^2 \tau_m^2)} + \frac{(1 - S^2) \tau}{(1 + \omega^2 \tau^2)} \right]$$

where $\frac{1}{\tau} = \frac{1}{\tau_e} + \frac{1}{\tau_m}$

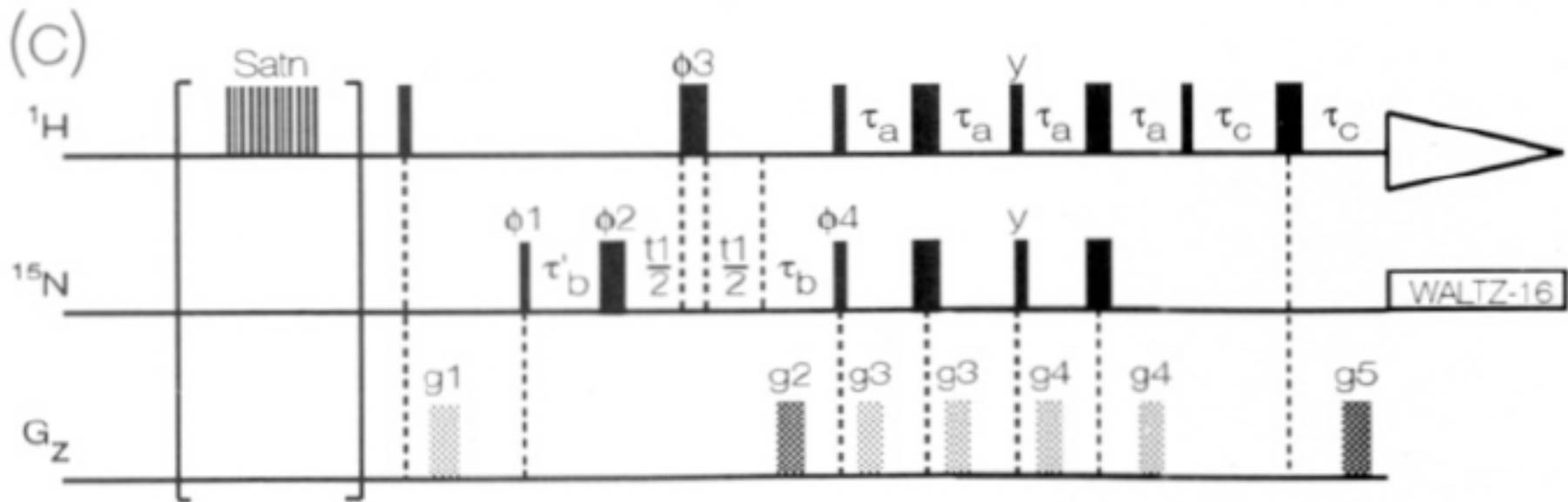


B_0



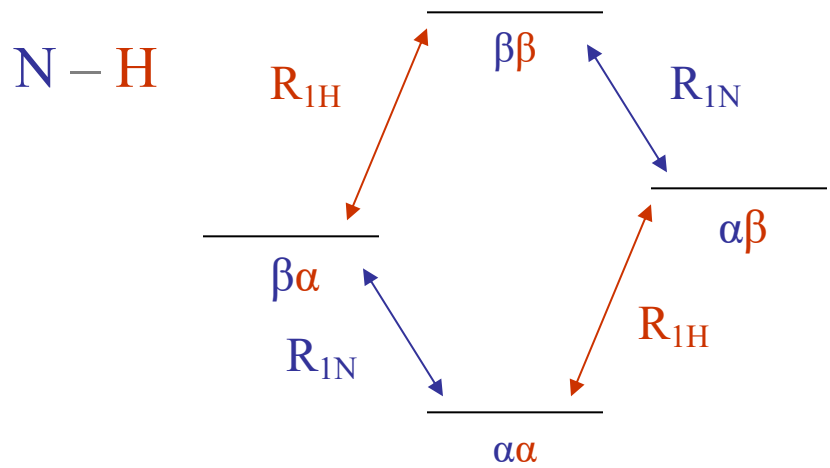
hNOE measurements

- Measure saturated and unsaturated experiments and take the intensity ratio for each peak



Farrow and Kay, Biochemistry, 1993

The heteronuclear NOE



$$M_N \propto (N_{\alpha\alpha} - N_{\beta\alpha}) + (N_{\alpha\beta} - N_{\beta\beta})$$

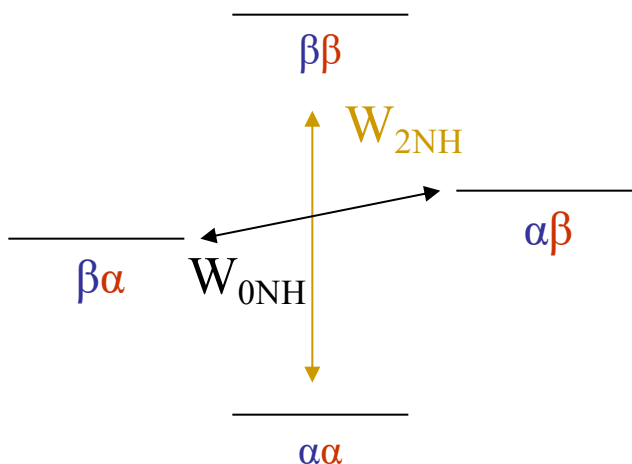
$$M_H \propto (N_{\alpha\alpha} - N_{\alpha\beta}) + (N_{\beta\alpha} - N_{\beta\beta})$$

Saturation equalizes $\beta\beta$ and $\beta\alpha$, $\alpha\beta$ and $\alpha\alpha \rightarrow M_H = 0$

R_1 transitions are an independent return to equilibrium

The heteronuclear NOE

N - H

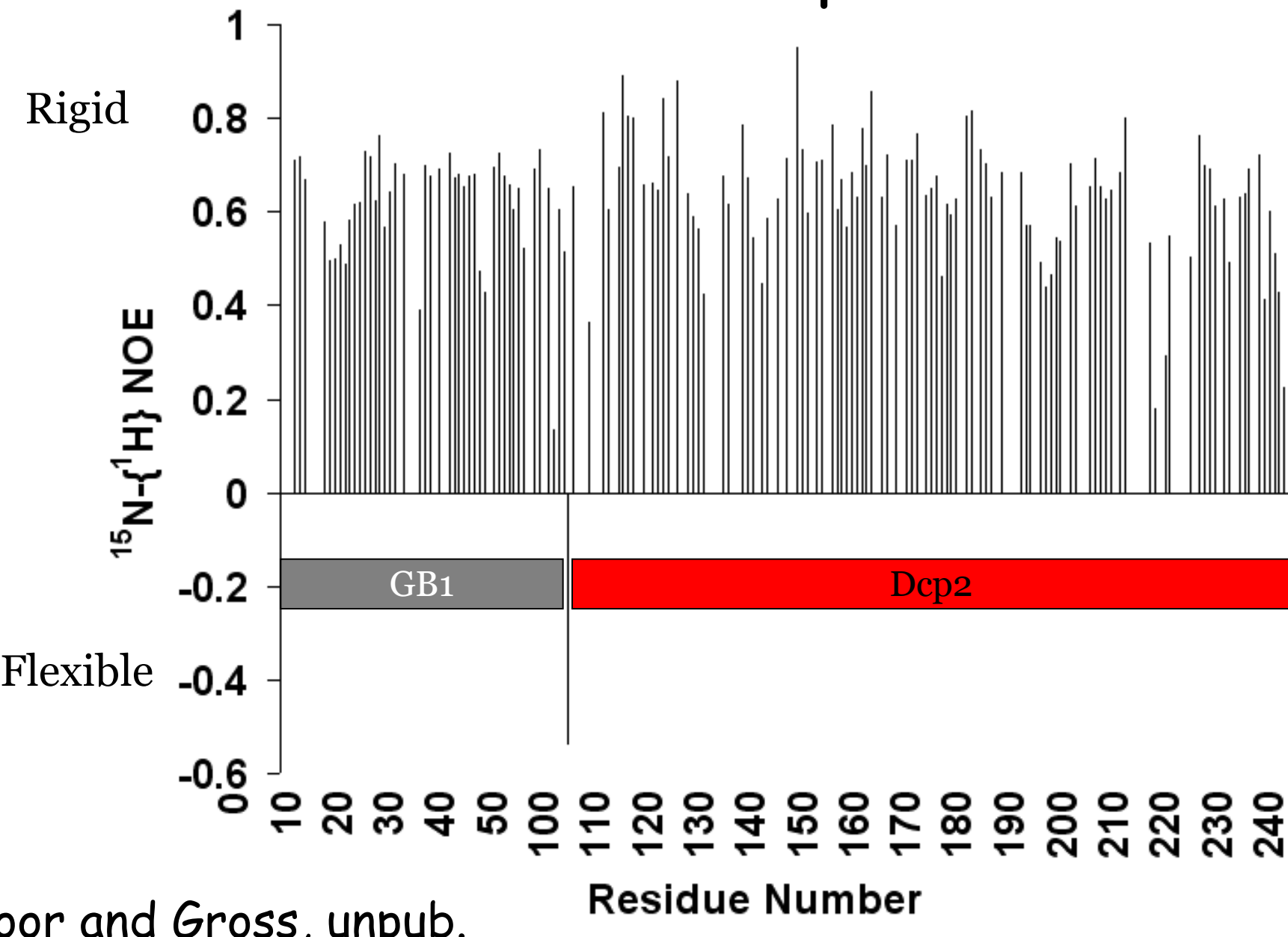


$$M_N \propto (N_{\alpha\alpha} - N_{\beta\alpha}) + (N_{\alpha\beta} - N_{\beta\beta})$$

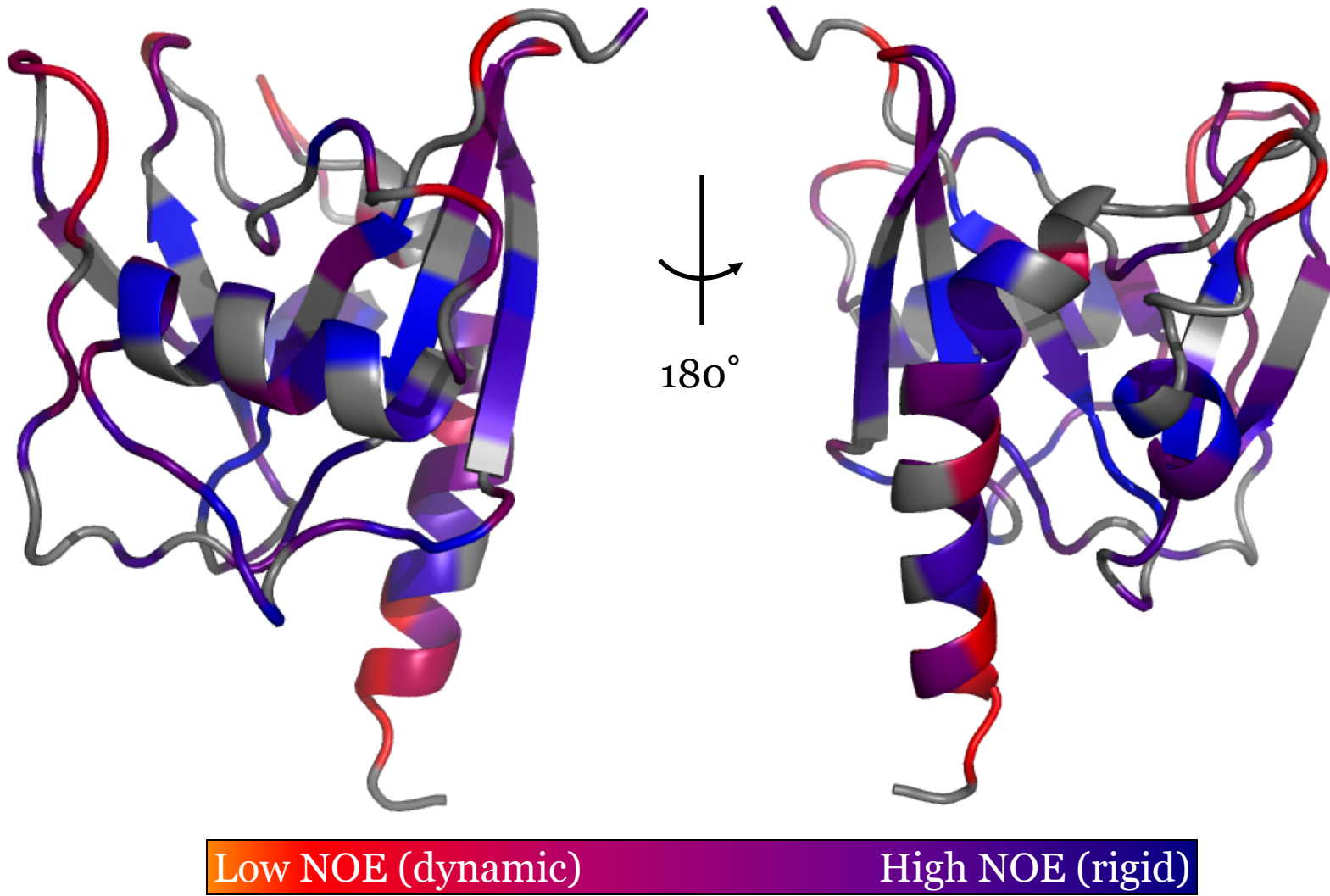
W_2 transitions increase $N_{\alpha\alpha}$ and decrease $N_{\beta\beta}$
→ M increases (positive NOE)
M_N **decreases** (negative NOE)

W_0 transitions increase $N_{\beta\alpha}$ and decrease $N_{\alpha\beta}$
→ M decreases (negative NOE)
M_N **increases** (positive NOE)

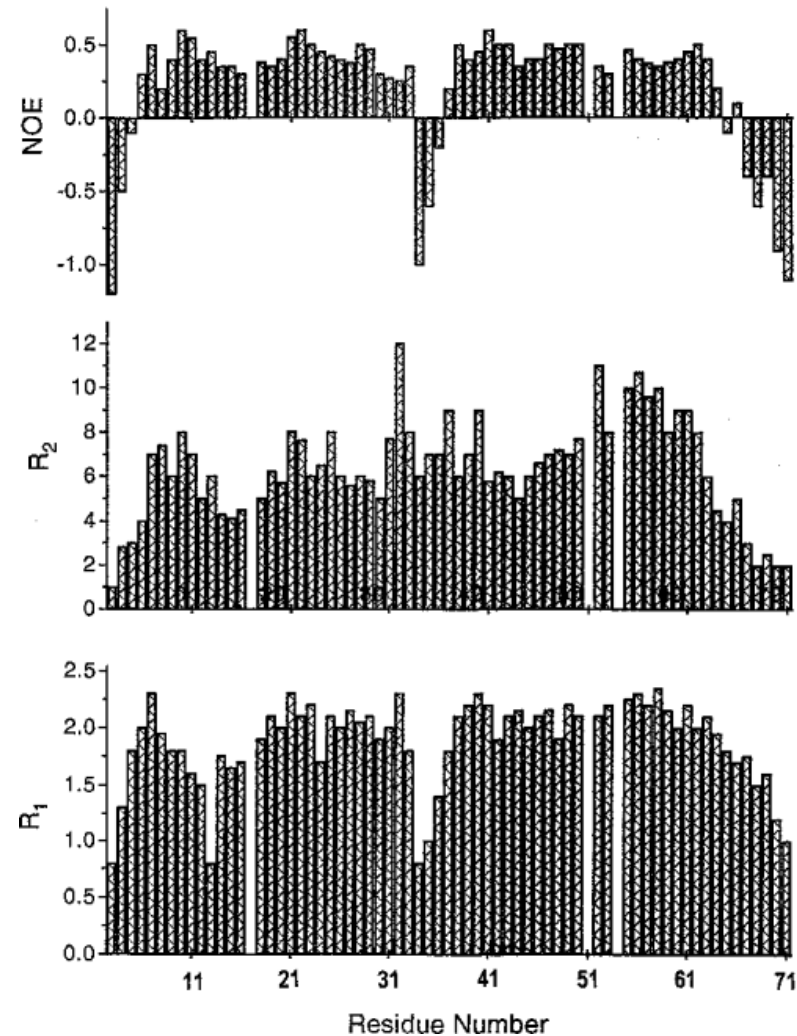
hNOE and Dcp2



hNOE versus structure



R1, R2 and NH-NOE: three relaxation rates

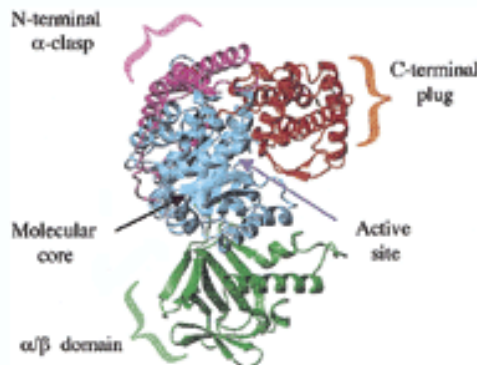


-> three fit parameters: τ_m, τ_e, S^2

Part IV:NMR of Assemblies

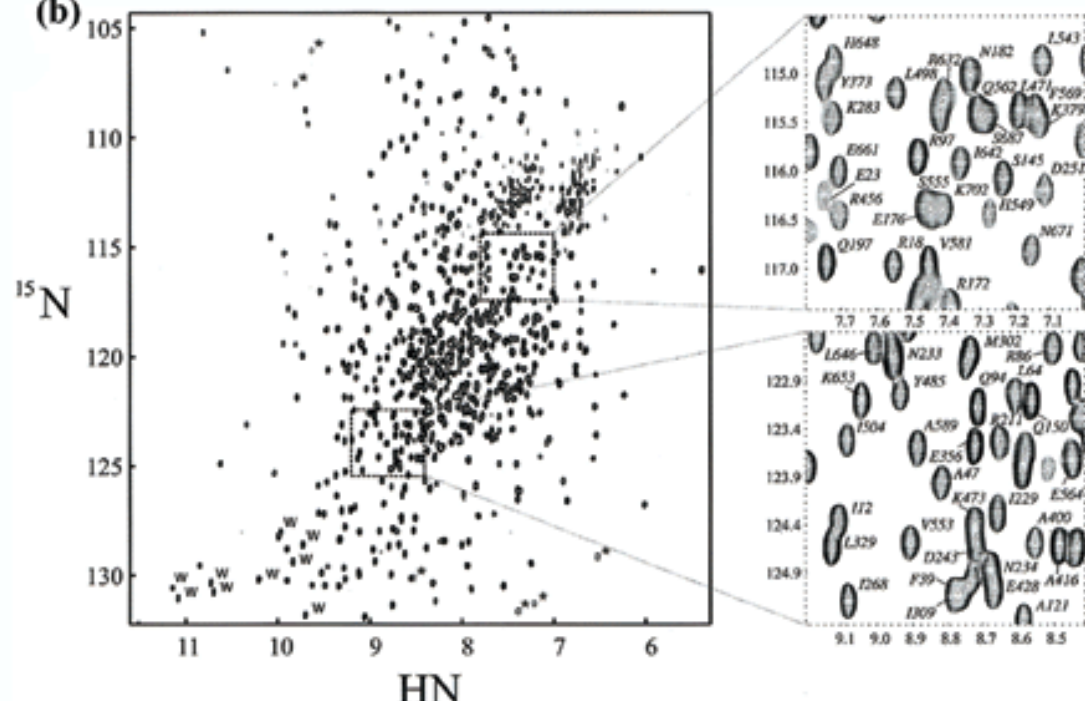
TROSY

(a)



Malate Synthase G
80 kDa

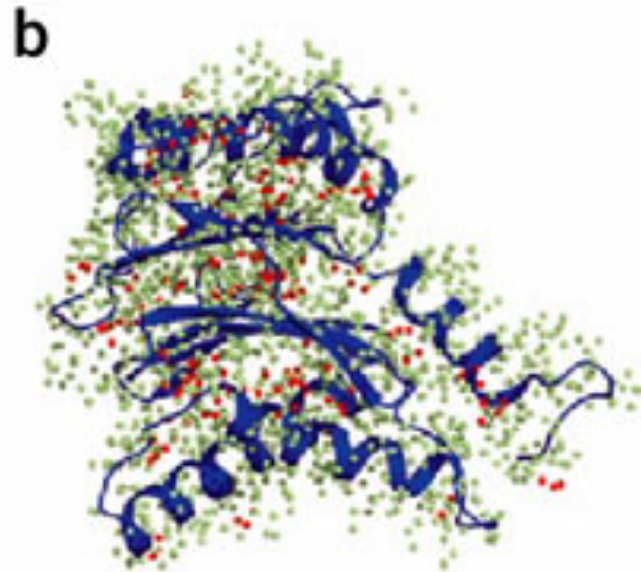
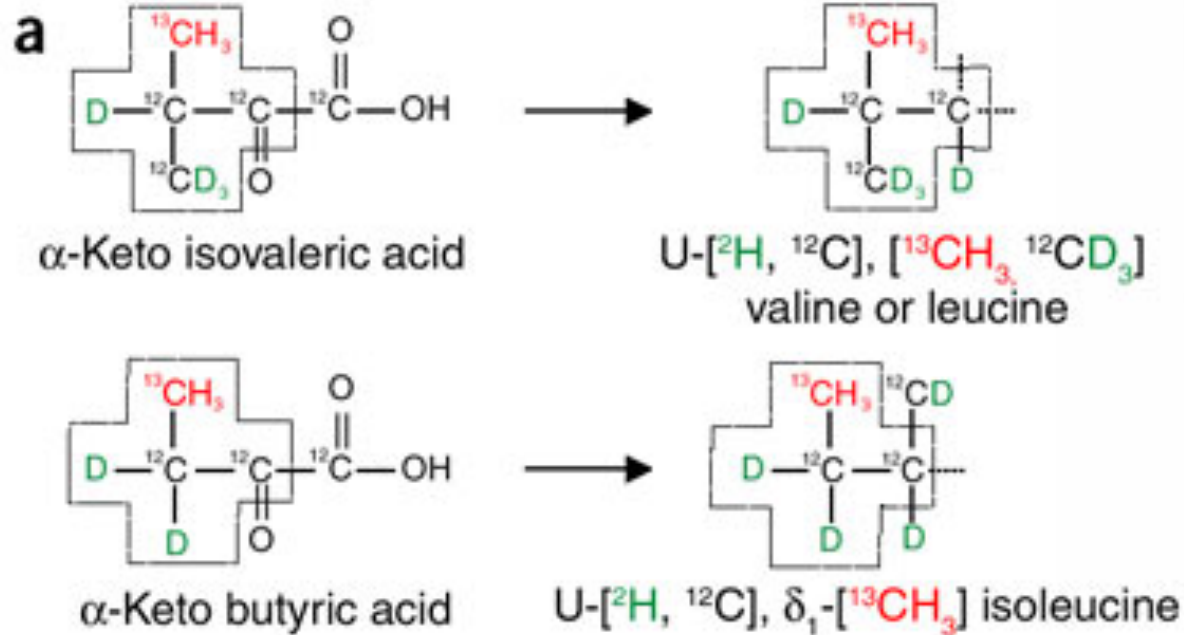
(b)



Turgarinov et al, JACS 2002

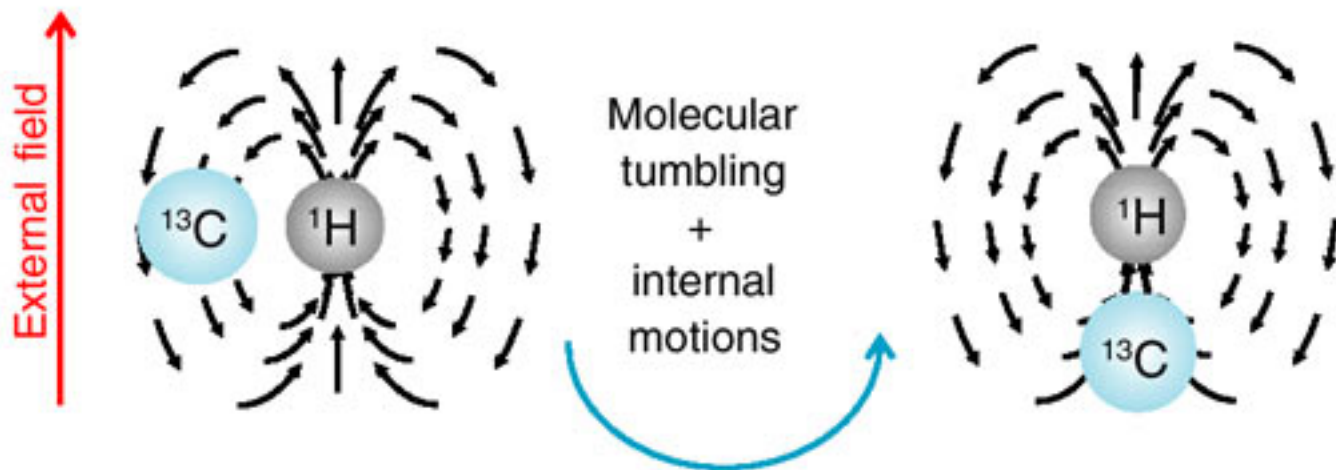
Same info as ^{15}N HSQC

Methyl-group labeling

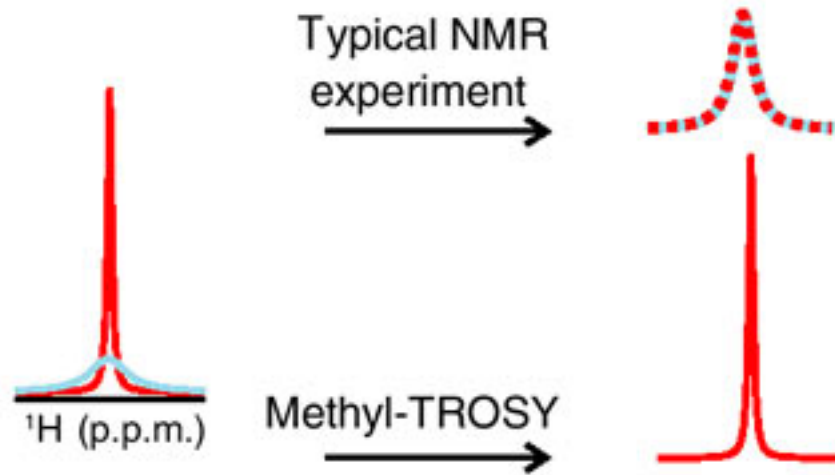


Methyl-TROSY

a



b

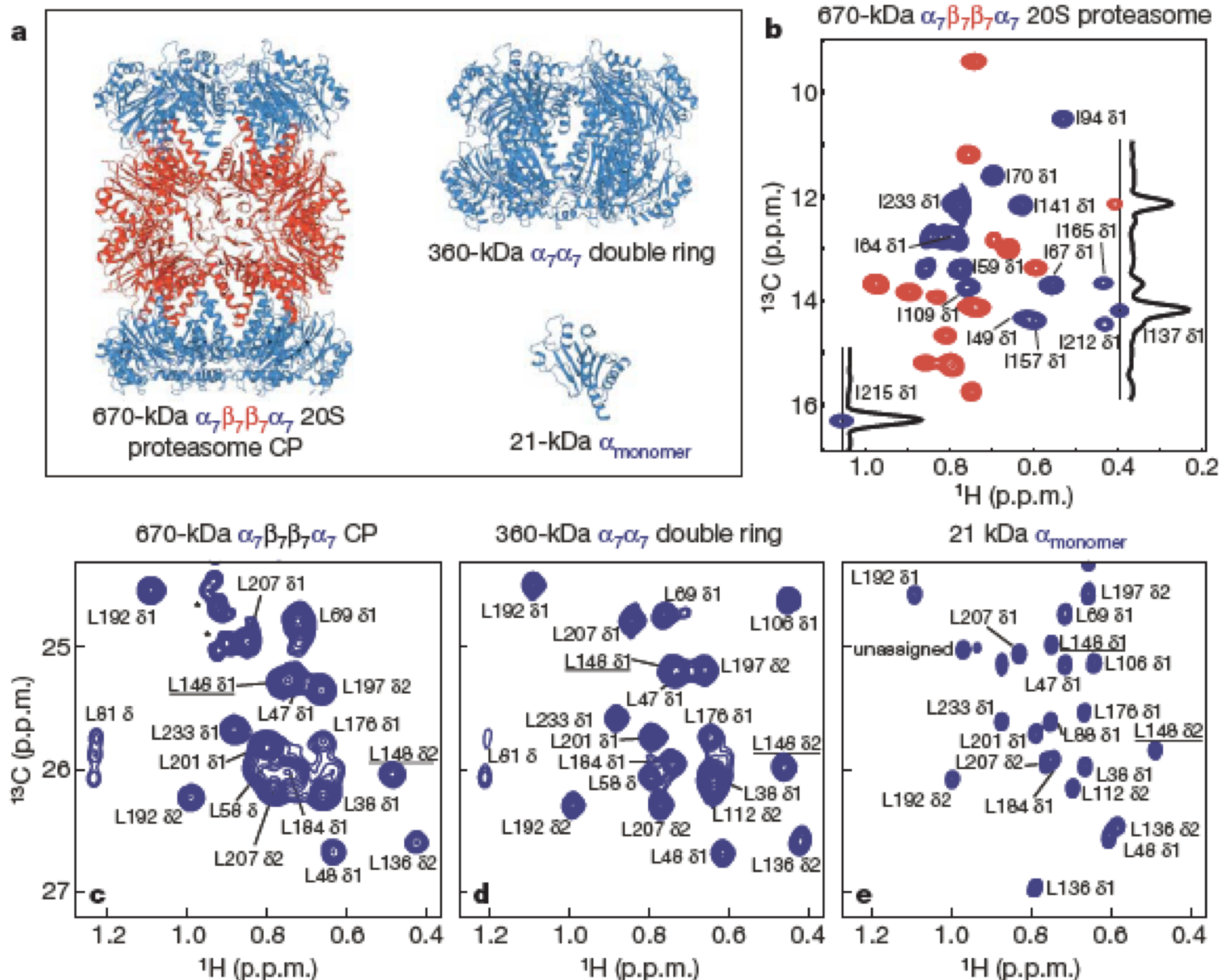


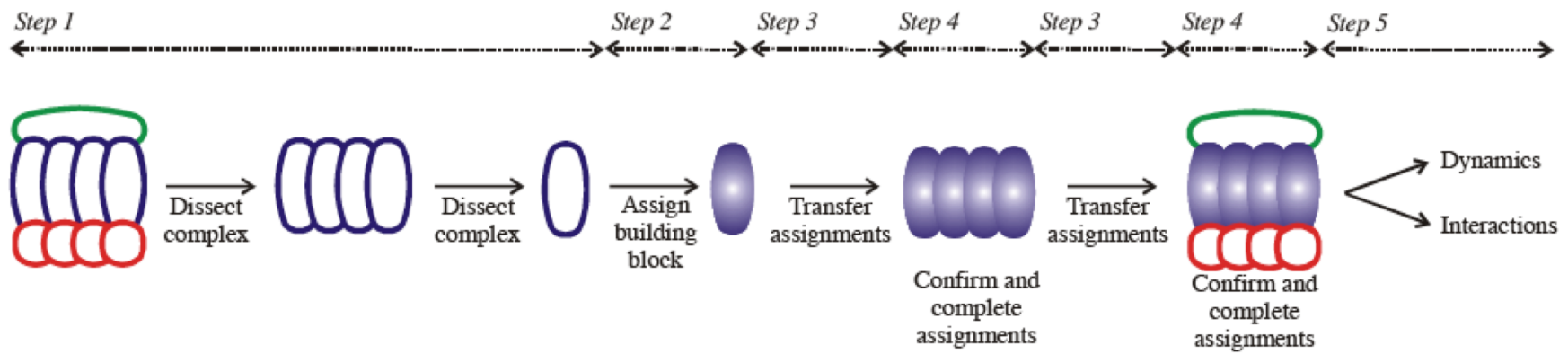
ARTICLES

Quantitative dynamics and binding studies of the 20S proteasome by NMR

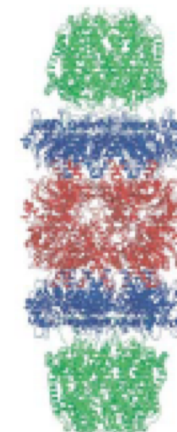
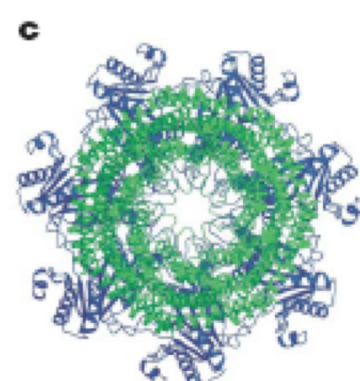
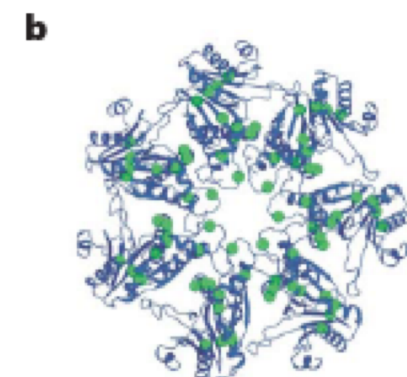
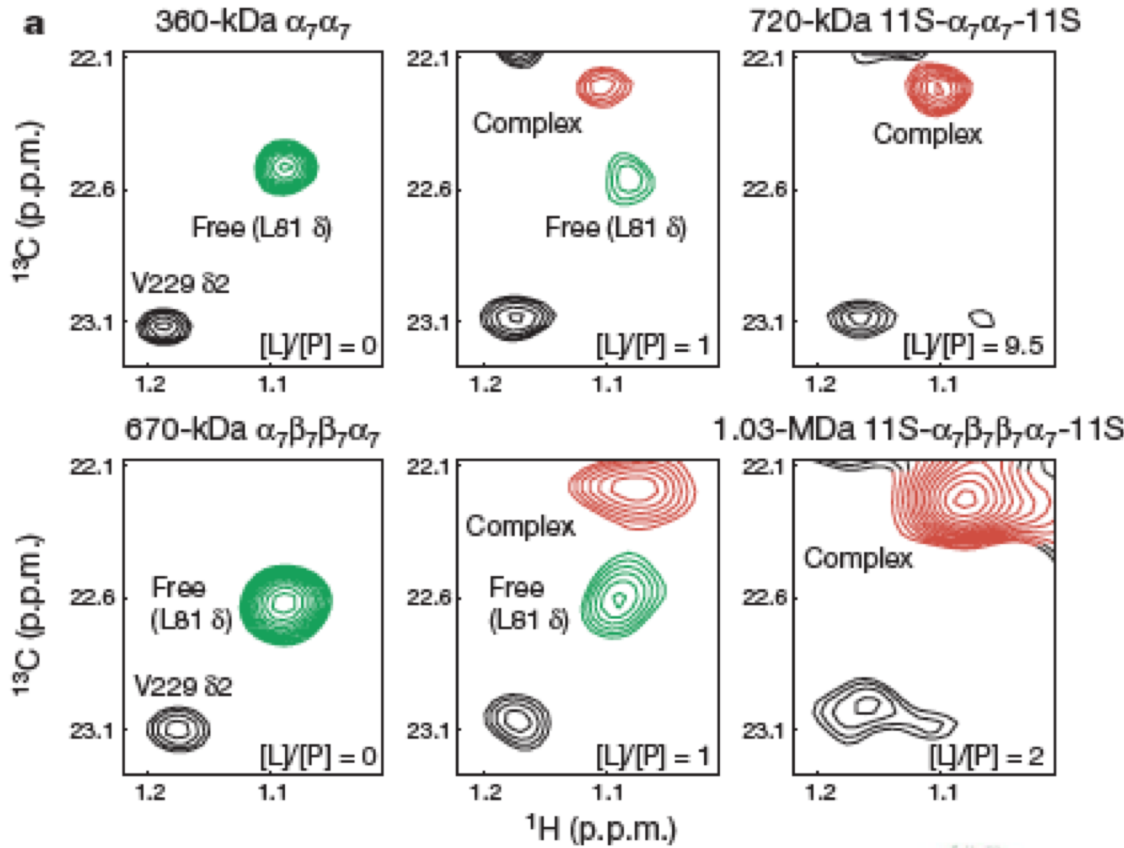
Remco Sprangers¹ & Lewis E. Kay¹

ILV METHYL ASSIGNMENTS OF 670 KDA COMPLEX

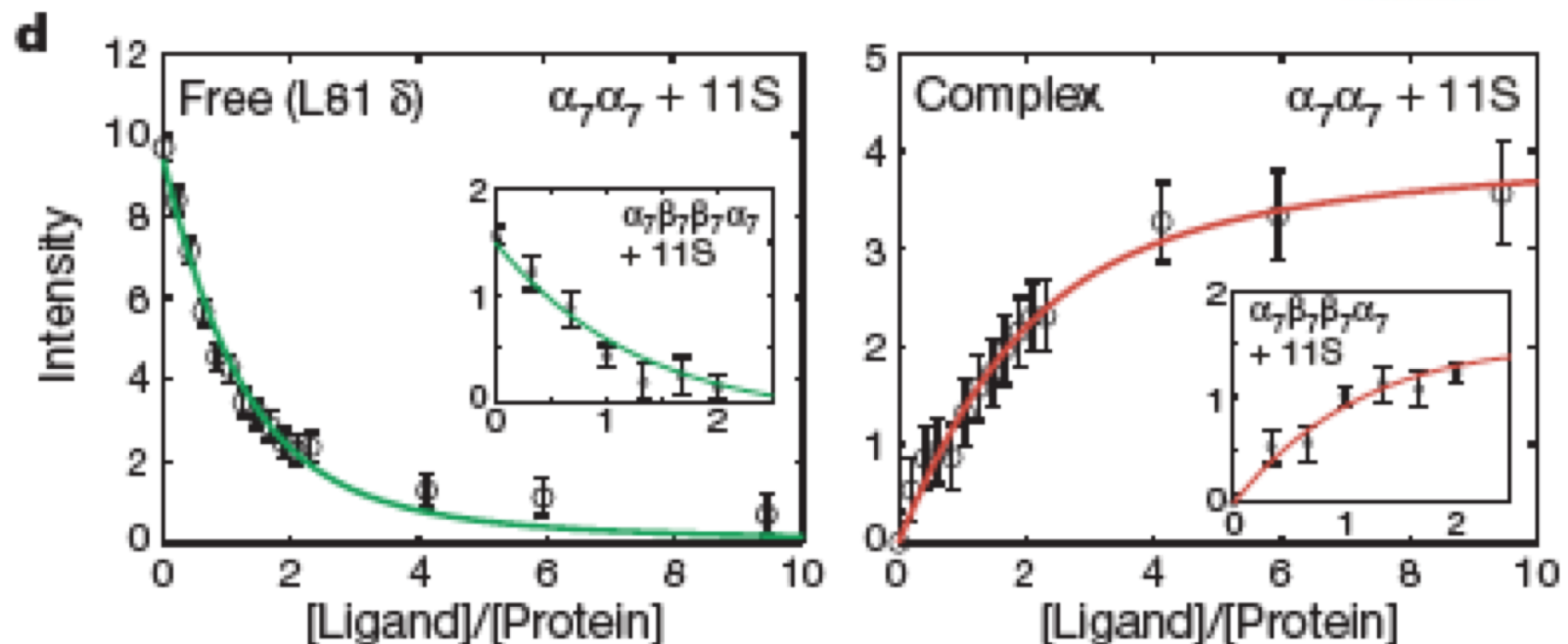




11S ACTIVATOR BINDING



11S BINDING CURVES

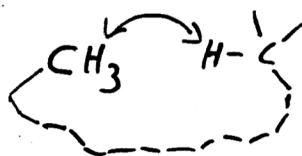
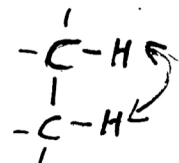


Part V: Structure Determination by NMR

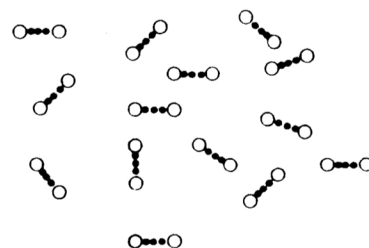
Calculating 3D structures: we need distance measurements & assignments

$$NOE = f(\tau_c) \cdot \frac{1}{r^6}$$

We can see distances that are
 $\leq 5 \text{ \AA}$

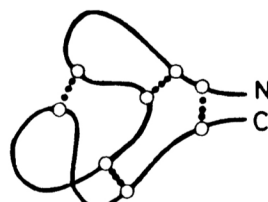


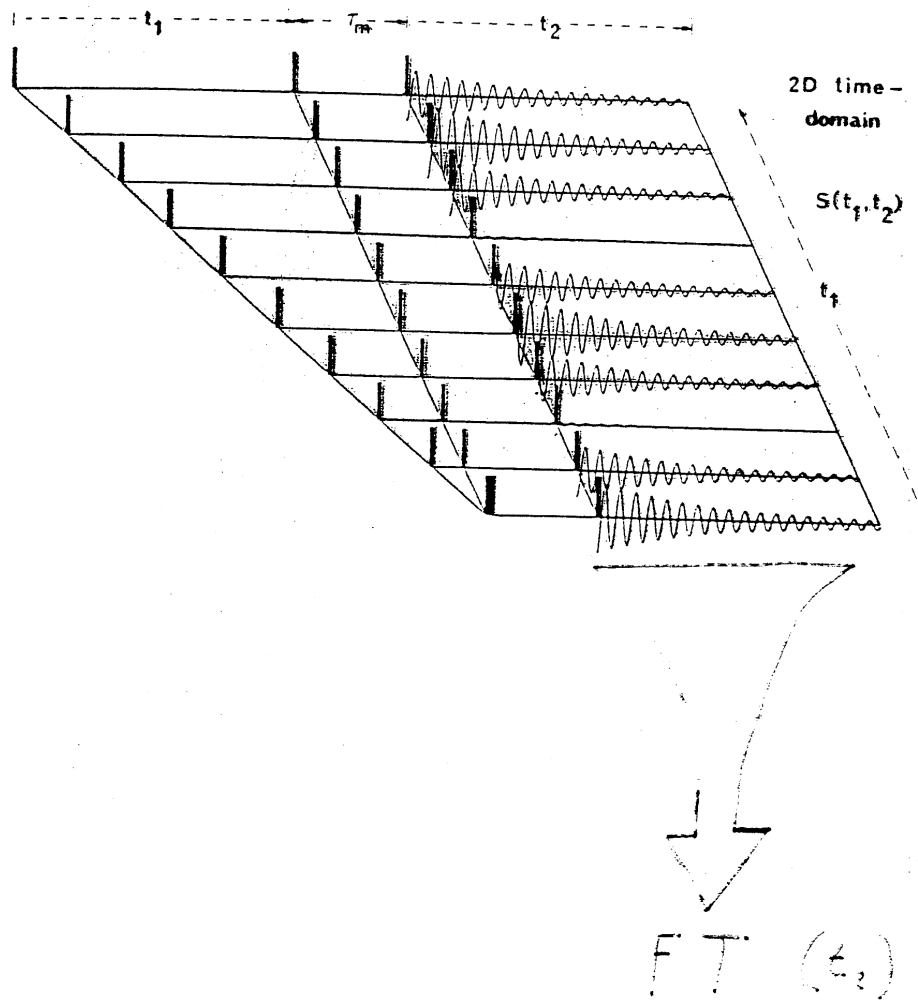
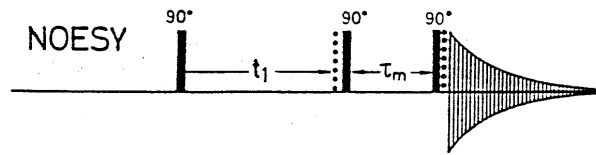
NO ASSIGNMENTS



N ————— C

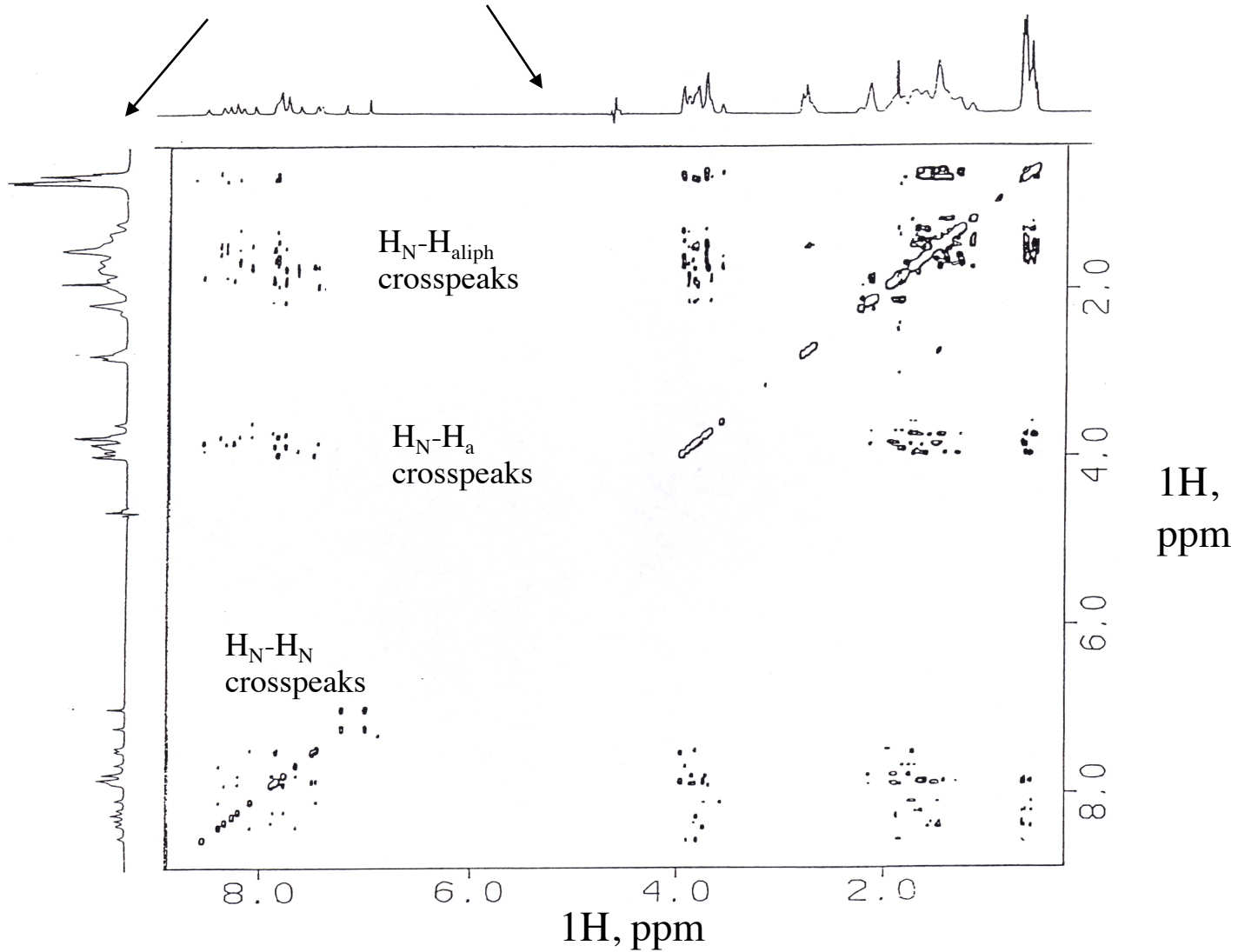
WITH ASSIGNMENTS





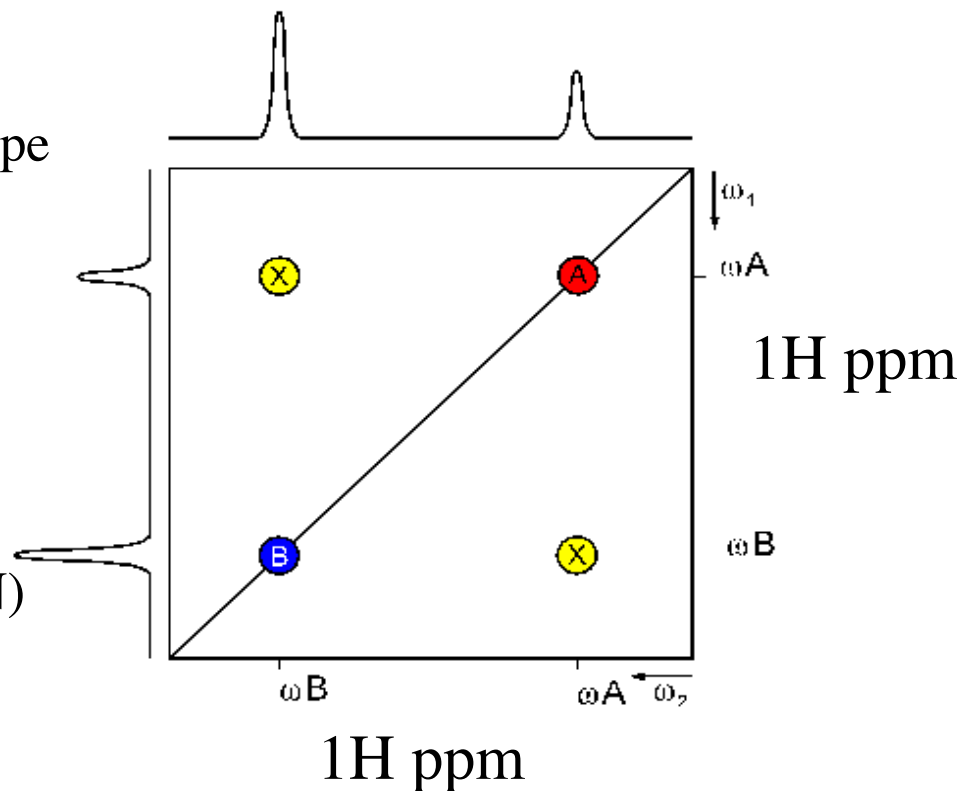
A Real 2D NOE Experiment of a Small Peptide

A projection through both dimensions gives a 1D spectrum



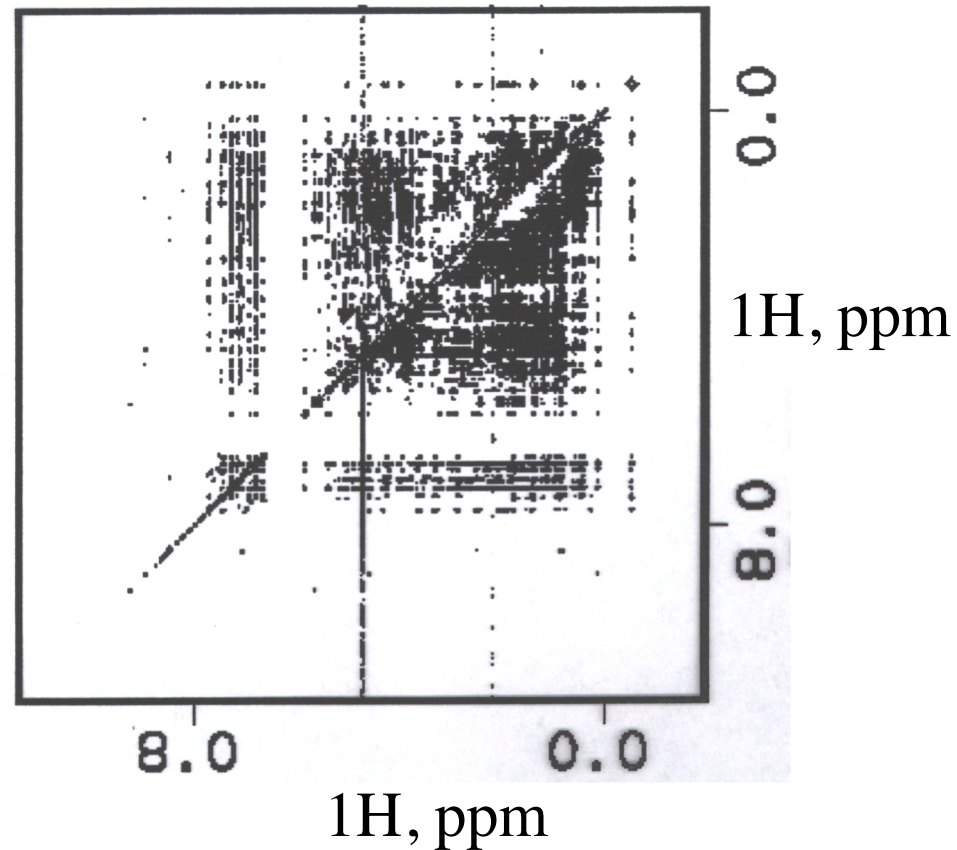
Interpretation of 2D NMR Spectra

- Crosspeaks are a measure of some type of interaction between 2 spins (NOE, J-coupling....)
- The intensity of the crosspeak often quantifies the interaction.
- A heteronuclear experiment (^1H - ^{15}N) would not have diagonal crosspeaks.



Higher Dimensionality 3 and 4D Heteronuclear Experiments on Isotopically Labeled (¹⁵N-¹³C) Proteins

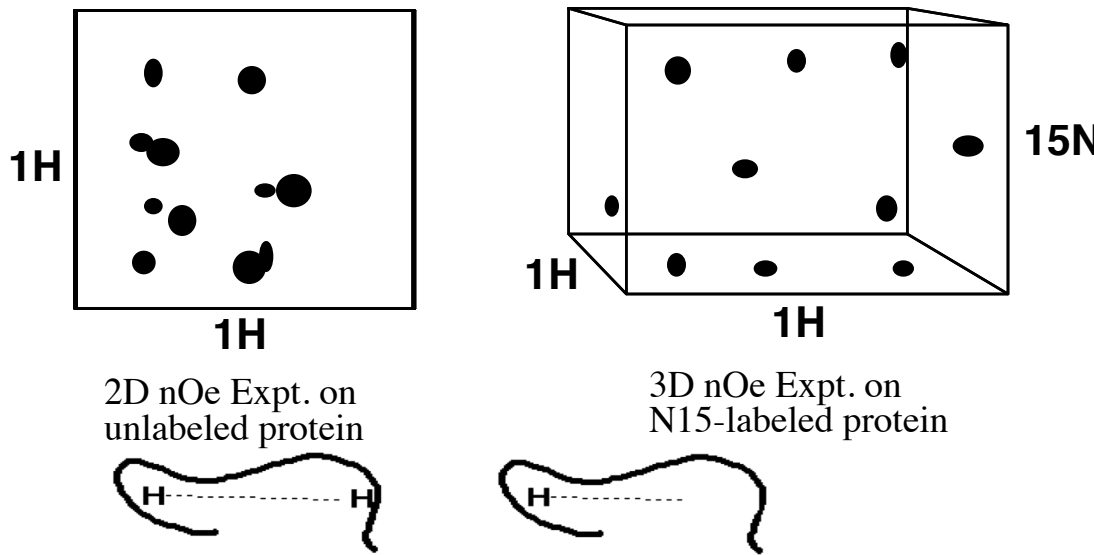
2D NOESY of a 76 residue protein homodimer (effectively 18kD) in D₂O



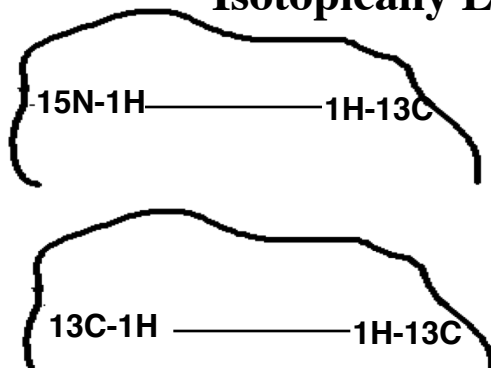
In practice, even small proteins have very crowded 2D spectra making assignment very difficult. In this case the fact that it is in D₂O simplifies the spectra because the amide protons exchange for deuterium and are not visible.

Benefit of C13 and N15 labeling of Proteins for NMR

Higher Dimensionality (3 and 4D) Experiments Reduce Overlap Compared to 2D Experiments



Many More Types of Experiments Can be Done on Isotopically Labeled Protein

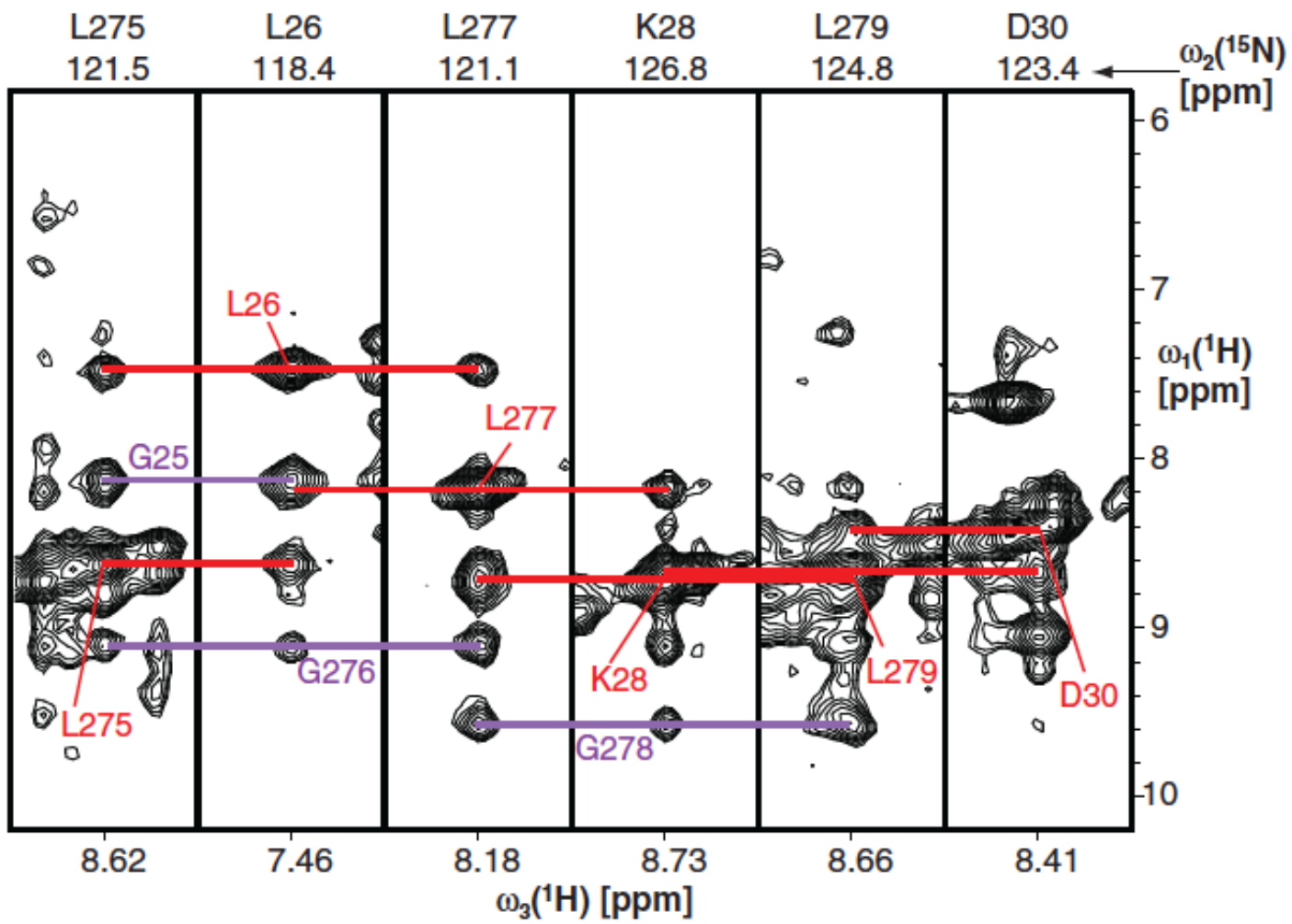


nOes between Protons Attached to ^{15}N and Protons Attached to ^{13}C

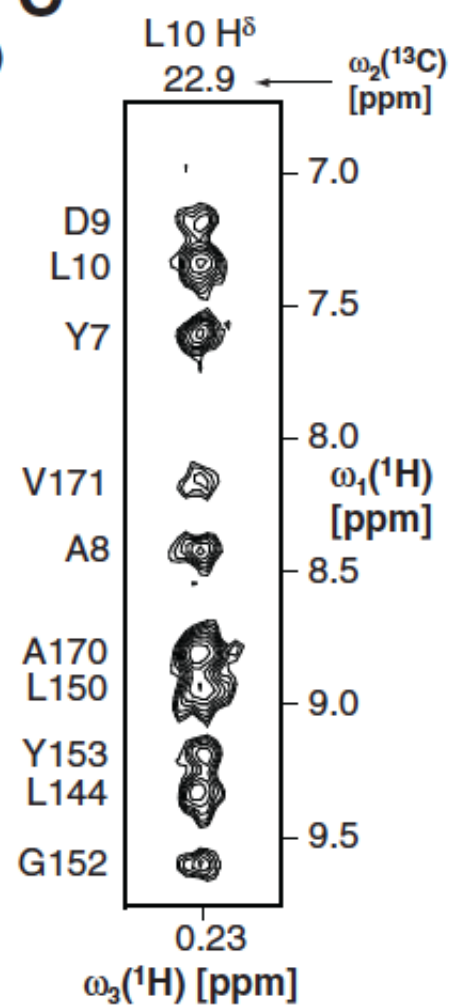
nOes between Protons Attached to ^{13}C and Protons Attached to ^{13}C

Examples of ^{15}N and ^{13}C dispersed NOESY

B



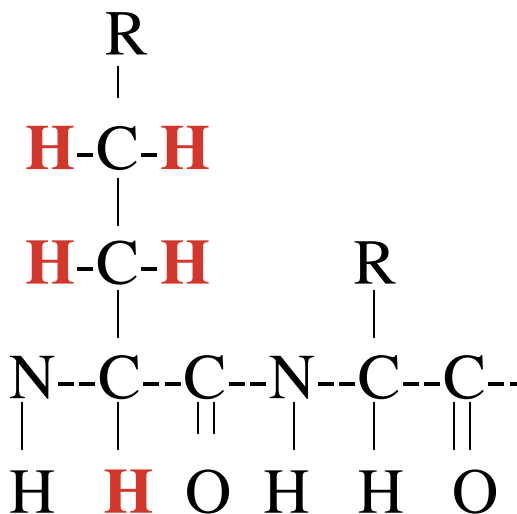
C



15N NOESY-HSQC

13C NOESY-HSQC

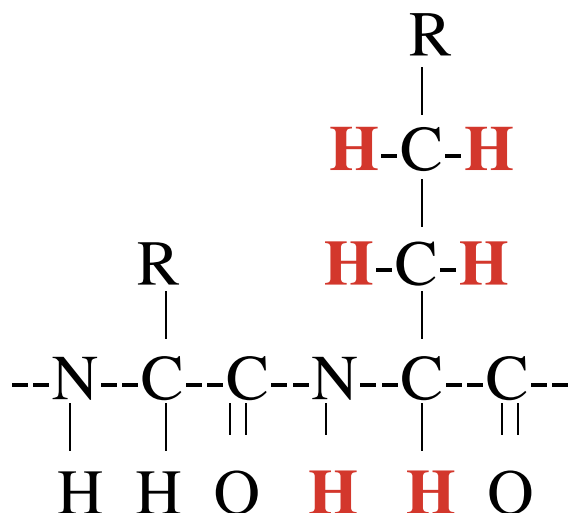
Side-chain protein assignments



H(CCO)NH-TOCSY

i - 1 res.

All Carbon's H's at i-1 to N-H pair.

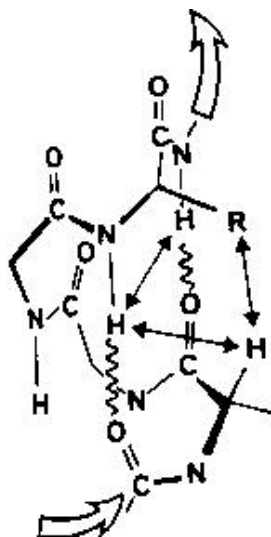


¹⁵N-TOCSY i res.

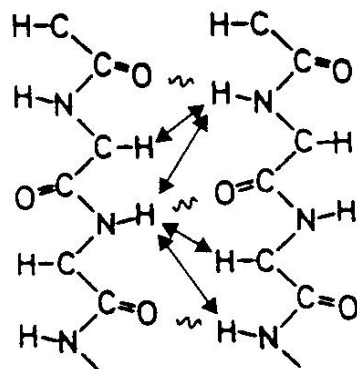
All H's at i to N-H pair.

TOCSY methods relies on through-bond J Couplings

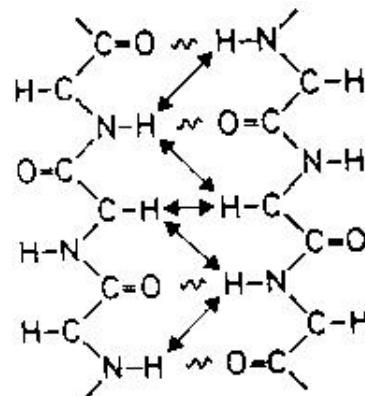
Close interatomic distances in secondary structures



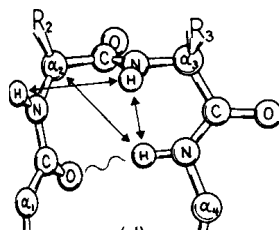
alpha-helix



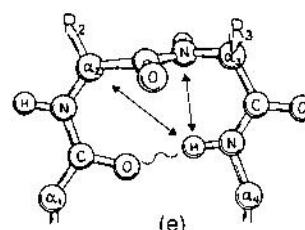
parallel beta-sheet



antiparallel
beta-sheet



type I turn



type II turn

THE RANGE OF ^{13}C CHEMICAL SHIFTS OBSERVED FOR EIGHT DIFFERENT PROTEINS

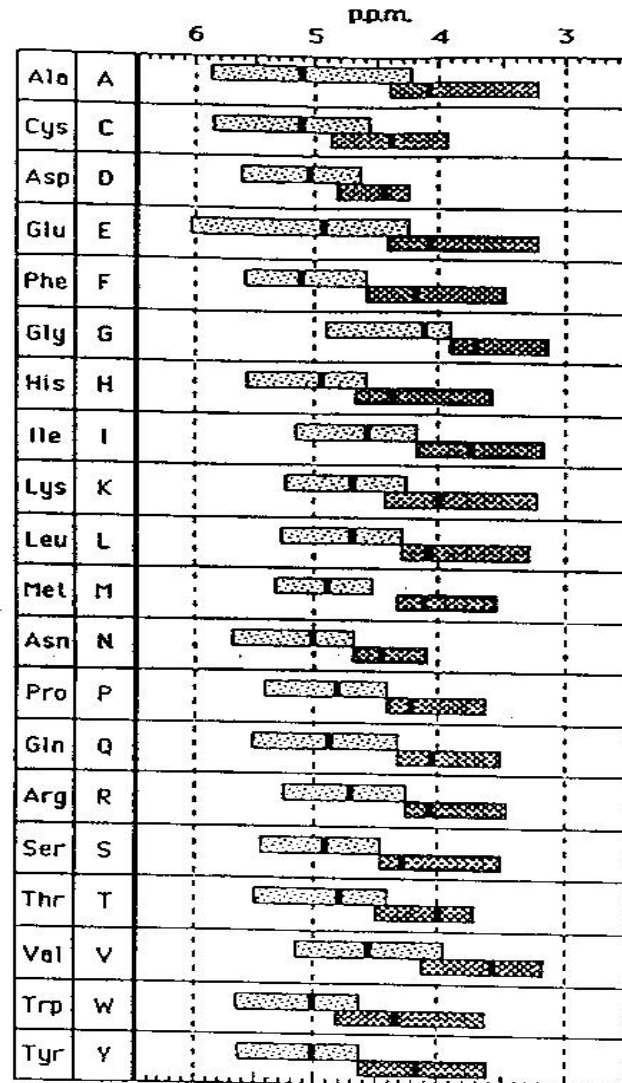
Res.	α	β	γ	δ	ϵ
Gly	42-48				
Ala	49-56	18-24			
Ser	55-62	61-67			
Thr	58-68	66-73	19-26		
Val	57-67	30-37	16-25		
Leu	51-60	39-48	22-29	21-28	
Ile	55-66	34-47	25-31	14-22	9-16
Lys	52-61	29-37	21-26	27-34	40-43
Arg	50-60	28-35	25-30	41-45	
Pro	60-67	27-35	24-29	49-53	
Glu	52-62	27-34	32-38		
.
.
.

WAGNER AND BRUHWILER, 1986...et al.

Or http://www.bmrb.wisc.edu/ref_info/statsel.htm

H^α chemical shifts and secondary structure

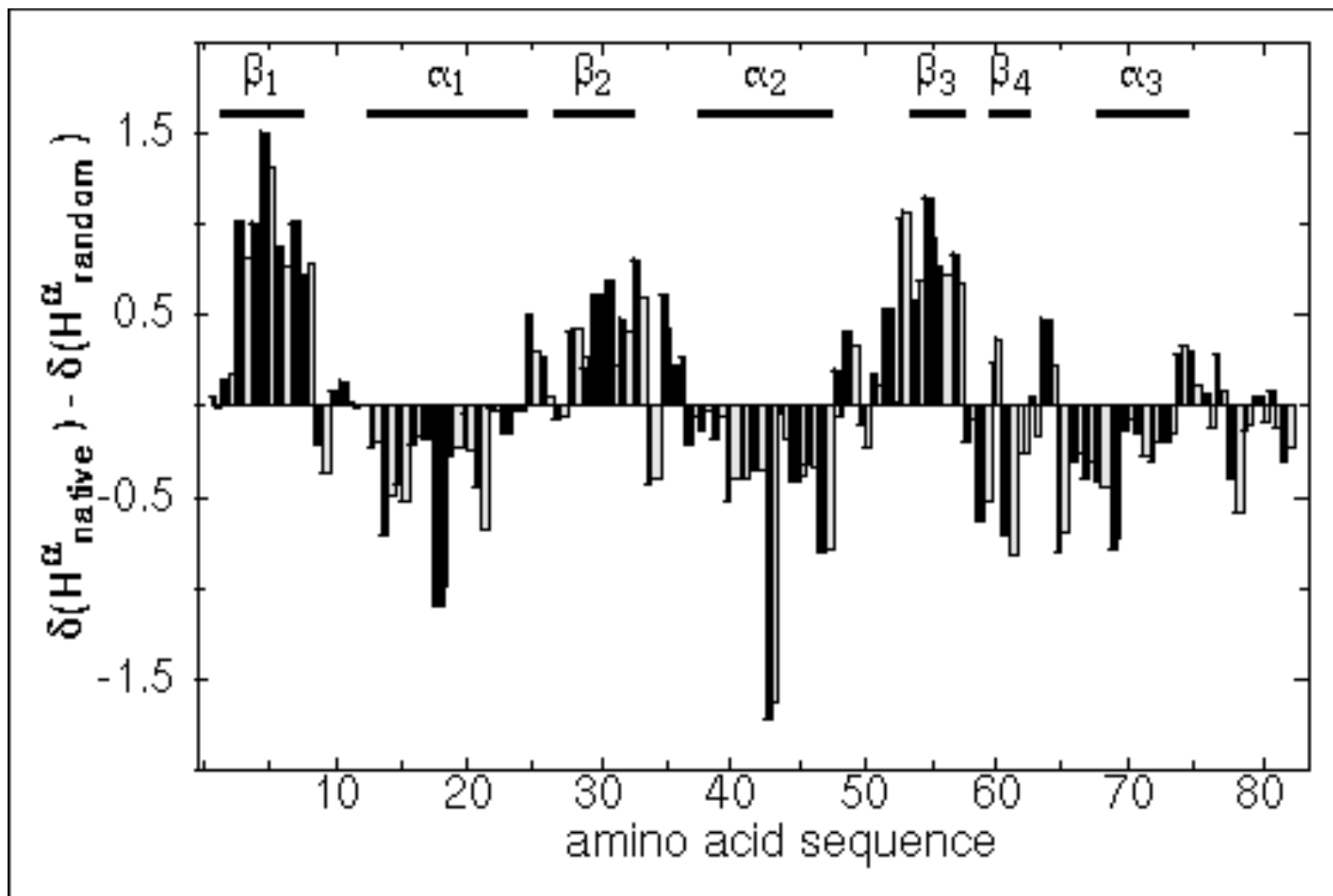
- the figure at right shows distributions of H^α chemical shifts observed in sheets (lighter bars) and helices (darker bars).
- H^α chemical shifts in α -helices are on average **0.39 ppm below** “random coil” values, while β -sheet values are **0.37 ppm above** random coil values.



Wishart, Sykes & Richards

J Mol Biol (1991) **222**, 311.

Secondary Shift vs Sequence



Reveals secondary structure !

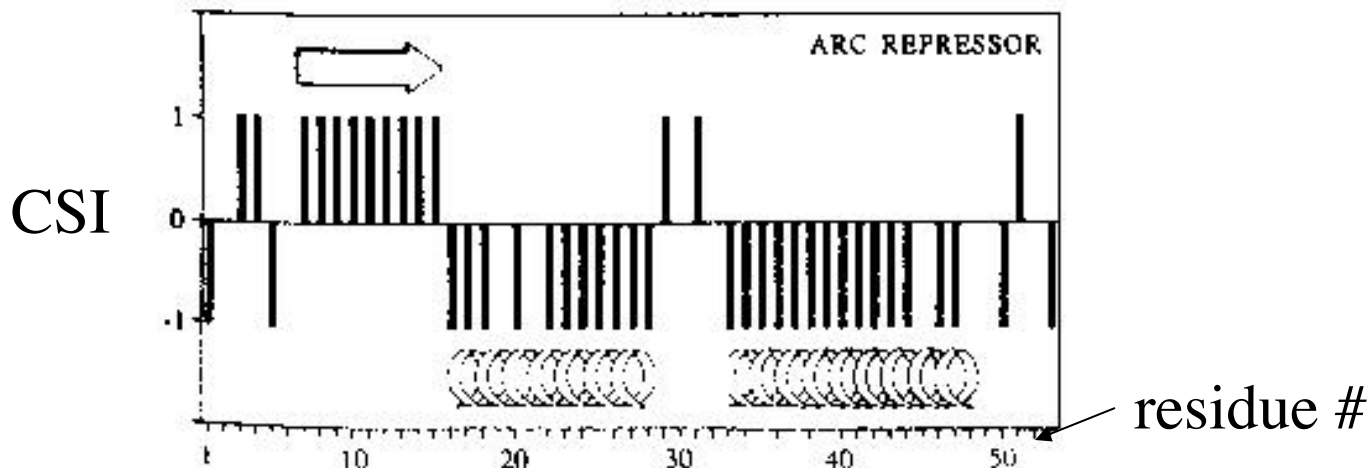
Chemical shift index (CSI)

- trends like these led to the development of the concept of the *chemical shift index** as a tool for assigning secondary structure using chemical shift values.
- one starts with a **table of reference values** for each amino-acid type, which is essentially a table of “random coil” H^α values
- CSI’s are then assigned as follows:

<u>exp' tl H^α shift rel. to reference</u>	<u>assigned CSI</u>
within ± 0.1 ppm	0
>0.1 ppm lower	-1
>0.1 ppm higher	+1

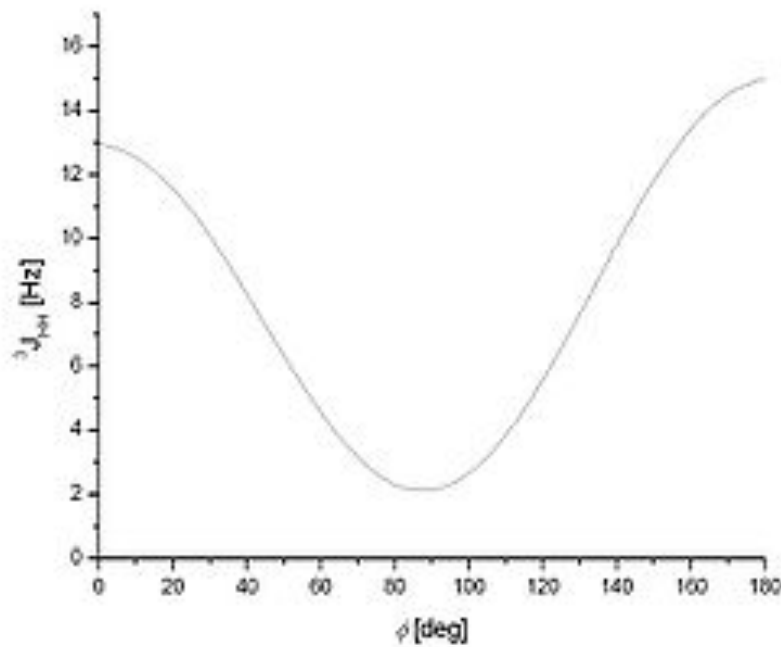
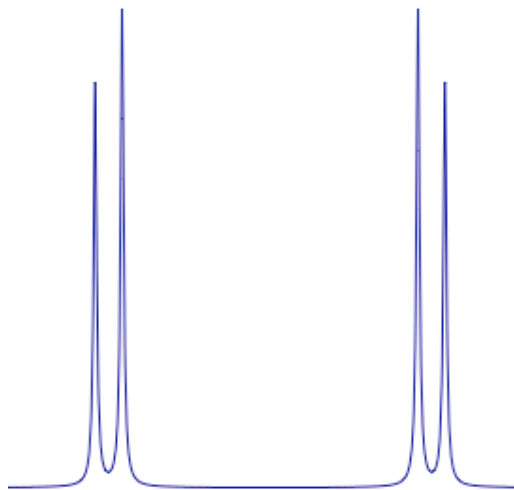
*Wishart, Sykes & Richards *Biochemistry* (1992) **31**, 1647-51.

Chemical shift indices



- any “dense” grouping of four or more “-1’ s”, uninterrupted by “1’ s” is assigned as a helix, while any “dense” grouping of three or more “1’ s”, uninterrupted by “-1’ s”, is assigned as a sheet.
- a “dense” grouping means at least 70% nonzero CSI’ s.
- other one regions are assigned as “coil”
- **this simple technique assigns 2ndary structure w/90-95% accuracy**
- similar useful relationships exist for $^{13}\text{C}^\alpha$, $^{13}\text{C}^{\text{C=O}}$ shifts

J couplings contain information on structure



$$J(\phi) = A \cos^2 \phi + B \cos \phi + C$$

3D structure calculation

- NMR provides information about structure
 - chemical shifts \Leftrightarrow local electronic environment
 - coupling constants \Leftrightarrow torsion angles
 - NOE, ROE \Leftrightarrow interproton distances
 - residual dipolar couplings \Leftrightarrow bond orientation
- and dynamics
 - relaxation times
 - NOE, ROE
- Most of the data describe
 - local environment of the protons
 - relative to each other
 - not the global conformation of the molecule

- **Distance**

NOE: The distance between i and j is a function of the NOE intensity $D_{ij} \sim C(\text{NOE}_{ij})^{-6}$

H-bonds: Identified by slowly exchanging amide H_N protons

- **Angles**

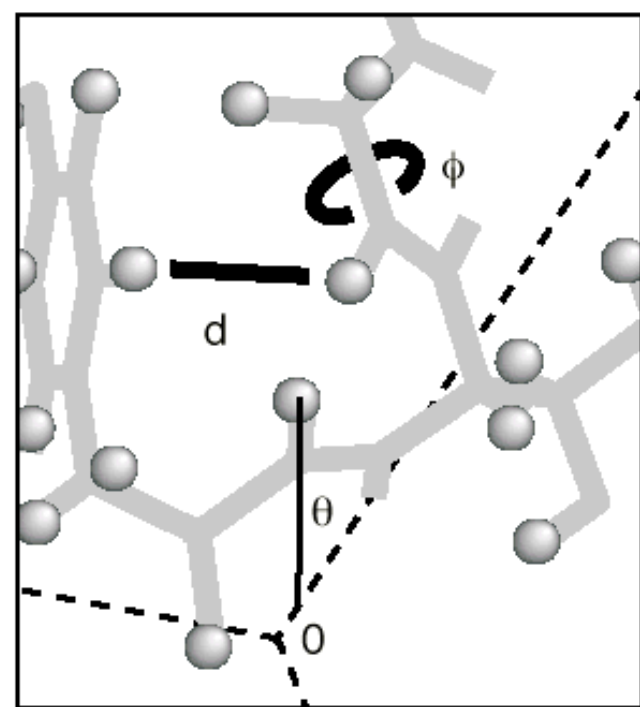
Side Chain χ and backbone torsion identified from J-coupling experiments

Chemical Shift also gives Angular Information

- **Residual Dipolar Couplings**

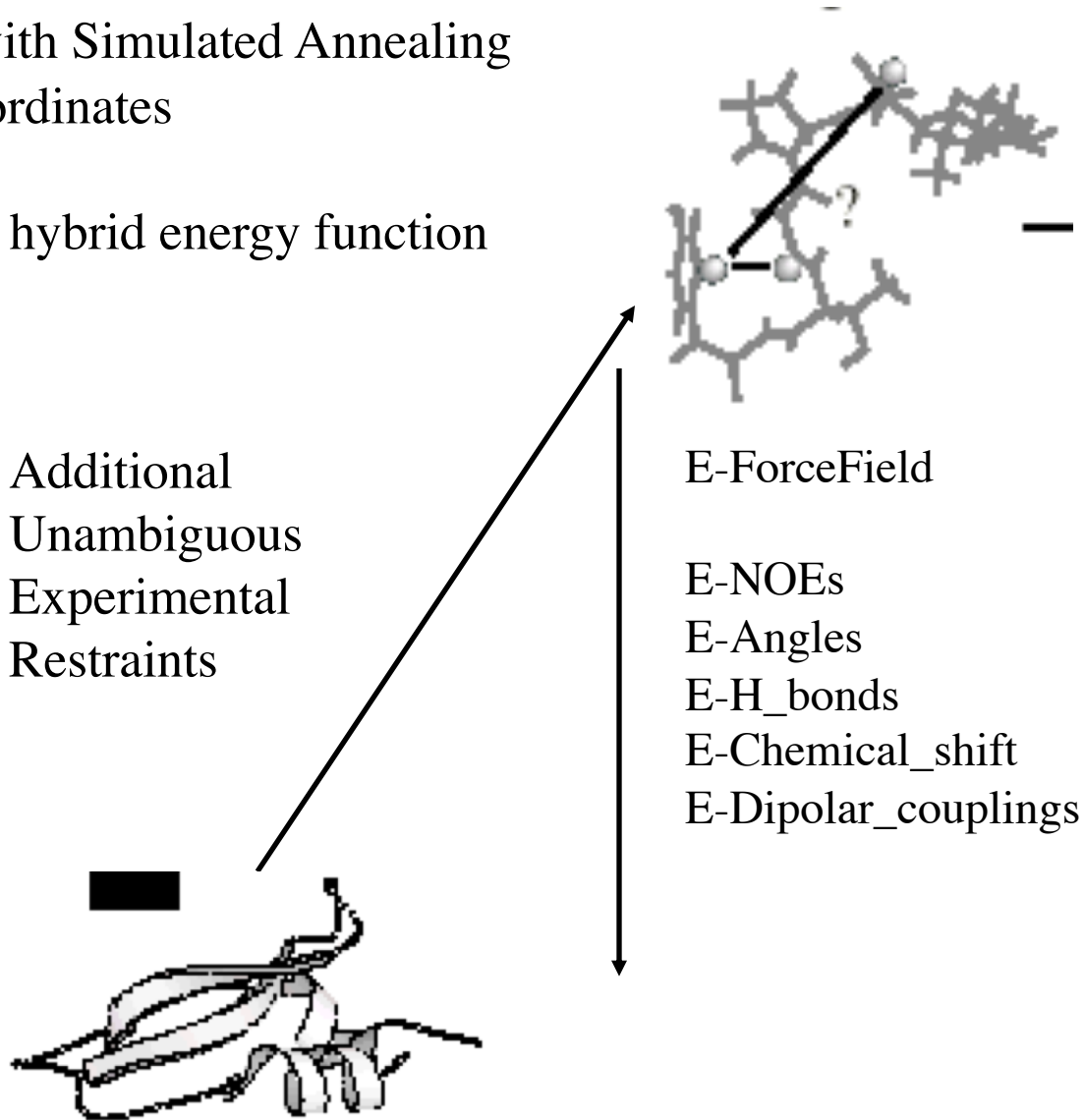
Bond Orientations Relative to an Alignment Tensor

Experimental data from NMR



3D structure calculation

- Molecular Dynamics with Simulated Annealing starting from random coordinates
- Goal is to minimize the hybrid energy function



The hybrid energy function

- Structure calculation = minimization of hybrid energy function (target function) which combines
 1. different experimental data
 2. *a priori* information (force field)

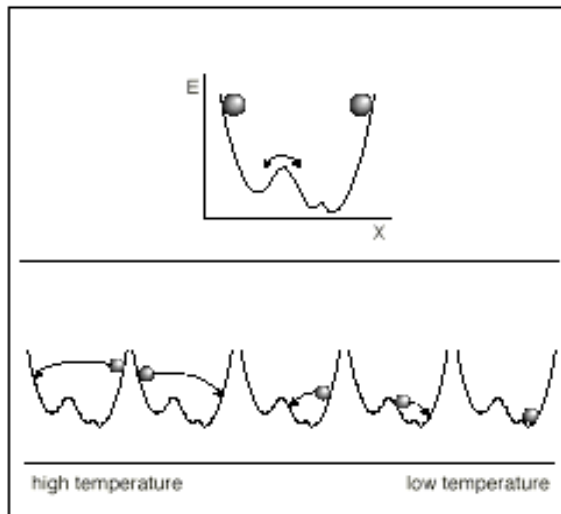
$$\begin{aligned}E_{hybrid} &= \sum_l w_l E_l = \\&\quad w_{bond} E_{bond} \\&+ w_{angle} E_{angle} \\&+ w_{improper} E_{improper} \\&+ w_{nonbonded} E_{nonbonded} \\&+ w_{unambig} E_{unambig} + w_{ambig} E_{ambig} + \dots \\&+ w_{torsion} E_{torsion} \\&+ w_{Jcoup} E_{Jcoup} \\&+ w_{RDC} E_{RDC} + \dots\end{aligned}$$

Minimization by molecular dynamics

- MD solves Newton's eqns. of motion:

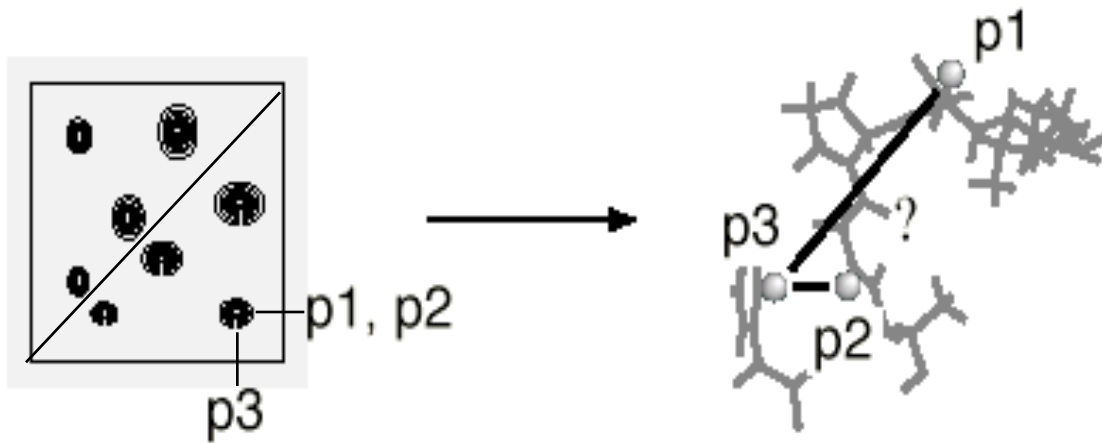
$$\frac{d^2\vec{r}_i}{dt^2} = -\frac{c}{m_i} \frac{\partial}{\partial \vec{r}_i} E_{hybrid}$$

- Molecular dynamics can overcome local energy barriers



- Temperature control and variation:
minimization by simulated annealing

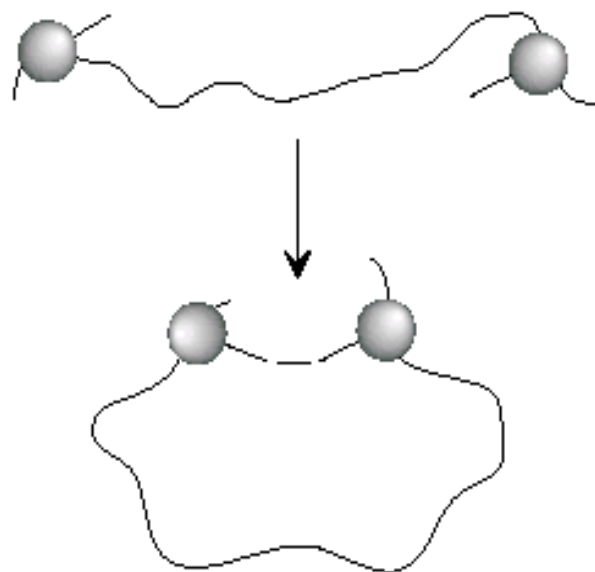
NOE ambiguities



- Key problem is ambiguity in NOE assignments
- Need for higher dimensional data: 3D & 4D
- Need for heteronuclear data
- Need for better calculational strategies that can deal with ambiguous data

Errors in data: error bounds

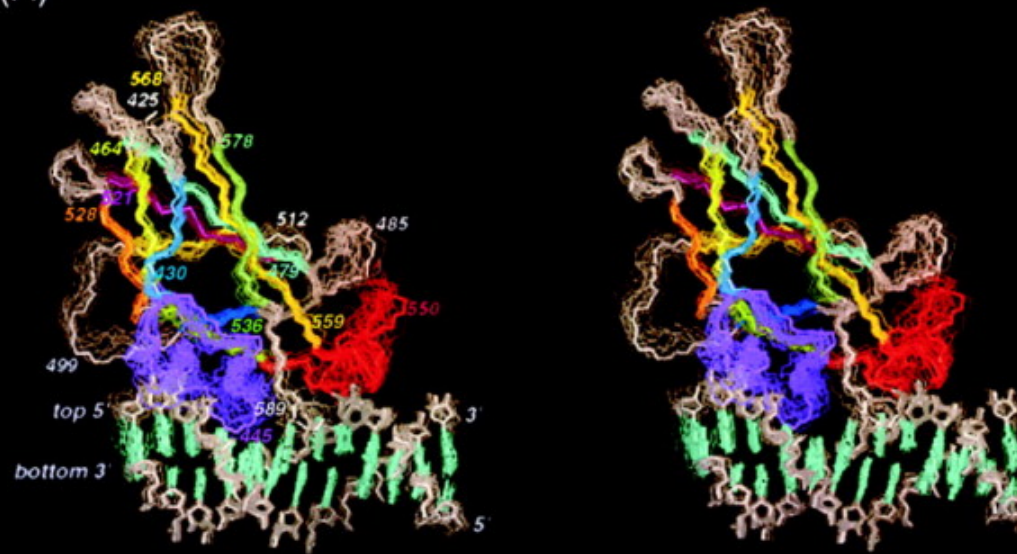
- Cumulative error in D_{ij} is treated by using loose error bounds $L \dots U$
- Precise value not (too) critical:
loose bounds restrict conformational space



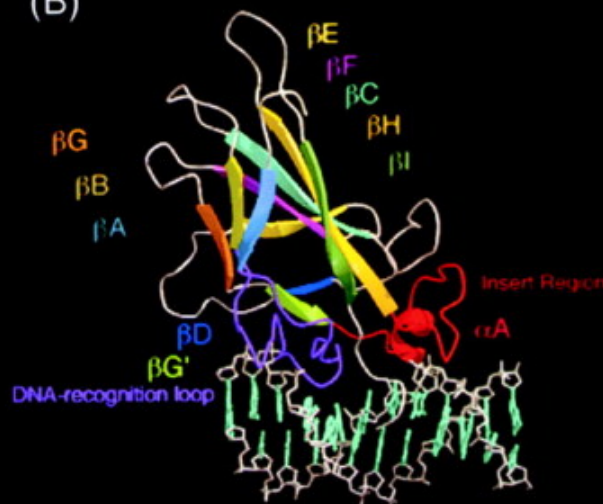
- However, consequences for:
 - precision of structure

Solution Structure of the Core NFATC1/DNA Complex

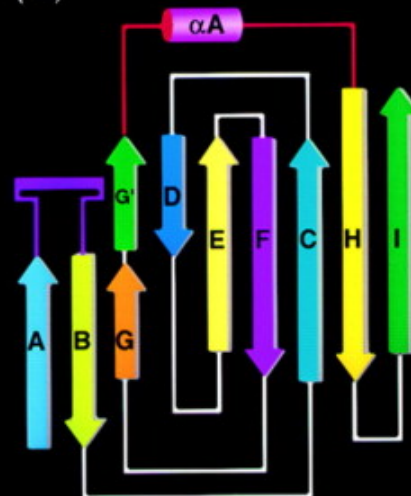
(A)



(B)



(C)



Need to evaluate restraint numbers, violations and precision

Table 1. Structural Statistics for NFATC1-DBD*/DNA Complex

Protein		
Amino acids residues sequentially assigned (nonproline)	162 of 167	
Effective distance constraints	1050	1050
Intraresidue	236	
Sequential ($ i - j = 1$)	374	
Medium-range ($ i - j \leq 4$)	86	
Long-range ($ i - j \geq 5$)	272	
H bonds	82	
Dihedral angle constraints	363	
DNA		
Effective distance constraints	276	
Intraresidue	146	
Sequential	131	
Interstrand	1	
H bond	58	
Protein-DNA interface		
Effective distance constraints	56	
Distance constraint violations > 0.2 Å (per structure)	1.81 ± 2.07	
Dihedral constraint violations > 3.0° (per structure)	1.44 ± 0.96	
X-PLOR potential energy ($E_{L,J}$, Kcal/mol, avg. per structure)	-501 ± 28.9	
R.m.s.d. to the mean for backbone heavy atoms of all β strands (residues 428–432, 460–464, 472–479, 493–495, 506–510, 515–521, 528–538, 559–568, 578–583)	0.62 ± 0.07	
R.m.s.d. to the mean for heavy atoms of all β strands (residues 428–432, 460–464, 472–479, 493–495, 506–510, 515–521, 528–538, 559–568, 578–583)	1.20 ± 0.14	
R.m.s.d. to the mean for backbone heavy atoms (residues 425–590)	1.14 ± 0.11	
R.m.s.d. to the mean for heavy atoms (residues 425–590)	1.58 ± 0.10	
R.m.s.d. to the mean for DNA heavy atoms (superposition of all DNA heavy atoms)	0.83 ± 0.21	
R.m.s.d. to the mean for protein + DNA heavy atoms (superposition of all β strand heavy atoms and DNA heavy atoms)	1.20 ± 0.16	
Ramachandran plot ^a		
	<u>Residues 425–590</u>	<u>Secondary Structures</u>
Most favorable region	60.4%	83.7%
Additionally allowed region	38.9%	14.0%
Generously allowed region	0.7%	2.3%
Disalloweed region	0.0%	0.0%

How were restraints measured?

^a Laskowski et al., 1996.

Analysis of Table

Table 1. Structural Statistics for NFATC1-DBD*/DNA Complex

Protein		
Amino acids residues sequentially assigned (nonproline)	162 of 167	
Effective distance constraints	1050	(circled in red)
Intraresidue	236	
Sequential ($ i - j = 1$)	374	
Medium-range ($ i - j \leq 4$)	86	
Long-range ($ i - j \geq 5$)	272	
H bonds	82	
Dihedral angle constraints	363	
DNA		
Effective distance constraints	276	
Intraresidue	146	
Sequential	131	
Interstrand	1	
H bond	58	
Protein-DNA interface		
Effective distance constraints	56	
Distance constraint violations > 0.2 Å (per structure)	1.81 ± 2.07	
Dihedral constraint violations > 3.0° (per structure)	1.44 ± 0.96	
X-PLOR potential energy ($E_{L,J}$, Kcal/mol, avg. per structure)	-501 ± 28.9	
R.m.s.d. to the mean for backbone heavy atoms of all β strands (residues 428–432, 460–464, 472–479, 493–495, 506–510, 515–521, 528–538, 559–568, 578–583)	0.62 ± 0.07	
R.m.s.d. to the mean for heavy atoms of all β strands (residues 428–432, 460–464, 472–479, 493–495, 506–510, 515–521, 528–538, 559–568, 578–583)	1.20 ± 0.14	
R.m.s.d. to the mean for backbone heavy atoms (residues 425–590)	1.14 ± 0.11	
R.m.s.d. to the mean for heavy atoms (residues 425–590)	1.58 ± 0.10	
R.m.s.d. to the mean for DNA heavy atoms (superposition of all DNA heavy atoms)	0.83 ± 0.21	
R.m.s.d. to the mean for protein + DNA heavy atoms (superposition of all β strand heavy atoms and DNA heavy atoms)	1.20 ± 0.16	
Ramachandran plot ^a		
	<u>Residues 425–590</u>	<u>Secondary Structures</u>
Most favorable region	60.4%	83.7%
Additionally allowed region	38.9%	14.0%
Generously allowed region	0.7%	2.3%
Disallowable region	0.0%	0.0%

How many NOE restraints?

>6 per residue is acceptable

^a Laskowski et al., 1996.

Analysis of Table

Table 1. Structural Statistics for NFATC1-DBD*/DNA Complex

Protein		
Amino acids residues sequentially assigned (nonproline)		162 of 167
Effective distance constraints		1050
Intraresidue		236
Sequential ($ i - j = 1$)		374
Medium-range ($ i - j \leq 4$)		86
Long-range ($ i - j \geq 5$)		272
H bonds		82
Dihedral angle constraints		363
DNA		
Effective distance constraints		276
Intraresidue		146
Sequential		131
Interstrand		1
H bond		58
Protein-DNA interface		
Effective distance constraints		56
Distance constraint violations > 0.2 Å (per structure)		1.81 ± 2.07
Dihedral constraint violations > 3.0° (per structure)		1.44 ± 0.96
X-PLOR potential energy ($E_{L,J}$, Kcal/mol, avg. per structure)		-501 ± 28.9
R.m.s.d. to the mean for backbone heavy atoms of all β strands		
(residues 428–432, 460–464, 472–479, 493–495, 506–510, 515–521, 528–538, 559–568, 578–583)		0.62 ± 0.07
R.m.s.d. to the mean for heavy atoms of all β strands		
(residues 428–432, 460–464, 472–479, 493–495, 506–510, 515–521, 528–538, 559–568, 578–583)		1.20 ± 0.14
R.m.s.d. to the mean for backbone heavy atoms		
(residues 425–590)		1.14 ± 0.11
R.m.s.d. to the mean for heavy atoms		
(residues 425–590)		1.58 ± 0.10
R.m.s.d. to the mean for DNA heavy atoms		
(superposition of all DNA heavy atoms)		0.83 ± 0.21
R.m.s.d. to the mean for protein + DNA heavy atoms		
(superposition of all β strand heavy atoms and DNA heavy atoms)		1.20 ± 0.16
Ramachandran plot ^a		
	<u>Residues 425–590</u>	<u>Secondary Structures</u>
Most favorable region	60.4%	83.7%
Additionally allowed region	38.9%	14.0%
Generously allowed region	0.7%	2.3%
Disalloweed region	0.0%	0.0%

How are NOE restraints distributed?

^a Laskowski et al., 1996.

Reading the NMR Statistics Structure Table

Table 1. Structural Statistics for NFATC1-DBD*/DNA Complex

Protein		
Amino acids residues sequentially assigned (nonproline)		162 of 167
Effective distance constraints		1050
Intraresidue		236
Sequential ($ i - j = 1$)		374
Medium-range ($ i - j \leq 4$)		86
Long-range ($ i - j \geq 5$)		272
H bonds		82
Dihedral angle constraints		363
DNA		
Effective distance constraints		276
Intraresidue		146
Sequential		131
Interstrand		1
H bond		58
Protein-DNA interface		
Effective distance constraints		56
Distance constraint violations > 0.2 Å (per structure)		1.81 ± 2.07
Dihedral constraint violations > 3.0° (per structure)		1.44 ± 0.96
X-PLOR potential energy (E_{LJ} , Kcal/mol, avg. per structure)		-501 ± 28.9
R.m.s.d. to the mean for backbone heavy atoms of all β strands		
(residues 428–432, 460–464, 472–479, 493–495, 506–510, 515–521, 528–538, 559–568, 578–583)		0.62 ± 0.07
R.m.s.d. to the mean for heavy atoms of all β strands		1.20 ± 0.14
(residues 428–432, 460–464, 472–479, 493–495, 506–510, 515–521, 528–538, 559–568, 578–583)		1.20 ± 0.14
R.m.s.d. to the mean for backbone heavy atoms		
(residues 425–590)		1.14 ± 0.11
R.m.s.d. to the mean for heavy atoms		
(residues 425–590)		1.58 ± 0.10
R.m.s.d. to the mean for DNA heavy atoms		
(superposition of all DNA heavy atoms)		0.83 ± 0.21
R.m.s.d. to the mean for protein + DNA heavy atoms		
(superposition of all β strand heavy atoms and DNA heavy atoms)		1.20 ± 0.16
Ramachandran plot ^a		
	<u>Residues 425–590</u>	<u>Secondary Structures</u>
Most favorable region	60.4%	83.7%
Additionally allowed region	38.9%	14.0%
Generously allowed region	0.7%	2.3%
Disalloweed region	0.0%	0.0%

How were H Bonds Determined?

^a Laskowski et al., 1996.

Reading the NMR Statistics Structure Table

Table 1. Structural Statistics for NFATC1-DBD*/DNA Complex

Protein		
Amino acids residues sequentially assigned (nonproline)		162 of 167
Effective distance constraints		1050
Intraresidue		236
Sequential ($ i - j = 1$)		374
Medium-range ($ i - j \leq 4$)		86
Long-range ($ i - j \geq 5$)		272
H bonds		82
Dihedral angle constraints		363
DNA		
Effective distance constraints		276
Intraresidue		146
Sequential		131
Interstrand		1
H bond		58
Protein-DNA interface		
Effective distance constraints		56
Distance constraint violations > 0.2 Å (per structure)		1.81 ± 2.07
Dihedral constraint violations > 3.0° (per structure)		1.44 ± 0.96
X-PLOR potential energy (E_{LJ} , Kcal/mol, avg. per structure)		-501 ± 28.9
R.m.s.d. to the mean for backbone heavy atoms of all β strands		
(residues 428–432, 460–464, 472–479, 493–495, 506–510, 515–521, 528–538, 559–568, 578–583)		0.62 ± 0.07
R.m.s.d. to the mean for heavy atoms of all β strands		
(residues 428–432, 460–464, 472–479, 493–495, 506–510, 515–521, 528–538, 559–568, 578–583)		1.20 ± 0.14
R.m.s.d. to the mean for backbone heavy atoms		
(residues 425–590)		1.14 ± 0.11
R.m.s.d. to the mean for heavy atoms		
(residues 425–590)		1.58 ± 0.10
R.m.s.d. to the mean for DNA heavy atoms		
(superposition of all DNA heavy atoms)		0.83 ± 0.21
R.m.s.d. to the mean for protein + DNA heavy atoms		
(superposition of all β strand heavy atoms and DNA heavy atoms)		1.20 ± 0.16
Ramachandran plot ^a		
	<u>Residues 425–590</u>	<u>Secondary Structures</u>
Most favorable region	60.4%	83.7%
Additionally allowed region	38.9%	14.0%
Generously allowed region	0.7%	2.3%
Disallowed region	0.0%	0.0%

How many intermolecular NOEs?

^a Laskowski et al., 1996.

Reading the NMR Statistics Structure Table

Table 1. Structural Statistics for NFATC1-DBD*/DNA Complex

Protein		
Amino acids residues sequentially assigned (nonproline)	162 of 167	
Effective distance constraints	1050	
Intraresidue	236	
Sequential ($ i - j = 1$)	374	
Medium-range ($ i - j \leq 4$)	86	
Long-range ($ i - j \geq 5$)	272	
H bonds	82	
Dihedral angle constraints	363	
DNA		
Effective distance constraints	276	
Intraresidue	146	
Sequential	131	
Interstrand	1	
H bond	58	
Protein-DNA interface		
Effective distance constraints	56	
Distance constraint violations > 0.2 Å (per structure)	1.81 ± 2.07	
Dihedral constraint violations > 3.0° (per structure)	1.44 ± 0.96	
X-PLOR potential energy (E_{LJ} , Kcal/mol, avg. per structure)	-501 ± 28.9	
R.m.s.d. to the mean for backbone heavy atoms of all β strands (residues 428–432, 460–464, 472–479, 493–495, 506–510, 515–521, 528–538, 559–568, 578–583)	0.62 ± 0.07	
R.m.s.d. to the mean for heavy atoms of all β strands (residues 428–432, 460–464, 472–479, 493–495, 506–510, 515–521, 528–538, 559–568, 578–583)	1.20 ± 0.14	
R.m.s.d. to the mean for backbone heavy atoms (residues 425–590)	1.14 ± 0.11	
R.m.s.d. to the mean for heavy atoms (residues 425–590)	1.58 ± 0.10	
R.m.s.d. to the mean for DNA heavy atoms (superposition of all DNA heavy atoms)	0.83 ± 0.21	
R.m.s.d. to the mean for protein + DNA heavy atoms (superposition of all β strand heavy atoms and DNA heavy atoms)	1.20 ± 0.16	
Ramachandran plot^a		
	<u>Residues 425–590</u>	<u>Secondary Structures</u>
Most favorable region	60.4%	83.7%
Additionally allowed region	38.9%	14.0%
Generously allowed region	0.7%	2.3%
Disallowed region	0.0%	0.0%

Criteria for publication:
No distance violations $> 0.5 \text{ \AA}$
No dihedral angle violations $> 5^\circ$

How many violations ?

^a Laskowski et al., 1996.

Read methods section to evaluate table

Resonance Assignments

1-HNCA/HN(CO)CA
2-Amino-acid specific labeling
3-NOESY experiments:
Homonuclear and heteronuclear

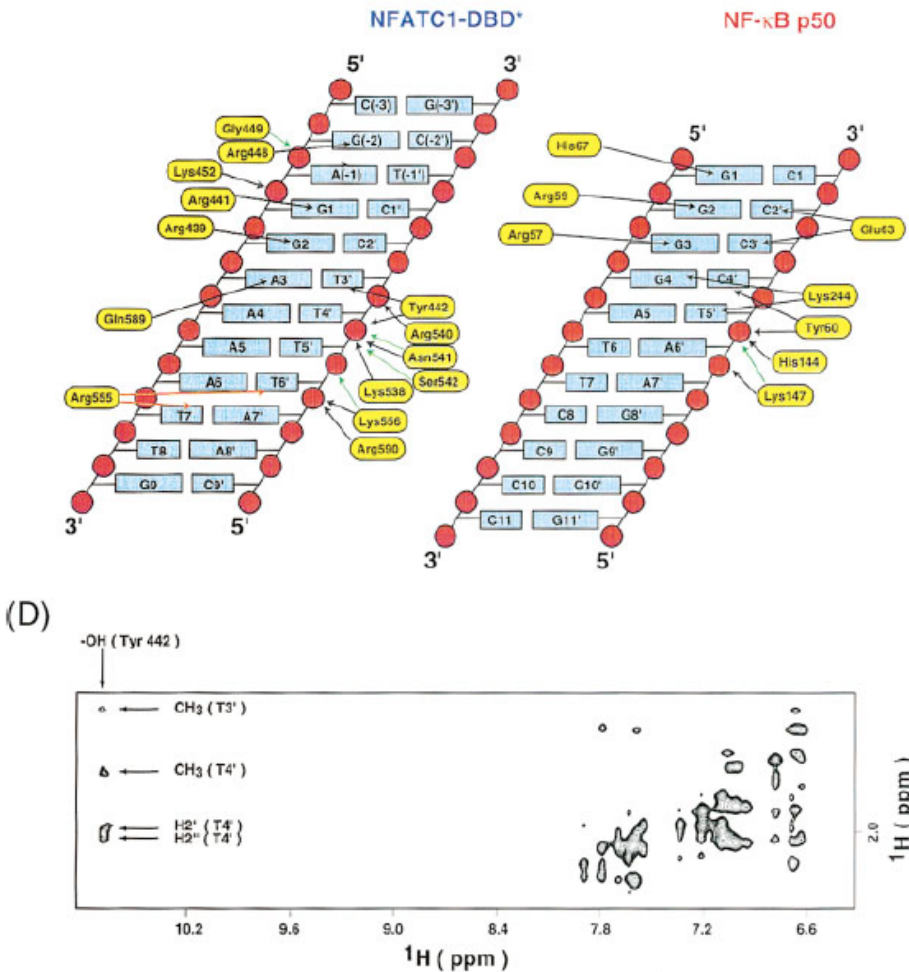
Distance Restraints

1-2D and 3D NOESY at longer mixing times to get weak NOEs
2-HD exchange to get hydrogen bonds

Many of these experiments performed with a specific labeling scheme to facilitate NOEs assignment

Side chain assignments from NOESY, caveats?

Assymmetric isotope labelling to get intermolecular NOEs



Protein is deuterated, DNA protonated experiment done in D₂O solvent
Caveats?

Structures of larger proteins and complexes

Sample Deuteration Increases Sensitivity and Resolution

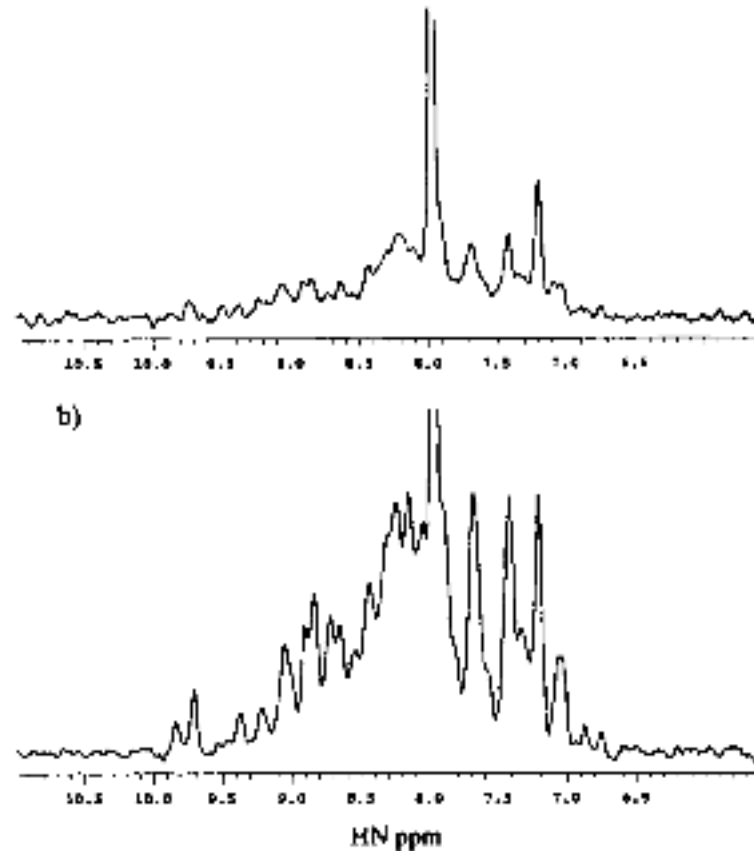
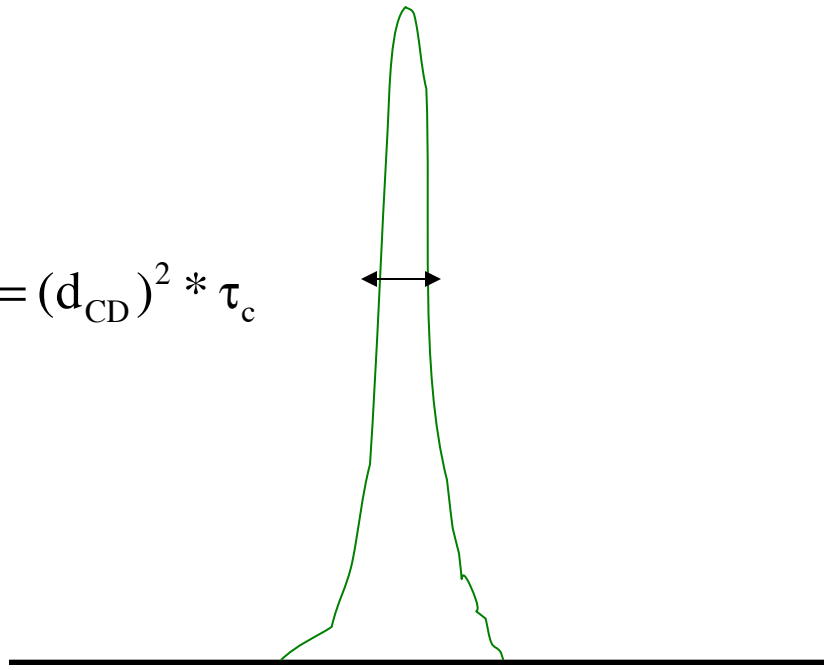
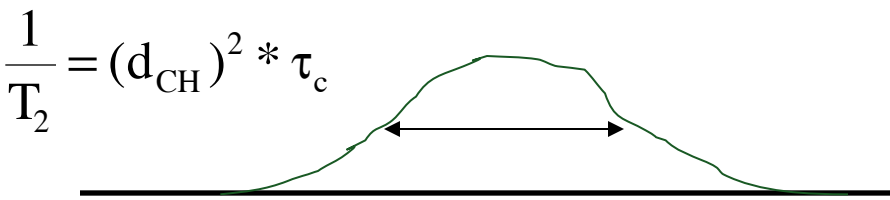


Figure 14. Comparative 1D spectra of fully protonated (a) and ~70% deuterated (b) ^{15}N , ^{13}C trpR using the HN(CA)CB scheme (Figure 2c). A total of 1024 transients were recorded for the ^3H sample and 6928 transients (1024×2.6^3) for the ^1H sample which is a factor of 2.6 more dilute. The rms noise levels are normalized in the plots.

Why does deuteration help?

$$d_{CH} = \frac{\gamma_C \gamma_H}{r^3} \frac{3\cos^2(\theta) - 1}{2}$$

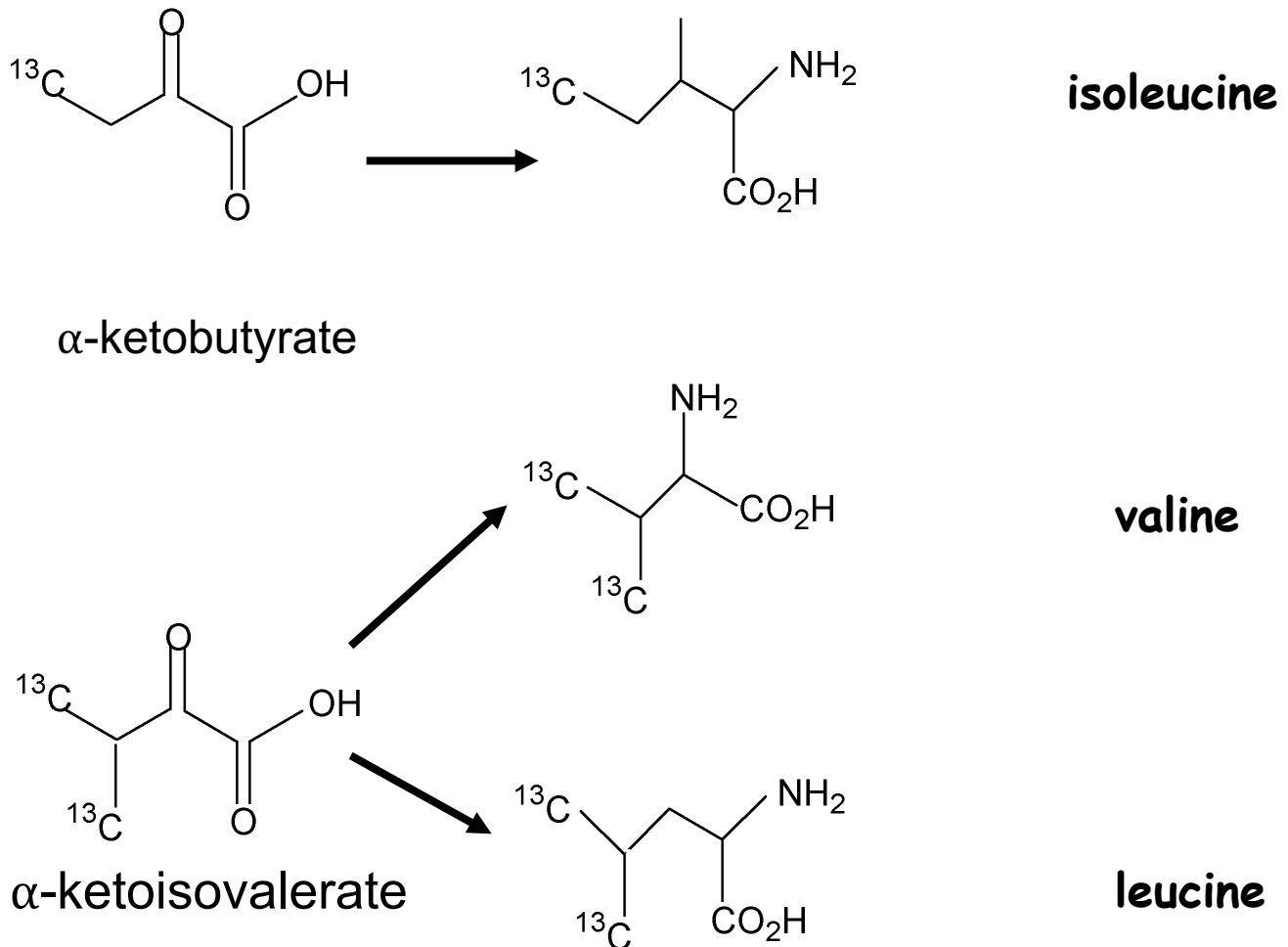
$$\frac{1}{T_2} = (d_{CD})^2 * \tau_c$$



Dipolar coupling for CH spin pair 6.5 times stronger than for CD--->roughly 50 fold reduction in linewidth with increase in S:N.

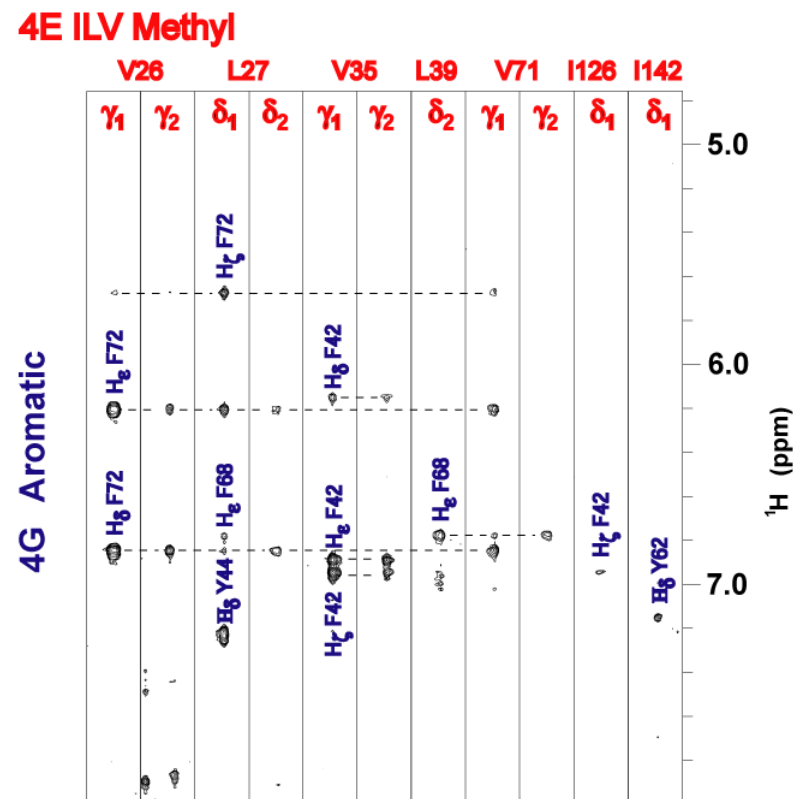
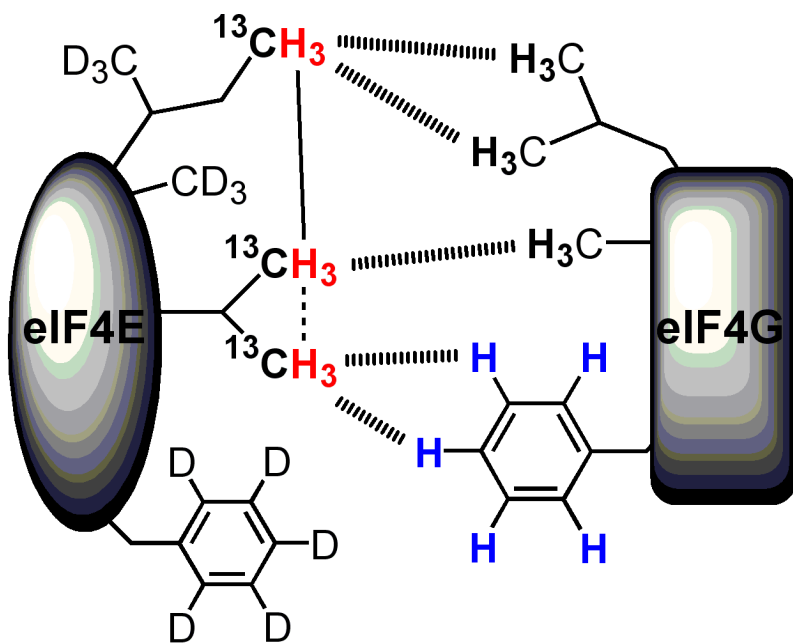
Need methods for measuring distance restraints in sparse 1H environment

Selective Re-introduction of Protons for NOE experiments



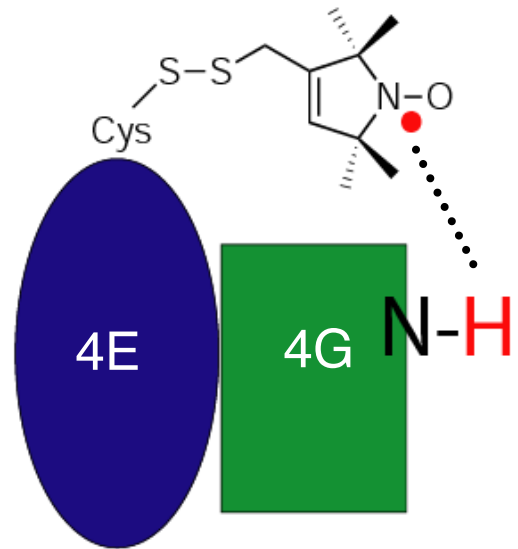
Grow E. coli in D₂O and deuterated glucose, add precursors to introduce 1H/13C methyl labels

Measurement of Intermolecular NOEs using Asymmetric Deuteration with ILV Labeling



Aromatic/methyl NOEs are unambiguously identified

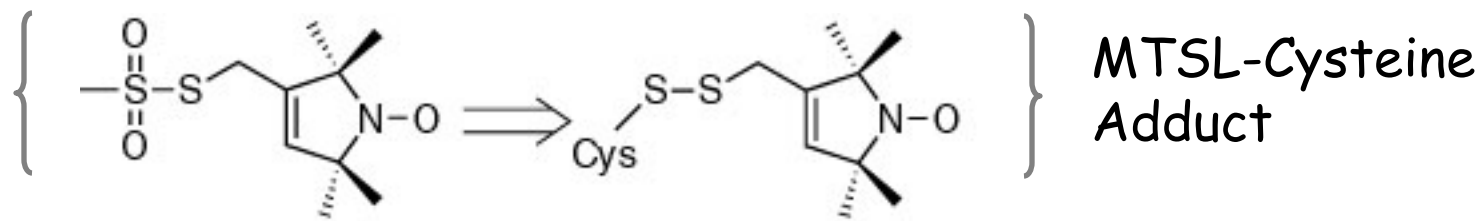
Determining Long Range Distances through Paramagnetic Relaxation Enhancements



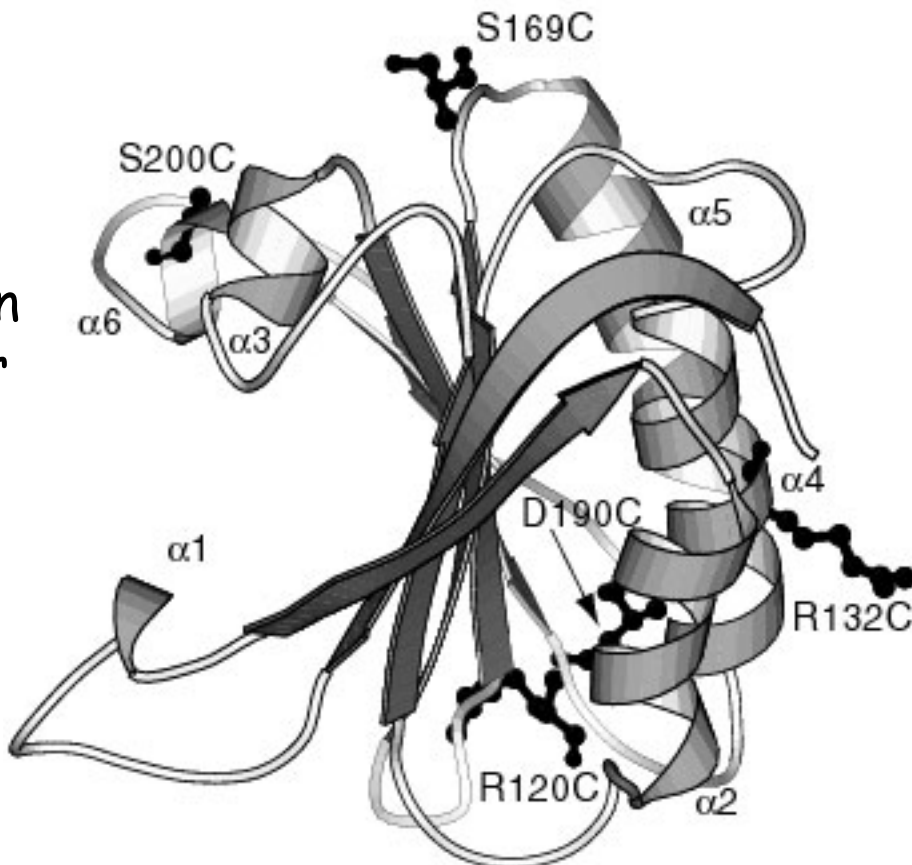
Dipolar broadening between unpaired electron and ¹H:
 $1/r^6$ dependence.

Provides long range distance information (15-20 angstroms)

Site-Directed Spin Labeling for PRE



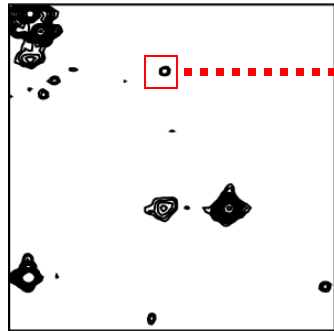
Cysteine mutation
in surface loop or
helix



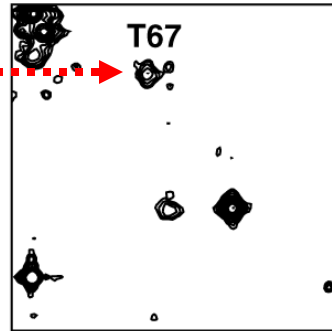
Record HSQC
In absence and
presence of
reductant

Paramagnet Relaxation Enhancement from Site-Directed Spin Labelling

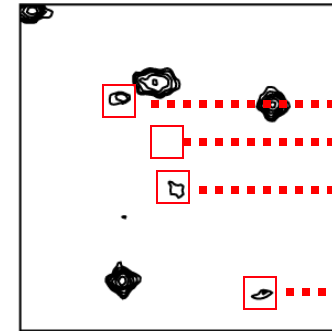
Oxidized



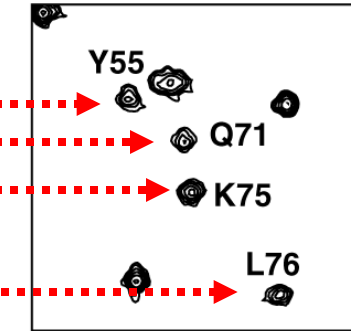
Reduced



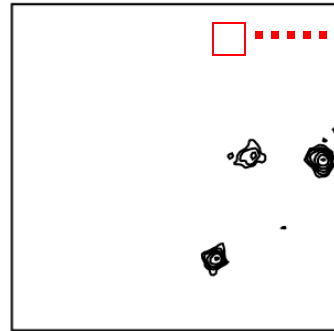
Oxidized



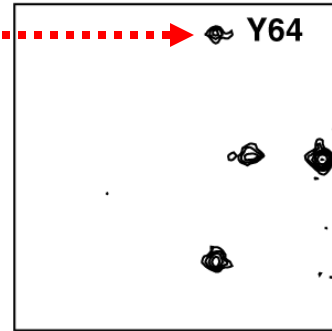
Reduced



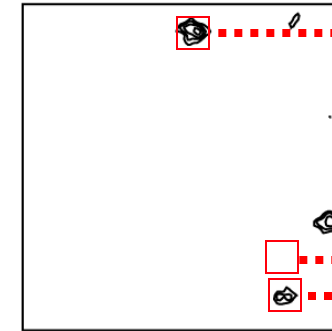
N-O•



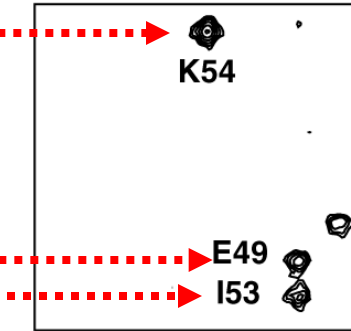
N-OH



N-O •

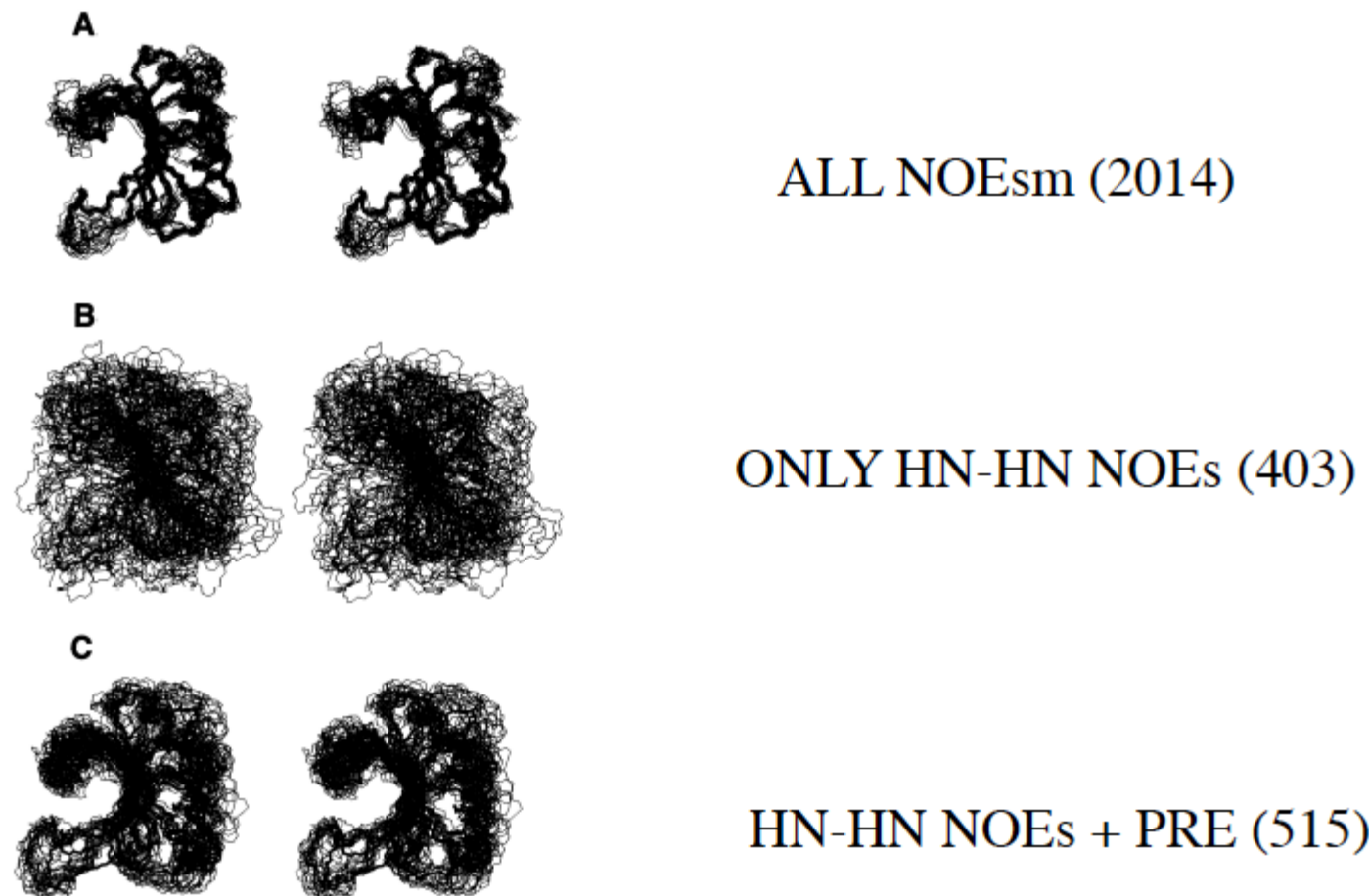


N-OH

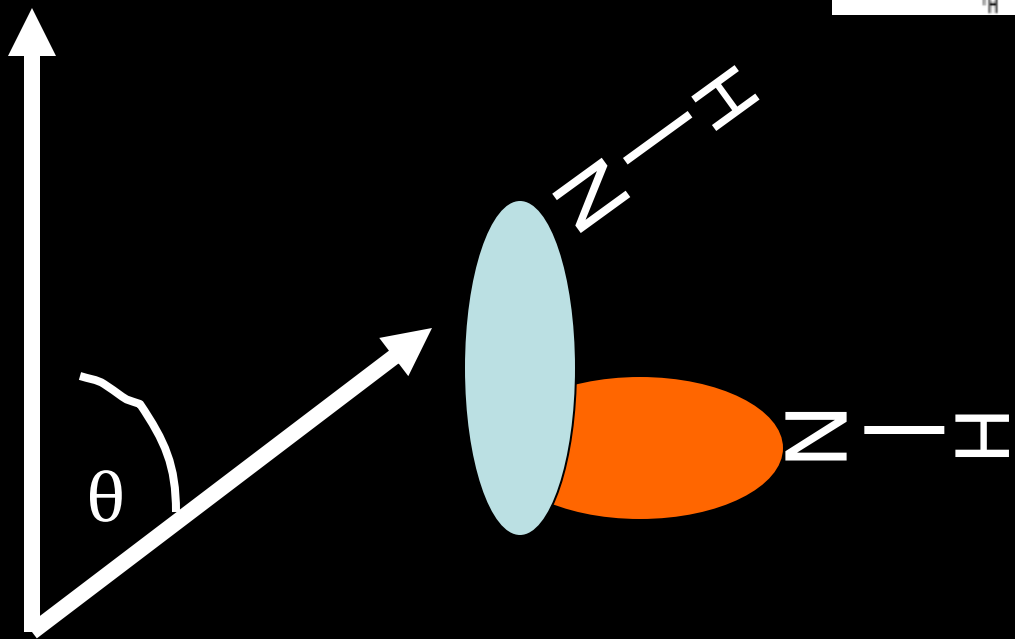
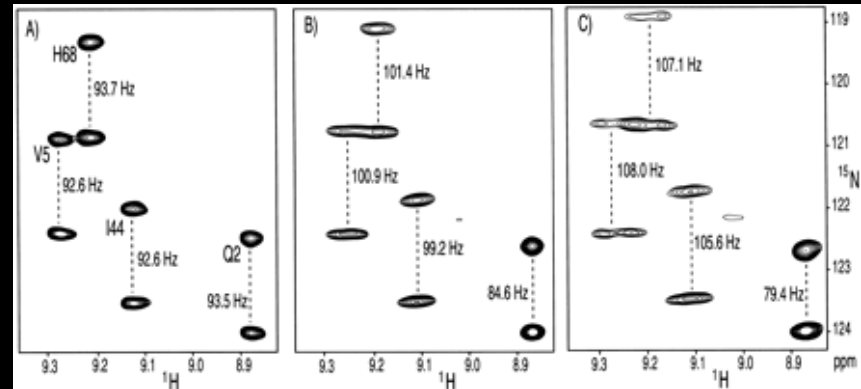
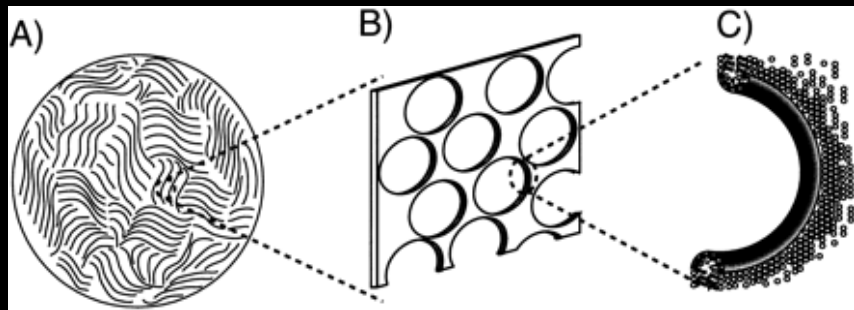


Intensity reduction from dipolar coupling ($1/r^6$), so distances can be extracted

Impact of PRE restraints for structure determination



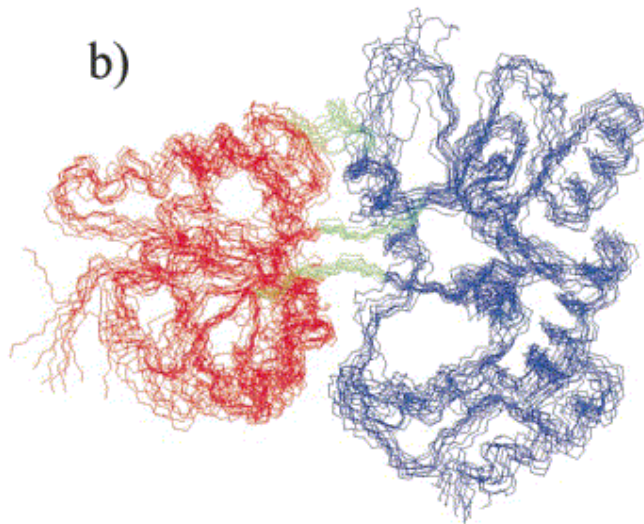
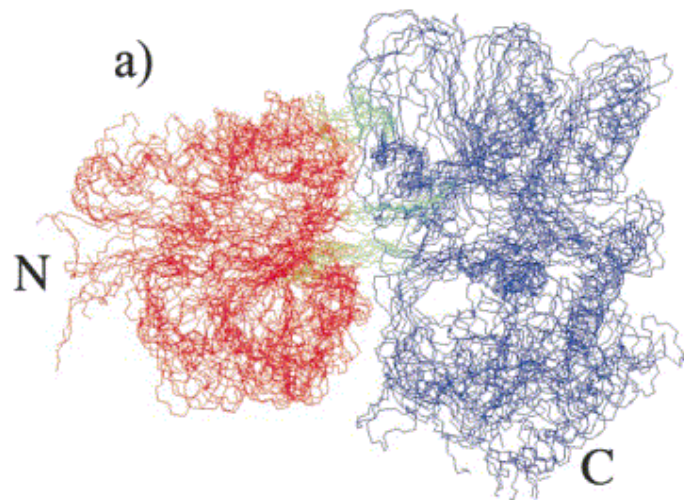
Residual Dipolar Couplings



$$d_{NH} [3\cos^2\theta - 1]/2$$

$$d_{NH} \sim \frac{\gamma_C \gamma_H}{r^3}$$

Impact of RDCs on Precision and Accuracy: MBP, a 42 kDa test Case



RMSD

Precision:	5.5 Å	2.2 Å
Accuracy:	5.1 Å	3.3 Å

From Mueller et. Al. JMB 300(1) 197-212 2000

Prospects for even Larger Proteins

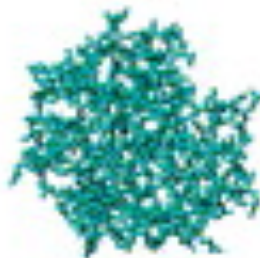
Ubiquitin
76 residues



Lysozyme
156 residues



Adenylate Kinase
214 residues



Maltose binding
protein (MBP)
370 residues



Malate synthase G
723 residues



- i. NMR assignments
- ii. Structure determination
- iii. Dynamics

requires ^{15}N , ^{13}C labeling

- i. NMR assignments
- ii. Global fold/structure determination
- iii. Domain orientation
- iv. Dynamics

requires ^{15}N , ^{13}C , ^2H labeling



X-ray

vs

NMR

- crystal
- single structure-best fit to electron density

- solution
- ensemble of 20-50 structures that equally fit experimental data

Limitations of NMR

- small proteins (20-30 kD max, although this is changing)
- must be soluble and nonaggregating at 1-3 mM conc
- lots of protein needed

Advantages of NMR

- don't need crystal
- observe protein in solution
- more than a method for determining structure
 - dynamics
 - ligand binding (drug/protein/DNA/etc)
 - protein folding
 - conformational change
 - chemistry, chemical reactions, protonation states.....